Phenomenological Study

Phenomenological Study on Volume Phase Transition of PNIPA Gels

HASHIMOTO, Chihiro

Phenomenological Study on Volume Phase Transition of PNIPA Gels

by
HASHIMOTO, Chihiro

ACKNOWLEDGEMENTS

The author wishes to express her deep gratitude to Professor Hideharu USHIKI for his constant guidance and encouragement in all phases of this work.

CONTENTS

GENERAL INTRODUCTION

Poly(N-isopropylacrylamide) (PNIPA) gels are well known as nonionic polymer gels showing volume phase transition induced by temperature. Hysteresis and various morphological changes are observed on swelling and shrinking processes of gels and such dynamical phenomena of gels can be expected as combined effects of thermodynamic instability and nonlinear elasticity. PNIPA gels shrink and become white after jumping above the critical temperature. Whitening slowly disappears and the gels become finally transparent. This final stage is regarded as the equilibrium state. The purpose of this research is to clarify such shrinking process of PNIPA gels from the viewpoint of macroscopic level using by graphical analysis method. This thesis is divided into five chapters.

Volume phase transition phenomena of gels is very interesting theme from the standpoint of the study of complex system. it is more important to discuss the relationship between experimental facts from the dynamical viewpoints of classification of space and time. PLASMA has been devised and built in our laboratory as a new apparatus from the above viewpoint(Part I). The flow of studies on volume phase transition of gels by PLASMA is reviewed and some results are introduced in part II.

Shrinking and whitening processes of synthesized disk-like PNIPA gels were studied at various constant temperatures, from critical temperature(T_c) to $T_c+\Delta T$ using by a CCD video camera or a single lens camera. PNIPA gels shrink and become turbid, then whitening slowly disappears and the gels become finally transparent. The number of dots of gels is evaluated using by a clipping procedure and defines the area of a gel S(t). The integral value of light intensities due to the whitening of gels is $W_1(t)$ and $W_2(t)$ is introduced as whitening per area of gel $W_1(t)/S(t)$. S(t) shows two-step shrinking and to fit it, the sum of exponential and stretched exponential functions was adequate using the 'χ^2 map method (Chapter 1-1). The exponential (first shrinking) is deduced as collective diffusion with infinitesimal deformation of an elastic body by T.Tanaka. In order to discuss the meaning of stretched exponential function with $\beta>1$, new theoretical concept 'integral transformation' was proposed. Applied this concept to secondary shrinking of PNIPA gels, assuming that gels consist of a lot of parts, each part shrinks step-like at $t=\tau$ and the distribution function of τ was defined as the derivative of stretched exponential function $D(\tau)$.(Chapter 1-2) $W_1(t)$ was explained by a sum of two whitening processes accompanied with shrinking one. Each process was directly explained by $D(\tau)$ and it indicates that whitening occurs like δ function in each part when each part shrinks, assuming that there are a lot of parts from the viewpoints

of mesoscopic level. (Chapter 2) Size of disk-like gels and jumping temperature were changed and the effects on both shrinking and whitening processes are discussed. Diameter of disk-like gels gives no change, while the time scale of $S(t)$ and $W_1(t)$ is elongated with increasing thickness of gels. The relationship between thickness of gels and average time of shrinking were expressed by T.Tanaka's formula mentioned above. Average time of firs and second shrinking shows a critical slowing down. First shrinking and first whitening are always synchronized at small temperature jump, while average time and the degree of asynchrous of second whitening undergoes slowly at large jumping temperature. It is due to the effect of elastic effects of gels chain. Except for the case of large temperature gap, whitening process is always synchronized with shrinking process, and it indicates that the shrinking process in macroscopic level is strongly related to whitening one in mesoscopic level. When gels are thick and jumping temperature is large, $S(t)$ shows 3 step shrinking and the possibility of multi-step shrinking was proposed. (Chapter 3) Sample gels were prepared by cutting out the synthesized sheet-like PNIPA gels with a cookie cutter, the shape of which was clover, diamond, heart and spade, respectively. Shape of gels dependence on $S(t)$, $W_1(t)$ and $W_2(t)$ was not observed, but all the gels show that the convexoconcave of the shape disappear in second shrinking and the shape is restored after shrinking. This deformation corresponds to the three-dimensional deformation of gels like Japanese original pouch 'Kinchaku'. The edge part of disk-like gels tends to turn over after first shrinking and it is due to the edge part's shrinking. Skin layer is formed as shrunken layer on the surface of gels after first shrinking process and the edge part exactly corresponds to skin layer itself. (Chapter 4) In addition, bubbles or interconnected network like neuron appear in gels in secondary shrinking. Power spectra on the surface of disk-like gels by 1-dimensional Fourier Transformation was done and has 3 modes, a sine, Markov noise and white noise. The temporal change of correlation strength of Markov noise is very similar to the temporal change of integral value of light intensities in gels. $W_1(t)$ corresponds to the temporal change of correlation strength of Markov noise on the surface of gels. In addition, size of periodic structure due to the network is small at large jumping temperature gap and it is compatible with the tendency of phase separation. (Chapter 5)

Part I. PLASMA

All materials are formed by their elements-in-theirselves and the relationship between dynamics of their elements. Their elements are divided into various classes of nature, and there is a spatial especial movement in each class. The schematic diagram of class organization based on a microscope photograph of Amoeba Limax is shown in Figure 1. Increasing the degree of magnification, the class organization of nature was understood from amoeba limax of microscope level, organella of light scattering level, biomembrane and phosphatidyl choline of molecular level, a methylene chain of functional group level, and to wave function of molecular orbital level. In spatial class organization of condensed matters, we can easily understand the class organization of natureit by dividing the classification into six levels (naked eye, microscope, light scattering, molecular, functional group, and molecular orbital levels). The concept of class organization in nature connects with the recent research theme of 'complex system', 'complex fluid', 'supermolecules', 'cluster', etc. It is very important to discuss the fundamental principle of the relationship between each class of nature in order to clarify the mechanism of structural formation processes in condensed matter. Especially it is necessary to discuss from the viewpoint of dynamics in order to understand the following vector development, reaction→ relaxation→transition→structural formation.

For the purpose of discussion about movement of elements in each class, a macromolecule is the best example because a macromolecule has a large number of motional degrees of freedom. The particular motional behaviour of each element is distributed into each class from a macroscopic class to a microscopic one. As its simple example, the schematic diagram of a space-time image of macromolecular dynamics is shown in Figure 2. The horizontal axis is space and the vertical one is relaxation time. There are many movements, for example, two state motions, local motions, segmental motions, cooperative diffusion, repetitive motions and so on.

Till now a new apparatus named PLASMA IV(Perfective Laboratory Automation System for Macromolecular Analysis) have been made in our laboratory from the viewpoint of spectroscopic measurements based on the concept mentioned above[1]. The schematic diagram of PLASMA IV is shown in Figure 3. The purpose of PLASMA is to analyze dynamics in the following 5 classes and the relationship between each motional class,

① Naked eye level (video graphics analysis)
② Microscope level
(graphics analysis of CCD images and spectroscopy using by a microscope)
③ Light scattering level
(two-dimensional static and dynamic light scattering analysis)

④ Molecular level
(various spectroscopic analysis with absorption, action, emission, depolarization spectra, pico- and nanoseconds time-resolved spectroscopic techniques)
⑤ Functional group level (image Raman scope with microscope)
PLASMA is controlled by our original program softs. In this report, we estimate the image of volume phase transition processes of gels more clearly based on naked eye level of PLASMA.

In recent years, many scientific researchers in the field of condensed matter begun to have the interest in various graphical analysis methods. Many biologists have been interested in the observation of livings using various microscopes in order to discuss the function of bio-organ. Students belonging to the faculty of biological and medical sciences have to learn the morphological techniques using various microscopes. On the other hand, some graphical methods were discussed based on fractal analysis in the field of space and earth sciences[2, 3]. They try to estimate the origin of some space phenomena. For example, they discussed the origin of the craters using photographs of the moon's surface. Graphical analysis method will be effective to clarify the origin of morphological phenomena in the field of condensed matter. In recent, many studies for crystal growth processes have been reported using graphical methods based on fractal analysis[4]. Therefore it is very important that various graphical analysis methods apply to the field of condensed matter.

References

1. Ushiki,H., W.Rettig, B.Strehmel, S.Schrader and H.Seifert, Eds. 'Applied Fluorescence in Chemistry Biology and Medicine', Springer, 325-370, 1999
2. A.S.Szalay and D.N.Schramm, Nature, 718(314) 1985
3. H.Mizutani, "Kureita no Kagaku", Tokyo Daigaku Syuppan-kai,Tokyo 1980
4. Brune,H., Romainczyk,C., Roder,H. and Kern,K., Nature, 469(369) 1994

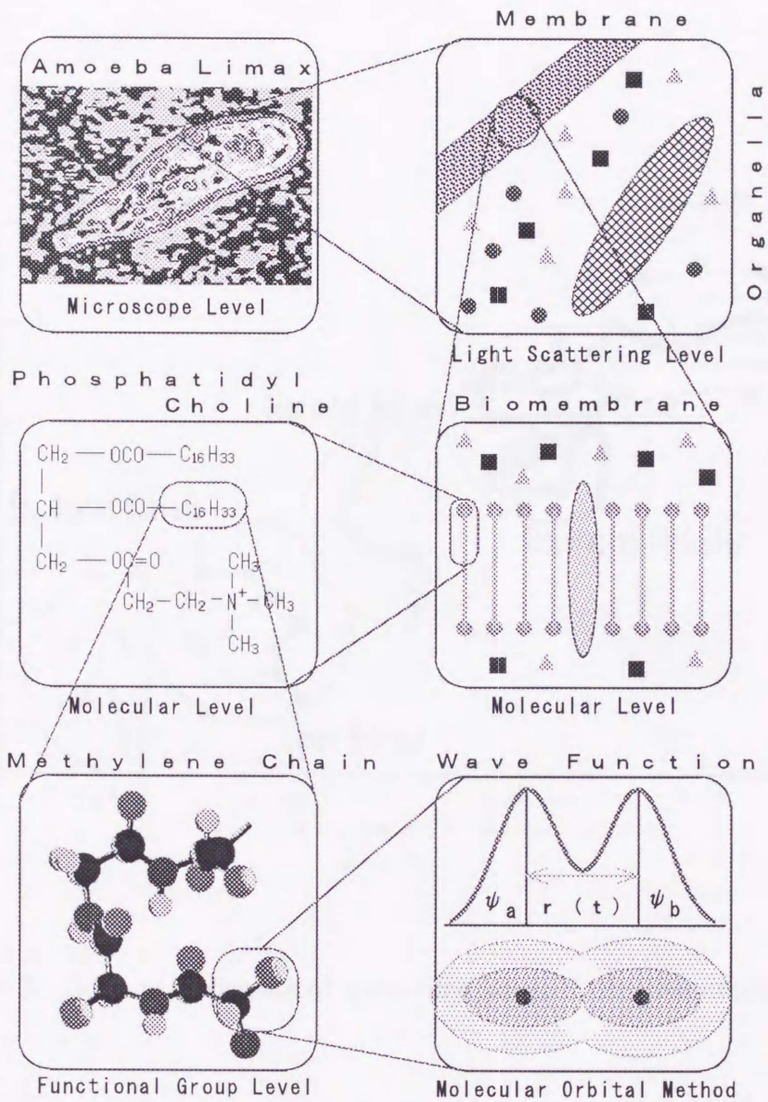

Figure 1. Schematic diagram of class organization in nature

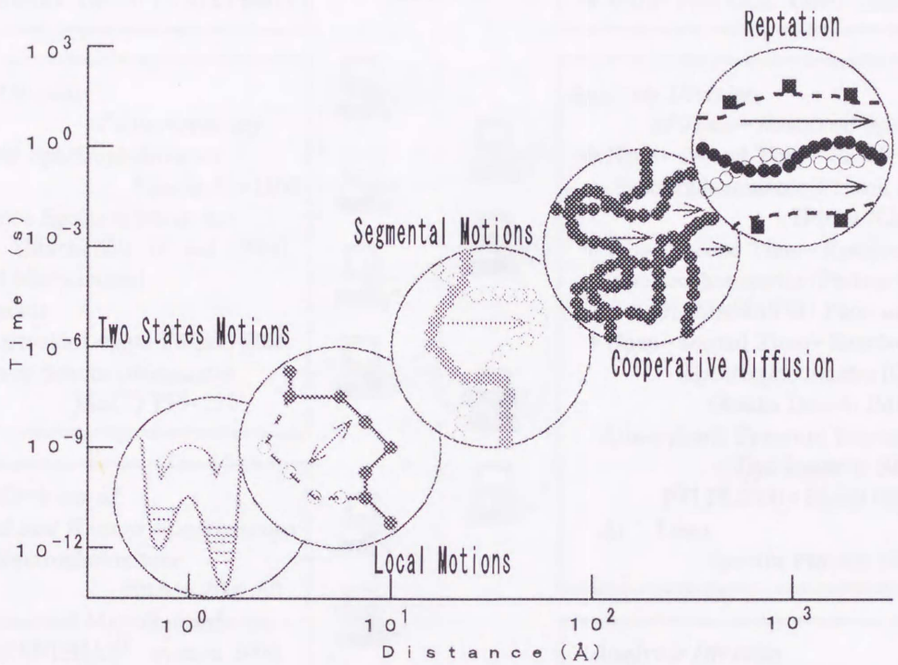

Figure 2. Schematic diagram of space-time image in macromolecules

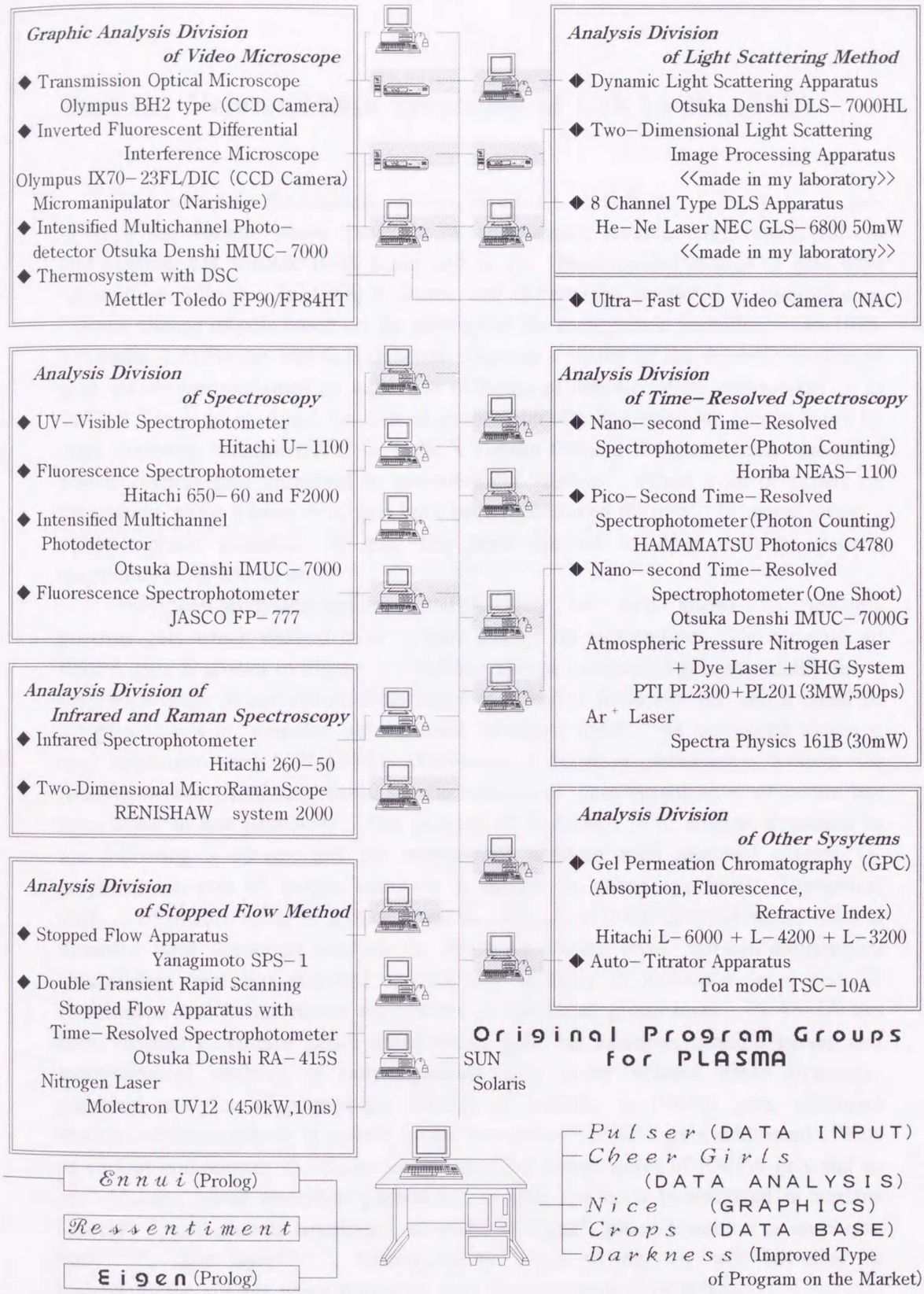

Figure 3. Schematic diagram of PLASMA IV
(Perfective Laboratory Automation System for Macromolecular Analysis IV)

Part II. Volume Phase Transition of Gels by PLASMA

Gels are three dimensional network swollen with solvent. Some polymer gels undergo the volume phase transition by surrounding stimuli, temperature, solvent composition, pH, electric field, stress and so on. Fundamental studies of gels were initiated as follows. In 1968, K.Dusek and D.Patterson predicted a discontinuous volume change of gels based on the analogy of the coil-globule transition[1]. In 1973, T.Tanaka, L.O.Hocker and G.B.Benedek proposed a theory of the dynamic motion of gels, which was explained by collective diffusion of polymer chain and solvent[2]. In 1977, T.Tanak et. al. found the critical phenomena of polyacrylamide gels in water by light scattering experiments[3]. In 1978, T.Tanaka found a distinct volume change of polyacrylamide gels immersed in acetone/water mixture[4]. Then a lot of papers on the volume phase transition of gels have been represented till now. In recent years, volume phase transition of gels has been applied to drug delivery system, micromachining and so on.

Poly(N-isopropylacrylamide) (PNIPA) gels are well known as nonionic polymer gels which show a large volume change by temperature. The structure of PNIPA gels is shown in Figure 1. Volume change process of gels essentially has a very wide range of movements from naked eye level to molecular one and it could be a typical thesis in "complex physics" and "complex fluid". As mentioned above, a new apparatus named PLASMA (Perfective Laboratory Automation System for Macromolecular Analysis) based on the concept of class organization of nature has been made in our laboratory. The purpose of PLASMA is to analyze dynamics in the following 5 classes and the relationship between each motional classes, ① graphical analysis of images using by a camera in naked eye level, ②graphical analysis of images using by a microscope in microscope level, ③two-dimensional and dynamic light scattering analysis in condense matter level, ④multi-dimensional spectroscopy and time-resolved spectroscopy analysis in molecular level and ⑤ two-dimensional image raman microscope in functional group level. PLASMA has been adapted to volume phase transition of gels, for example, titration curves and morphological analysis of polyacrylamide gels under volume phase transition, graphical analysis of permeating process of solvents in PNIPA gels, rotational motions of chromophore in volume phase transition of PNIPA gels, additional effects of various components to volume phase transition temperatures of PNIPA gels and so on. Volume phase transition phenomena of gels has been investigated in various aspects[5, 6], coil-globule transition[7], structure of water[8], phase transition as an elastic body[9, 10], skin layer[11, 12], heterogeneities[13] and so on. It will be clear to understand the volume phase transition from the viewpoint of PLASMA.

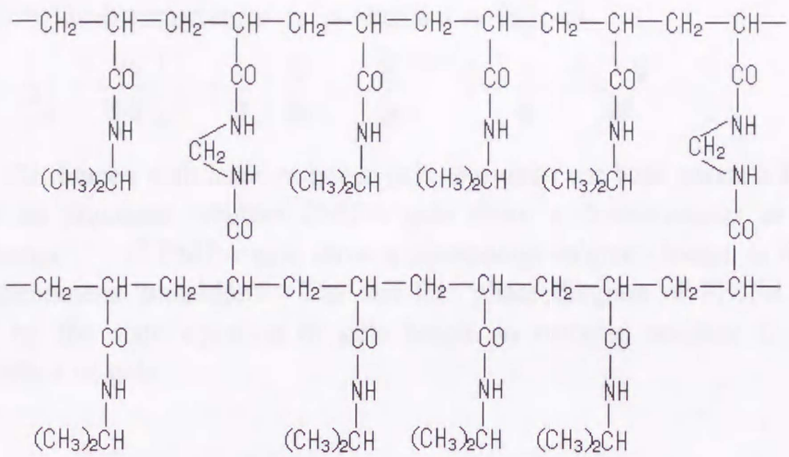

Figure 1. Structure of Poly(N-isopropylacrylamide)

1. Volume Phase Transition of Gels and Osmotic Pressure[6]

Phase diagram of gels has been discussed and the concept of discussion will be shown here. If gels are immersed in solvents, they swell or shrink as shown in Figure 2. It is a different feature from powder or solid. The state of gels is theoretically defined as the infinity of molecular weight by crosslinkage, on the other hand, experimentally defined as the point in which the viscosity diverges in sol-gel transition.

Phase diagram of PNIPA gels is shown in Figure 3. Volume phase transition of gels has been explained using by osmotic pressure. Osmotic pressure of gels π is defined by

$$\Pi = -\left(\frac{\partial F}{\partial V}\right)_T . \qquad (1)$$

where F is free energy change after mixing of solvents and an unstrained polymer network and V is total volume of gels. It is often presented that such expression of phase diagram of gels is similar to that of Van der Waals fluid formally. π consists of $\pi_{elastic}$, π_{mixing} and π_{ion}, which denote the contributions of the elastic free energy, mixing free energy and free energy due to ions, respectively.

$$\Pi = \Pi_{elastic} + \Pi_{imixing} + \Pi_{ion}$$

$$= \upsilon kT\left[\left(\frac{\Phi}{2\Phi_0}\right)-\left(\frac{\Phi}{\Phi_0}\right)^{1/3}\right]-\frac{NkT}{v}\left[\Phi+\ln(1-\Phi)+\chi\Phi^2\right]+\upsilon fkT\left(\frac{\Phi}{\Phi_0}\right) \qquad (2)$$

where ϕ is the volume fractions of polymer network and ϕ_0 is the volume fraction of polymers when the gel network has a random walk configuration. The polymer-solvent interaction parameter χ, the Boltzmann constant k, the Avogadro's number N, the absolute temperature T, the molar volume of the solvent v, the number of counter ions per chain f, and the number of chains per unit volume of gels ν are also used. Phase diagram of gels has been explained as π=0, that is an equilibrium

state. The reduced temperature τ is obtained as follows.

$$\tau \equiv \left(\frac{1}{2}-\chi\right) = \frac{vu}{N\phi^2}\left[\left(f+\frac{1}{2}\right)\left(\frac{\phi}{\phi_0}\right)-\left(\frac{\phi}{\phi_0}\right)^{1/3}\right]-\frac{1}{\phi}-\frac{\ln(1-\phi)}{\phi^2}-\frac{1}{2} \qquad (3)$$

Equation (3) agrees with ionic polymer gels, but does not hold good in PNIPA gels. There is an argument whether PNIPA gels show a discontinuous or continuous volume change[26]. If PNIPA gels show a continuous volume change, is it suitable to call the phenomena 'transition'? The fact that phase diagram of PNIPA gels is not explained by the state equation of gels based on osmotic pressure is due to the elasticity effect of gels

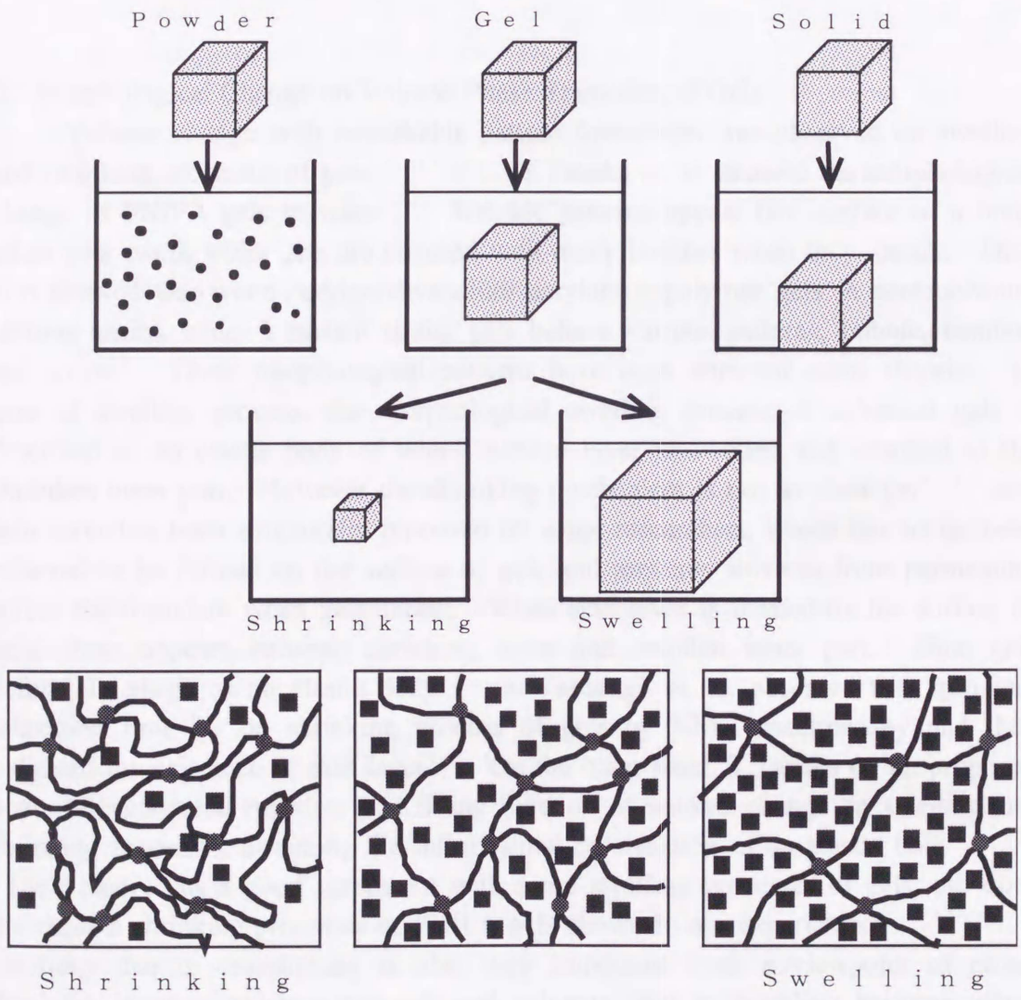

Figure 2. Characteristics of gels

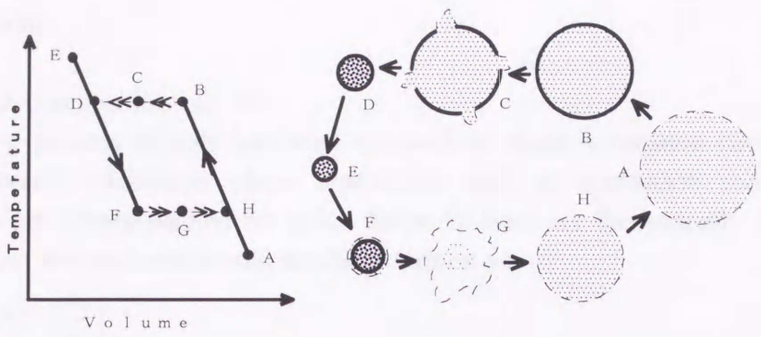

Figure 3. Morphological change of PNIPA gels on swelling and shrinking processes after temperature quench and jump, respectively. Gels are described on the concept of 'skin layer' as one of the elastic effects.

2. Morphological Change on Volume Phase Transition of Gels

Volume change with remarkable pattern formations was observed on swelling and shrinking processes of gels[11, 17-20]. T.Tanaka et. al. showed the morphological change of PNIPA gels in water[12]. Wrinkle patterns appear like surface of a brain when gels swell, while gels are covered with many bubbles when they shrink. They also showed that when acrylamide/sodium acrylate copolymer gels in acetone/water mixture shrink under a certain strain, gels behave various patterns, bubble, bamboo and so on[7]. These morphological patterns have been attracted many theorist. In case of swelling process, the morphological swelling process of spherical gels is described as an elastic body of which surface layer is swollen and attached to the shrunken inner part. However the shrinking mechanism is not so clear yet[6, 21] and skin layer has been structurally proposed by some researchers, which has so far been believed to be formed on the surface of gels and prevents solvents from permeating across the boundary when gels shrink. When skin layer is formed on the surface of gels, shear appears between shrinking layer and swollen inner part. Then gels deform its shape as an elastic body[13]. H.Yasunaga et. al. observed two spin-spin relaxation time T_2 on shrinking process of gels by NMR spectroscopy and they indicated the existence of skin layer[14]. On the other hand, T.Tanaka et. al. proposed a single exponential function as a fitting function of volume change on swelling and shrinking processes, assuming the infinitesimal deformation of an elastic body[22, 23]. Their theory has a good agreement with some swelling processes of gels, but does not explain shrinking processes of PNIPA gels shown in our experiments[12, 15-19]. Elasticity due to crosslinking is also very important from a viewpoint of phase demixing between polymer network and solvents, that is, coupling between phase transition and elasticity[6] is an essential concept for shrinking process of gels. Dynamics of gels are expected as combined effects of thermodynamic instability and nonlinear elasticity. H.Tanaka has studied asymmetric molecular dynamics in polymer solution[16], considering volume phase transition phenomena of gels as an

expanded problem.

3. Spinodal Decomposition of Gels

Shrinking process of gels has been assumed as phase separation between gels chain and solvents. However phase separations such as nucleation and spinodal decomposition are poorly studied for gels. Spinodal lines are theoretically defined as K=0, where K is the isothermal bulk modulus written as

$$K = -V\left(\frac{\partial \Pi}{\partial V}\right)_T . \qquad (4)$$

Spinodal lines are also defined as that longitudinal density fluctuation diverges at $K+4/3\,\mu = 0$, where μ is shear modulus[6].

Let us consider whitening process of gels on volume phase transition. It is well known that PNIPA gels shrink and become white just after temperature jump above critical temperature. Then the whitening slowly disappears. The whitening of gels has so far been believed as fluctuations accompanied with phase separation between polymer chain and solvents. Y.Li et al. showed that early shrinking process of PNIPA gels could correspond to spinodal decomposition from temporal turbidity change of gels[30] using by mean-field linear Cahn-Hillard-Cook (CHC) theory[32]. According to the theory, the scattered light intensity I_s is related to the fluctuation growth rate $R(q)$ as follows,

$$I_s(q,t) \sim \exp(2R(q)t) , \qquad (5)$$

where q is the scattering wavevector and t is time. R.Bansil et al. showed the spinodal ring by two-dimensional light scattering of PNIPA gels and also described the time evolution of the scattered light in the early shrinking stage by the linear CHC theory[31]. Both groups didn't observe the disappearance of whitening and the connection with phase diagram is not clear. Increasing and decreasing of scattering light was also observed on phase separating process of polymer solution, but scattering light has been usually studied from the viewpoint of q, not t[33-34]. Determination of spinodal line of gels was discussed with the structure factor by T.Tanaka and A.Onuki[6].

4. Studies on Gels by PLASMA

4-1. Additional effects of various metal ions to volume phase transition temperatures of PNIPA gels[35]

PNIPA is soluble in water and has phase diagram which shows the LCST (lower critical solution temperature). It is said to be due to the hydrophobic effects. Coil-globule transition and additional effects of surfactants have been researched recently. Interaction between water molecules and N-isopropyl groups can be assumed to be sensitive to addition of various compounds, temperature and so on. The dependence of added metal ion on volume phase transition temperature of PNIPA gels was discussed as follows.

The aqueous solutions with PNIPA gels were prepared by the addition of 20

sorts of nitrate salt. The dependence of added alkali metal ion on volume phase transition temperature (Tc) is shown in Figure 4. Tc decreases with an increase in concentration of any metal ion. This phenomena can be explained by the following theory based on the statistical mechanics model which is developed from Ising model, not the equation of state method using osmotic pressure mentioned above.

〈Statistical mechanics model〉

1. Assuming Ising model based on cells of gels, total number of cells N is represented as follows.

$$N = N_c + N_v \tag{6}$$

where N_c and N_v are the number of cells which have water clusters and are vacant, respectively.

2. Free energy of gels is explained as follows,

$$G_{network}(T, N_v) = N_v(\varepsilon + \alpha T) \tag{7}$$

where ε and α are enthalpy and entropy changes in a cell by discharging water cluster, respectively.

3. Free energy of Ising model is explained as follows,

$$G_{ising}(T, N_V) = \frac{N_C N_V z J}{N} - kT \ln\left(\frac{N!}{N_C!\, N_V!}\right) \tag{8}$$

where z and J are the neighboring number between cell clusters and interaction coefficient of Ising model, respectively.

Introducing the state variable $X=(N_C-N_V)/N$, total free energy of gels is explained as

$$G(T,N_V) = N\left[\frac{(\varepsilon+\alpha T)(1-X)}{2} + \frac{zJ(1-X^2)}{4} + kT\left(\frac{1+X}{2}\right)\ln\left(\frac{1+X}{2}\right) + \left(\frac{1-X}{2}\right)\ln\left(\frac{1-X}{2}\right)\right] \tag{9}$$

Equation (7) is trasfered to equation (8) for the temperature at which the probability of existence shows to be highest. Consequently the critical temperature Tc of volume phase transition of PNIPA gels is written as

$$T = 2\frac{273.15 + T_0}{2 - z\ln(1-\eta[M^{n+}])} - 273.15 \tag{10}$$

where T_0 is the critical temperature of PNIPA gels in water and $a(=1-\eta[M^{n+}])$ is chemical activity coefficient. Curve fittings for concentration of various metal ion vs Tc are shown in Figure 5. Our obtained plotted curves about univalent, divalent and trivalent metals agree with equation (8) very well. Relationship between surface charge density of metal ions ρ $(=n/4\pi r^2)$ and hydrated force η value are shown in Figure 6. The hydrating effect of metal ions is given a master curve based on ρ. It can be assumed that metal ions attract water molecules and an decrease in chemical activity coefficient affect the critical temperature of PNIPA gels. Our proposed theoretical model is very effective in order to analyze not only added effect of metal ion but also that of hydrated organic compounds and polymers such as various alcoholic group and Polyethyleneoxide (PEO) and so on. Phase diagram of PNIPA in water/PEO mixtures is shown in Figure 11 and equation (8) holds good. If $1<\eta[M^{n+}]$, T divergent $-\infty$ in equation (8). It indicates that there is no critical temperature in the region of $[M^{n+}]>1/\eta$ and it is. The drastic change of solution

nature is induced over $\eta C=1$ where C is the concentration of PEO as shown in Figure 7. This phenomenon was named 'Hydrating-induced solution transition'. PNIPA gels are very sensitive to environment mentioned above and it will be due to week interaction between polymer chains and water molecules.

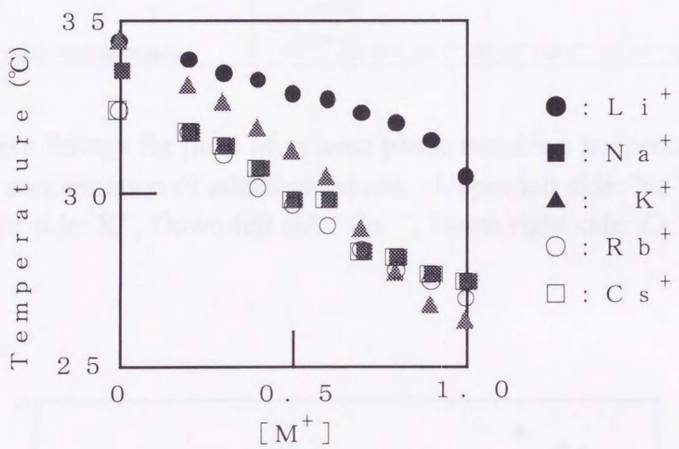

Figure 4. Relationship between volume phase transition temperature and molar concentration of added metal ion

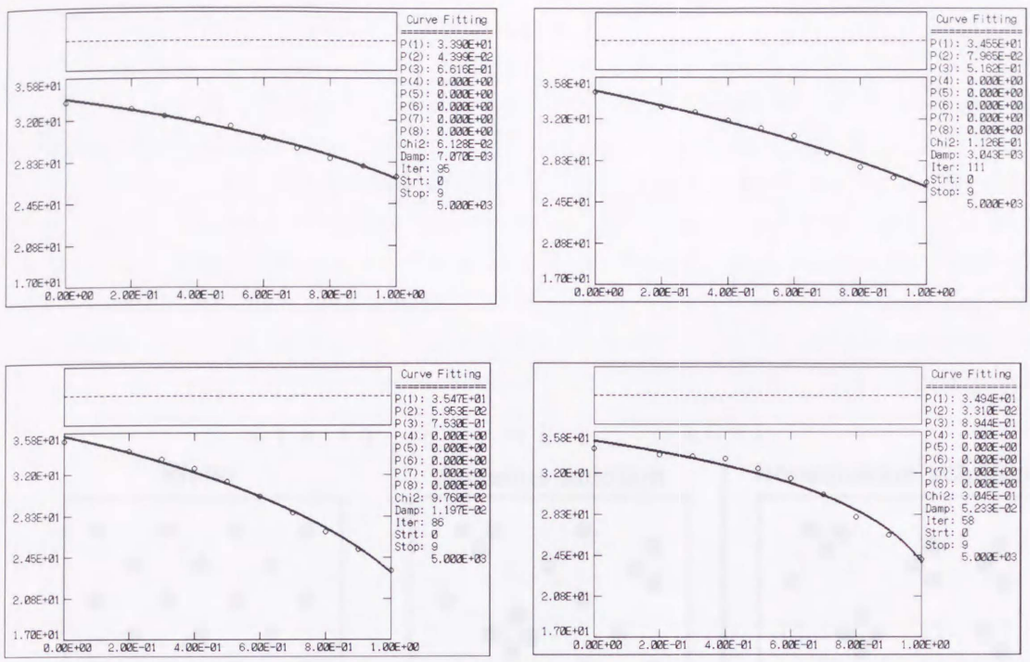

Figure 5. Curve fittings for plots of volume phase transition temperature vs. molar concentration of added metal ion. Upper-left side: Na^{+}, Upper-right side: K^{+}, Down-left side: Ca^{2+}, Down-right side: Cr^{3+}

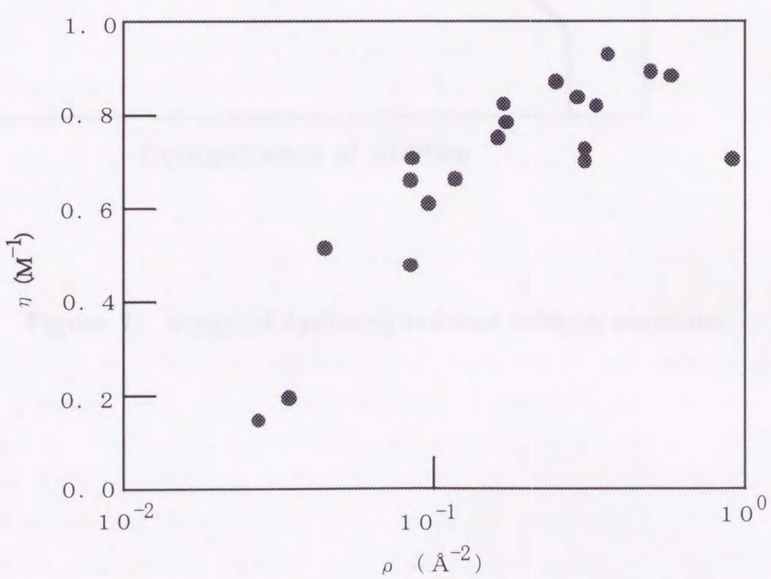

Figure 6. Relationship between surface charge density of metal ions ρ $(=n/4\pi r^2)$ and hydrated force η value

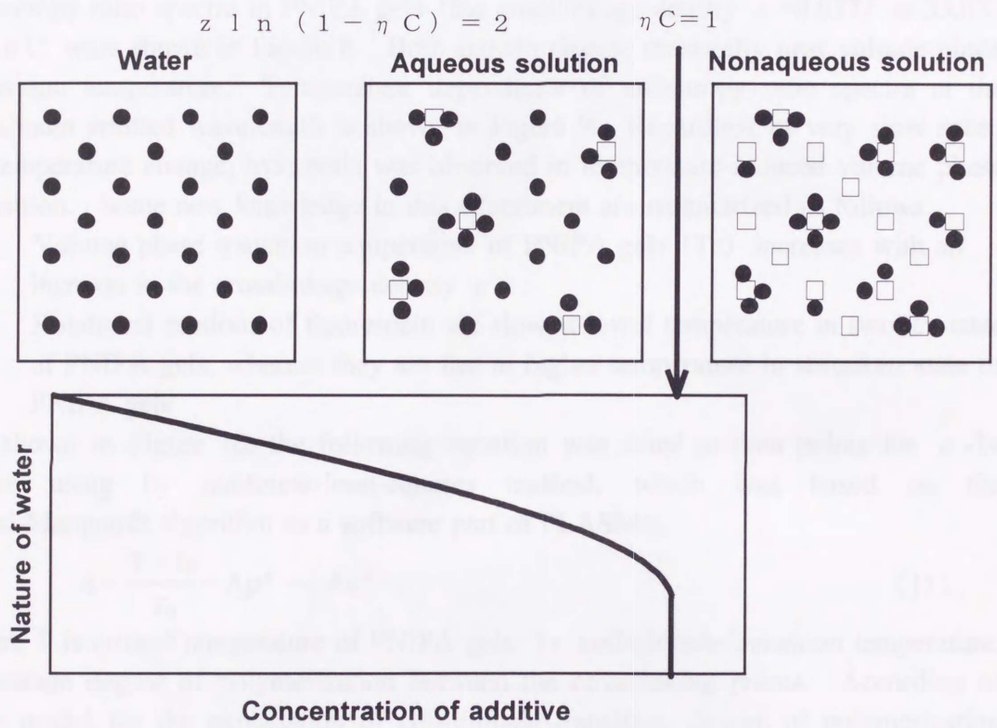

Figure 7. Image of hydrating-induced solution transition

4-2. Volume Phase Transition in Molecular Level[35]

Dynamics of volume phase transition of gels in microscopic level has been discussed using by light scattering method, NMR spectroscopy and so on. According to fluorescence probe method which is effective to discuss dynamics in micro level, it is reported that molecular motions drastically change near the volume phase transition point of gels. In order to clarify volume phase transition of gels in microscopic level, spectrosopy measurements of fluorescence in PNIPA gels were done near the volume phase transition temperature. PNIPA gels were prepared in a thin cell with fluoresceine aqueous solution. The cooling or heating rate of sample solution was 0.3mK/s and one spectrum was measured per about 16ms. The emission and anisotropy ratio spectra in PNIPA gels (the crosslinkage density ρ =0.037) at 33.0℃ -39.0℃ were shown in Figure 8. Both spectra change drastically near volume phase transition temperature. Temperature dependence of anisotropy ratio spectra at the maximum emitted wavelength is shown in Figure 9. Regardless of very slow speed of temperature change, hysteresis was observed in temperature-induced volume phase transition. Some new knowledge in this experiment are summarized as follows

1. Volume phase transition temperature of PNIPA gels (Tc) increases with an increase in the crosslinkage density ρ.
2. Rotational motions of fluorescein are slow at lower temperature in swollen state of PNIPA gels, whereas they are fast at higher temperature in shrunken state of PNIPA gels.

As shown in Figure 10, the following equation was fitted to data points for ρ -Tc curve using by nonlinear-least-squares method, which was based on the quasi-Marquardt algorithm as a software part of PLASMA.

$$\varepsilon = \frac{T - T_0}{T_0} = A\rho^{\beta} \sim An^{-\beta} \qquad (11)$$

where T is critical temperature of PNIPA gels, T_0 coil-globule transition temperature, n average degree of polymerization between the crosslinking points. According to blob model for the explanation of coil-globule transition, degree of polymerization dependence on crossover temperature in scaling law of polymer chain is represented as follows.

$$\tau = \frac{1 - \theta}{T} \sim n^{-1/2} \qquad (12)$$

From the viewpoint of molecular level, volume phase transition phenomena of PNIPA gels can be assumed to be assembled coil-globule transition phenomena of polymer chains which have various degree of polymerization between the crosslinking points. On the other hand, the fact that rotational motion of fluorecein is slower in swollen state than shrunken one does not coincide with the motional behaviour of PNIPA side-chains near coil-globule transition. PNIPA gels soak up a lot of water in swollen state, so water solvents may make some structure in gels as shown in Figure 11. If the image is correct, it is concluded that diffusion rate of water solvents are slower in swollen state than in shrunken state in case of PNIPA gels.

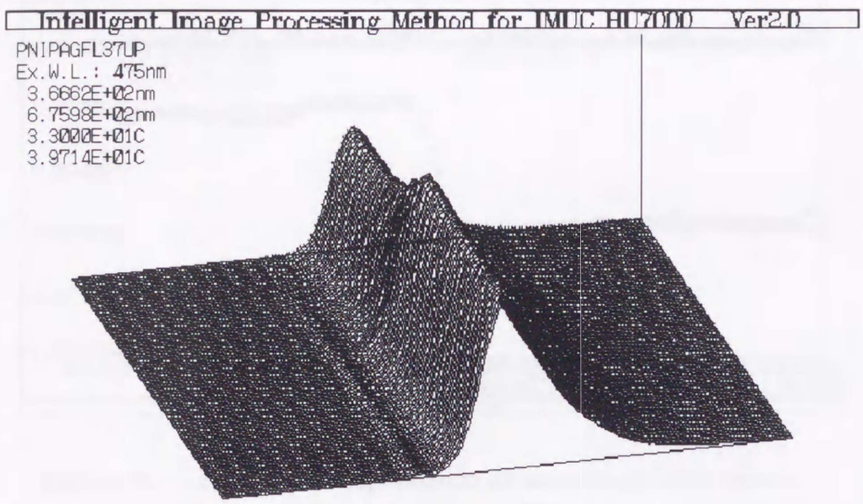

(a)

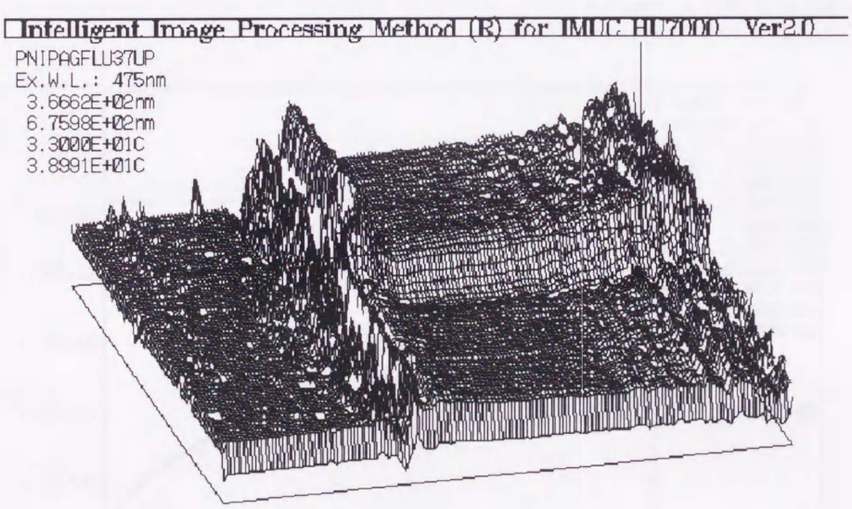

(b)

Figure 8. Emission and anisotropy ratio spectra in PNIPA gels
(a) Emission spectra (b) Anisotropy ratio spectra

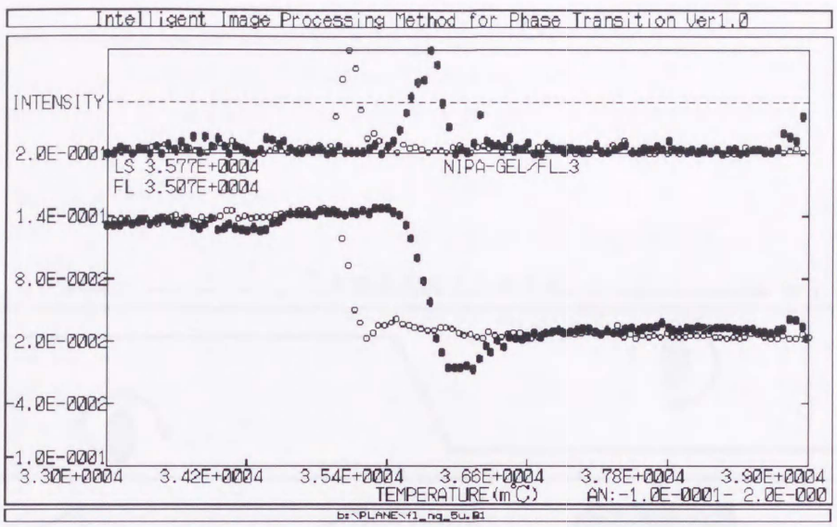

Figure 9. Temperature dependence of anisotropy ratio spectra on heating (●) and cooling (○) processes

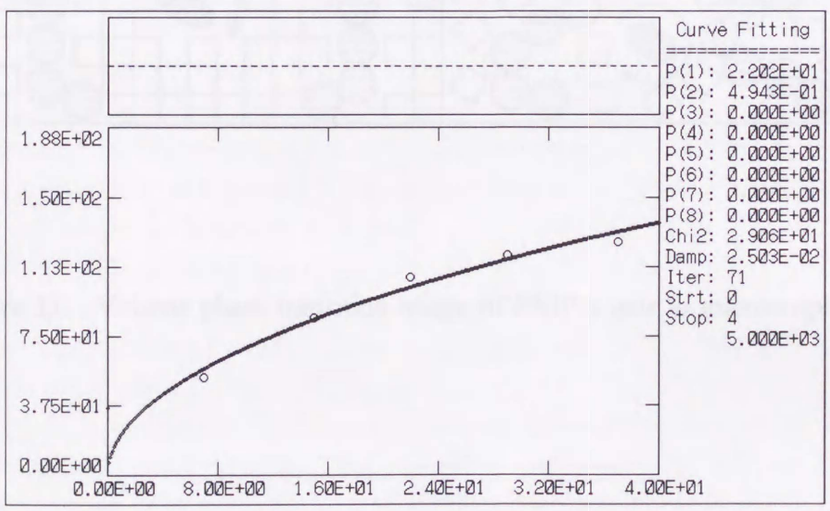

Figure 10. Plots of anisotropy ratio against crosslinkage density and curve fitting of equation (11) to the plot data

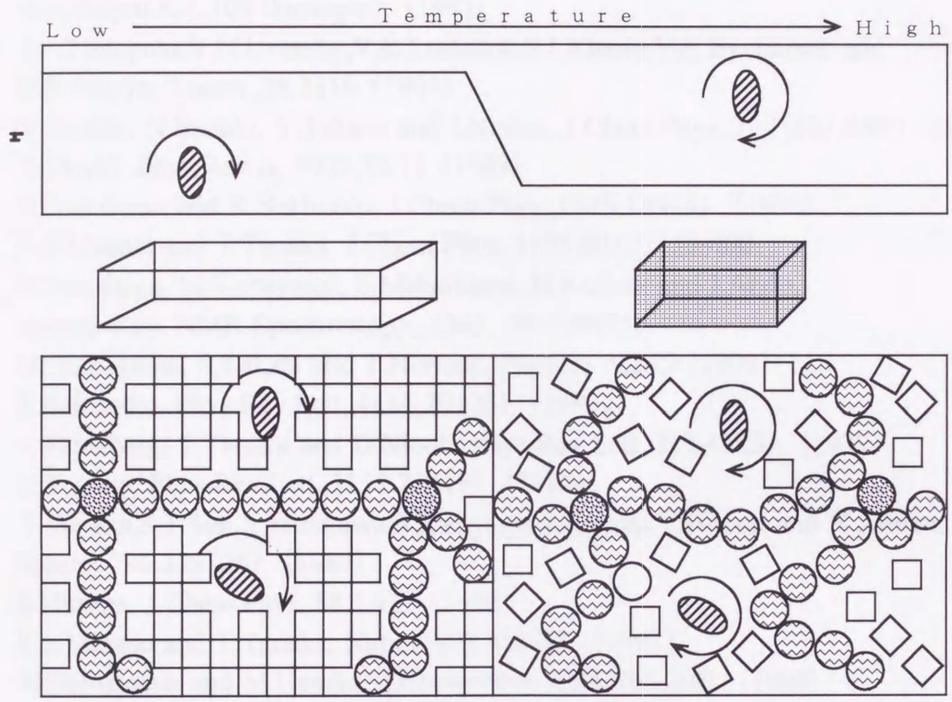

Figure 11. Volume phase transition image of PNIPA gels in microscopic level

References

1. K.Dusek and D.Patterson, J.Polym.Sci.,A-2,1217 (1968)
2. T.Tanaka, L.O.Hocker and G.B.Benedek, J.Chem.Phys.,59,9,5151 (1973)
3. T.Tanaka, S.Ishiwata and C.Ishimoto, Phys.Rev.Lett.,38,14,771 (1977)
4. T.Tanaka, Phys.Rev.Lett.,40,820 (1978)
5. H.G.Schild, Prog.Polym.Sci.,(17),163 (1992)
6. K.Dusek (Editor), Responsive Gels: Volume phase transitions I, Adv.Polym.Sci.,109 (Springer) (1993)
7. E.I.Tiktopulo,V.N.Uversky,V.B.Lushchik,S.I.Klenin,V.E.Bychkova and O.B.Ptitsyn, Macro.,28,7519 (1995)
8. Y.Suzuki, N.Suzuki, Y.Takasu and I.Nishio, J.Chem.Phys.,107(15),5890 (1997)
9. A.Onuki, Phys.Rev.A, 5932,39,11 (1989)
10. H.Nakazawa and K.Sekimoto, J.Chem.Phys.,1675,104(4) (1996)
11. E.S.Matsuo and T.Tanaka, J.Chem.Phys.,1695,89(3) (1988)
12. H.Yasunaga, M.Kobayashi, S.Matsukawa, H.Kurosu and I.Ando, Annual Rep. NMR Spectroscopy, (34), 39 (1997)
13. M.Shibayama, S.Takata and T.Norisue, Physica A,245 (1998)
14. K.Sekimoto, Phys.Rev.Lett.,4154,70(26) (1993)
15. A.Hochberg, T.Tanaka and D.Nicoli, Phys.Rev.Lett.,217,43(3) (1979)
16. H.Tanaka, Phys.Rev.Lett.,3158,71(19) (1993)
17. T.Tanaka,S.T.Sun,Y.Hirokawa,S.Katayama,J.Kucera,Y.Hirose and T.Amiya, Nature,,796,325(26) (1987)
18. S.Hirotsu, J.Chem.Phys.,88,1,427 (1988)
19. E.S.Matsuo and T.Tanaka, Nature,482,358(6) (1992)
20. M.Shibayama and M.Uesaka, J.Chem.Phys.,4350,105(10) (1996)
21. B.Barriere, K.Sekimoto and L.Leibler, J.Chem.Phys.,1735,105(4) (1996) K.Sekimoto,N,Suematsu and K.Kawasaki, Phys.Rev.A,39(9),4912 (1989)
22. T.Tanaka and D.J.Fillmore, J.Chem.Phys.,1214,70(3) (1979)
23. Y.Li and T.Tanaka, J.Chem.Phys.,1365,92(2) (1990)
24. Y.Hirokawa and T.Tanaka, J.Chem.Phys.,6379,81(12) (1984)
25. S.Hirotsu, Y.Hirokawa and T.Tanaka, J.Chem.Phys.,87(2) (1987)
26. C.Wu and S.Zhou, Macro.,30,574 (1997)
27. H.Ushiki, F.Tsunomori, K.Hamano, Rep.Prog.Polym.Phys.,Jpn.,37,463 (1994)
28. T.Nakagawa and Y.Oyanagi, "Saishou Nijou-hou Niyoru Jikken-Data Kaiseki", Tokyo Daigaku Syuppan-kai,Tokyo (1982)
29. "Koubunshi Kagaku no kiso" (2nd edition), Tokyo kagakudoujin (1994)
30. Y.Li, G.Wang and Z.Hu, Macromolecules, 4194,28 (1995)
31. R.Bansil, G.Liao and P.Falus, Physica A, 346, 231 (1996)
32. J.W.Cahn and J.E.Hilliard, J.Chem.Phy., 688,31(3) (1959); J.W.Cahn, J.Chem.Phy., 93,42(1) (1965)
33. H.Furukawa, Adv.Phys., 703, 34(6) (1986)

34. A.T.Bharucha-Reid, "Elements of the Theory of Markov Processes and their Applications", McGraw-Hill, New York (1960)
35. H.Ushiki and C.Hashimoto, Polym.Proc., 46, 273 (1997)

Graphical Analysis for Gels Morphology

Chapter 1. Shrinking Pocess

1-1. Shrinking Process of PNIPA Gels

1-1-1. Abstract

A new graphical analysis method is proposed for measurement of gels morphology on volume phase transition. Poly(N-isopropylacrylamide) (PNIPA) gels shrink and become white after jumping above the critical temperature. Whitening slowly disappears and the gels become finally transparent. This final stage is regarded as the equilibrium state. The shrinking and whitening of disk-like PNIPA gels have been monitored using a CCD video camera, and both area and whitening of the gels have been evaluated from time-resolved images using a new graphical analysis method. We showed that gels underwent a two-step shrinking in synchronism with the whitening process. To fit the time-dependent shrinking process, the sum of exponential and stretched exponential functions was adequate using the 'χ^2 map method'. The exponent characterizing the stretched exponential was found to be greater than one. The meaning of fitting parameters is determined on the assumption that the skin layer collapses in the second shrinkage.

1-1-2. Introduction

Some polymer gels show large discontinuous volume change upon change of temperature[1], solvent composition[2, 3, 4], pH[5], electric field[6], stress[7] ... Considerable interest has been devoted to this phase transition that has been explained from various point of view : considering gels as an elastic body[8, 9], using phase transition formation[10], heterogeneities[11], assuming coil-globule transition[12], or structure of water[13] .... There is little discussion about dynamics on volume phase transition of gels from the viewpoint of macroscopic level. As one of interesting dynamical phenomena, various morphological patterns were observed when gels swell/shrink. In the case of PNIPA gels in water, wrinkle patterns appear when gels swell, while gels are covered with many bubbles when they shrink[1]. When acrylamide/sodium acrylate copolymer gels in acetone/water mixture shrank under a certain strain, various patterns were observed such as bubble, bamboo and so on[3]. These patterns have attracted theorists and have been explained by considering the gels as elastic bodies. Sekimoto et al discuss the deformation of gels by taking account of 'Skin layer'[9], structurally proposed as a shrunken layer formed on the surface of gels when gels shrink. They showed that the skin layer is useful to explain various morphological changes when gels shrink. Shrinking accompanying bubble formation of cylindrical PNIPA gels was recently reported by Shibayama et al [14] who showed that the actual observation is very complex. The mechanism is not

so clear on shrinking process yet.

Tanaka et al. propose a single exponential function to fit the volume change during the swelling and shrinking processes, assuming infinitesimal deformation of an elastic body[14]. Their theory is in good agreement with some swelling processes of gels, but cannot explain the two-step shrinking of PNIPA gels[1, 15-21]. Tanaka et al. showed the two-step shrinking of spherical PNIPA gels and interpret the cause of two-step shrinking by assuming skin layer, which prevents solvents from permeating across the boundary[1]. Tomari et al. thermodynamically showed the possibility of two-step swelling/shrinking on the assumption of skin layer[21]. Using NMR spectroscopy, Yasunaga et al. observed two spin-spin relaxation time T_2 on shrinking process of PNIPA gels and reported the existence of skin layer[22]. The question of the relationship between the skin layer and the origin of the two-step shrinking process still remains.

PNIPA gels are nonionic polymers showing a large volume change by changing temperature[1]. Just after above the critical temperature, gels shrink and become white. The whitening slowly disappears and the gels become finally transparent. This final state is regarded as the equilibrium state. In this report, the mechanism of the phase transition is discussed based on phenomenological kinetic analysis using graphic images.

1-1-3. Experimantal

1) Sample Preparation

N-isopropylacrylamide (NIPA; monomer) was obtained from Kohjin Chem. Co. and recrystallized in a benzene/n-hexane mixture. N,N'-methylenebisacrylamide (BIS; cross-linker), ammonium persulfate (APS; initiator), N,N,N',N'-tetramethylethylenediamine (TEMED; accelerator) were purchased from Wako Co. and used without further purification. Aqueous solution of NIPA (655mM), BIS, TEMED and APS was polymerized between glass plates with a spacer; thickness was about 0.3 mm. It was undisturbed at 20°C for one day. The synthesized sheet-like gels were taken from the glass plates and washed several times with a large amount of distilled water for about a week. Disk-like gels were prepared by cutting the sheet-like gels with a cookie cutter. The sample was put into a 2.0mm thickness cell filled with distilled water, as shown in Figure 1. The cell was sealed with epoxy resin. The critical temperature (T_c) was close to 34.1°C based on cloud point measurement. Gel diameter was about 28.0 mm at about 20.9°C and is plotted against temperature in Figure 2. The diameters ratio $d_{34.1°C}/d_{20.9°C}$ was 0.32, where d and suffix are the diameter of the gel and observed temperature, respectively. Crosslinkage density of the gel is given by $2N_c/(N_c+N_m)$, where N_c and N_m are molar concentrations of cross-linker and monomer, respectively, and was obtained 8.8×10^{-3} in this study.

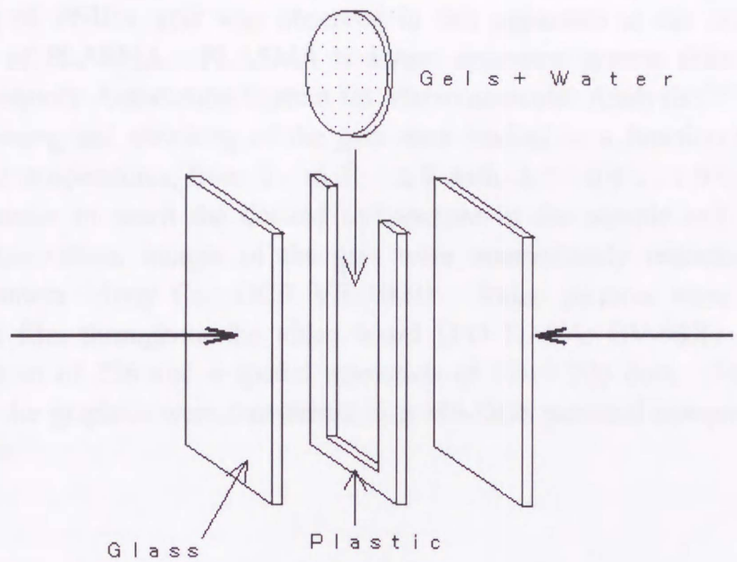

Figure 1. Sample cell for volume phase transition measurement of PNIPA gels

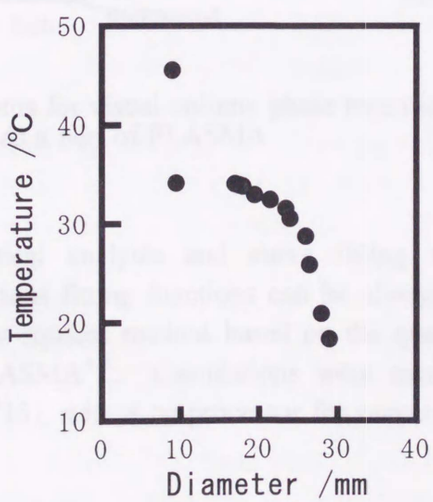

Figure 2. Diameter of disk-like PNIPA gel as a function of temperature.

2) Experimental Procedure

As shown in Figure 3, the sample cell was immersed in a thermostated water bath at $\pm 0.02^{\circ}C$. The sample gels are lighted from above by a white light source. The shrinking of PNIPA gels was observed in this apparatus at the macroscopic level as a part of PLASMA. PLASMA is a new apparatus system abbreviation at "Perfective Laboratory Automation System for Macromolecular Analysis"[23].

The whitening and shrinking of the gels were studied as a function of time at various constant temperatures, from T_c to $T_c+\Delta T$ with ΔT= 0.4°C, 1.0°C, 3.0°C. It took 2-3 minutes to reach the desired temperature in the sample cell. Besides direct visual observation, images of the gels were intermittently recorded using a digital video camera (Sony Co.: DCR VX-1000). Video pictures were converted into RGB form files throughout the video board (I·O DATA: GV-98X) at a light intensity resolution of 256 and a spatial resolution of 320×200 dots. From the G (green) plane, the graphics were transferred to a MS-DOS personal computer by our original software[24].

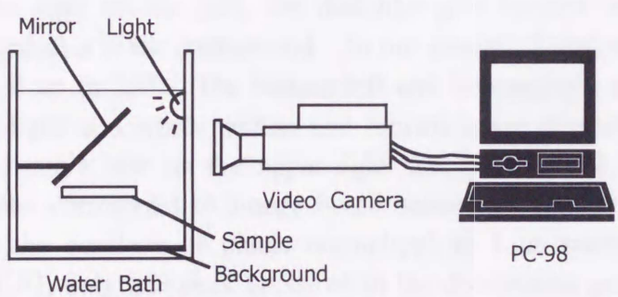

Figure 3. Apparatus for visual volume phase transition measurement of gels as a part of PLASMA.

Programs for graphical analysis and curve fitting were made by Turbo PASCAL (Borland). Various fitting functions can be always estimated for all data curves using nonlinear-least-squares method based on the quasi-Marquardt algorithm as a software part of PLASMA[25]. Calculations were carried out on a personal computer (NEC:PC-9821V13) with a co-processor for numerical calculations (Intel: 8087/80287).

1-1-4. Results and Discussions

1) Visual Observation

Typical shrinking of disk-like PNIPA gels was observed visually as follows. PNIPA gels are transparent and adhere to the fingers at 20°C before shrinking. When the gels are immersed in a water bath above T_c+0.4°C, they first shrink

monotonically. If lighted from above by a white light source (Fig. 3), they become bluish white due to intense multiple scattering. Bluish white gels are less adhesive than transparent ones, gels stop shrinking for a while. During this first step, and the gels become bluish white, because if the gels are taken from the water at that point and poured into cold water, then become transparent from the outside with bluish white core. While the bluish white gels stop shrinking, some white points appear in the gels and the edges of the disk-like gels become white. Many bubbles and shrinking appear. The disk-like gels shrink abruptly again with deformation. Gel shape is restored after shrinking and whitening begins to disappear slowly. The gels show white and transparent spots randomly. With time the white spots slowly disappear and finally the gels become completely transparent.

2) Graphical Analysis Method for Volume Phase Transition of Gels

Graphical analysis diagrams for disk-like gels at the initial and final stages on shrinking are shown in Figure 4(a) and (b), respectively. Since PNIPA gels are transparent at first, we cannot get images of disk-like gels clearly using a video camera. So a white plastic disk was used to estimate the initial gel size. On increasing scattered light on the gels, the disk-like gels become white and can be observed clearly against a black background. In our graphical analysis, the resolution of light was from 0 up to 255. The bottom-left and bottom-right side graphs show the distribution of light in a whole picture and limited space of a whole picture, that is, within a closed curve line on the upper-right side of Figure 4. The horizontal axes of these graphs correspond to image board sensitivity from 0 to 255, and the vertical axes give the numbers of pixels normalized to 1 at maximum value. As shown in Figure 4(b), only one peak appeared in the distribution graph when PNIPA gels became finally transparent. The intensity background was not zero. As shown in Figure(4), there are two peaks when the gels are white. The first peak with lower intensity is mainly attributed to light distribution of the background, while the second peak with higher intensity is due to whitenings. Maximum intensity of the scattered light against a perfectly transparent sample corresponds to 63, shown as the vertical dotted line in bottom graphs. Therefore a clipping procedure has to be used to process the image : we count 0 if intensity of a pixel is less or equal to 63 (background) and 1 if comprised of 64 and 255 (gels). Using such a procedure, we obtain black and white images of the disk-like gels as shown on the upper-right side of Figure 4. Note the presence on the same side in Figure 4 of a second gel sample of smaller size which can be studied in the same time. Sometimes some noise occurs in the area uncovered by the gels, leading to pixel intensity greater than 63. To remove these pixels, we consider only lightened pixels inside a given domain drawn around the shrunken gels, that is, the area surrounded by a closed curve on the upper-right side of Figure 4. Here we introduce typical parameters $S(t)$, $W_1(t)$ and $W_2(t)$ transferred from the monitored graphical image. The number of black dots within the closed curve line defines the area of a gel $S(t)$, normalized to 1 at the

initial value of area obtained using a white plastic disk of size the same as before shrinking. The integral value of the second peak area on the bottom-right side is the area of whitening gels $W_1(t)$, normalized to 1 at maximum value. $W_2(t)$ is introduced as whitening per area of gel $W_1(t)/S(t)$, normalized to 1 at maximum value. The shrinking of volume phase transition of PNIPA gels will be discussed based on $S(t)$, $W_1(t)$ and $W_2(t)$.

Besides clipping, upper-left side shows contour maps of light based on the following. We count light intensity difference between neighboring pixels and put black dots by clipping. Light intensity suddenly changes around the black spots.

Temporal change in the clipping images of PNIPA gels and distribution after temperature jump is shown in Figure 5. The black domain due to whitening of gels becomes gradually smaller with time. As shown in Figure 5-(g), the gels are spotted with black and white, indicating that gels are randomly spotted with white and transparent parts when whitening disappears. When the gels become finally transparent, black domains disappear completely as shown in Figure 5-(h). The second peak due to whitening on the right side, shifts to higher intensity with time. The peak shifts back to lower intensity and finally disappears in Figure 5-(h).

Plots of $S(t)$ (●), $W_1(t)$ (□) and $W_2(t)$ (○) as a function of time and at various ΔT are shown in Figure 6. $S(t)$ first decreases monotonically and remains constant for a while, then decreases and approaches a certain constant value. In Figure 6-(b), the two-step shrinking is clearly observed in temperature-induced volume phase transition of PNIPA gels. Since disk-like gels have anisotropic shape and show large deformation buckling was suppressed by putting sample gels between glass plates. The two-step shrinking of gels has so far been measured by diameter change of spherical and cylindrical gels[1, 13-15] at 200 to 600 μm in the swollen state. This study shows that the two-step shrinking has no relation to the gel deformation.

As shown on Figure 6, $W_1(t)$ and $W_2(t)$ first increase sharply and decrease gradually, reaching 0 at the final stage. The time at which $S(t)$ reaches a minimum corresponds to the time at which $W_2(t)$ is a maximum. The time of $W_2(t)$ is synchronized with that of $S(t)$ for different ΔT.

The sample gels sometimes stuck to glass plates, and probably due to the adhesiveness of transparent PNIPA gels. In most cases, these gels did not shrink and never became white. If the fixed part was taken off, it started to shrink and be white. This indicates that gels will not be white without shrinking. Synchronism between $S(t)$ and $W_2(t)$ shows shrinking of PNIPA gels strongly related to whitening.

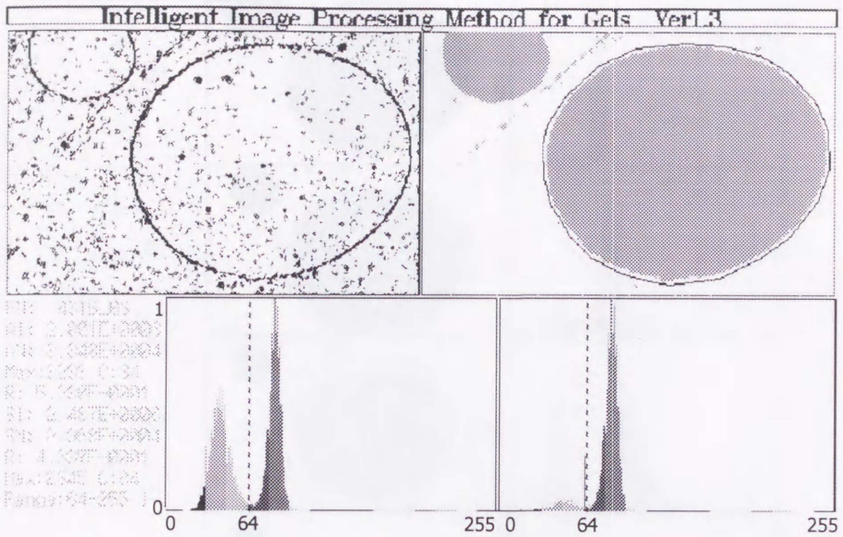

(a)

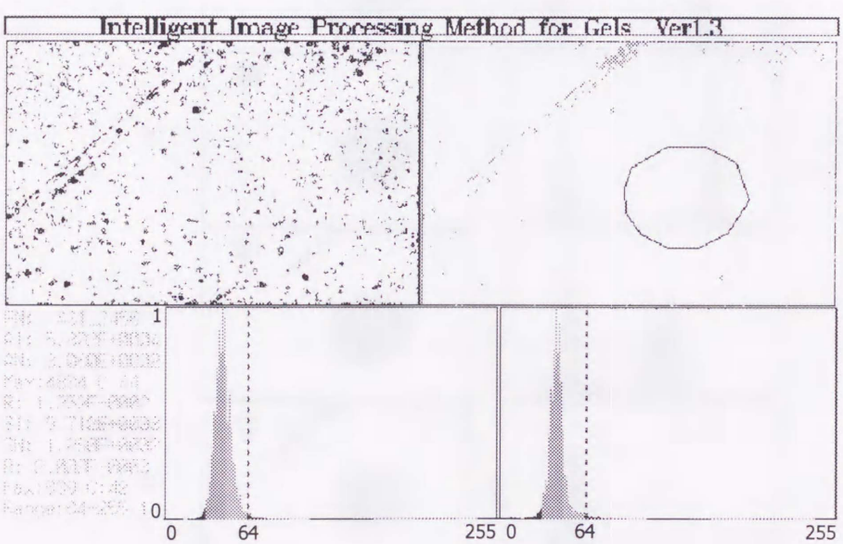

(b)

Figure 4. Graphics analysis of volume phase transition of disk-like PNIPA gels. Thickness and diameter of gels are 0.4mm and 61mm, respectively.
Time after jump to $\Delta T=1.0^{\circ}C$ is (a)3minutes and (b)2456minutes, respectively.
Upper-left side: contour maps of light intensities base on a differential operation.
Upper-right side: black and white images of the disk-like gels by a clipping procedure
Bottom-left side: distribution of light intensity.
Bottom-right side: distribution of light intensity within closed curve of the vision depicted in upper-right side.

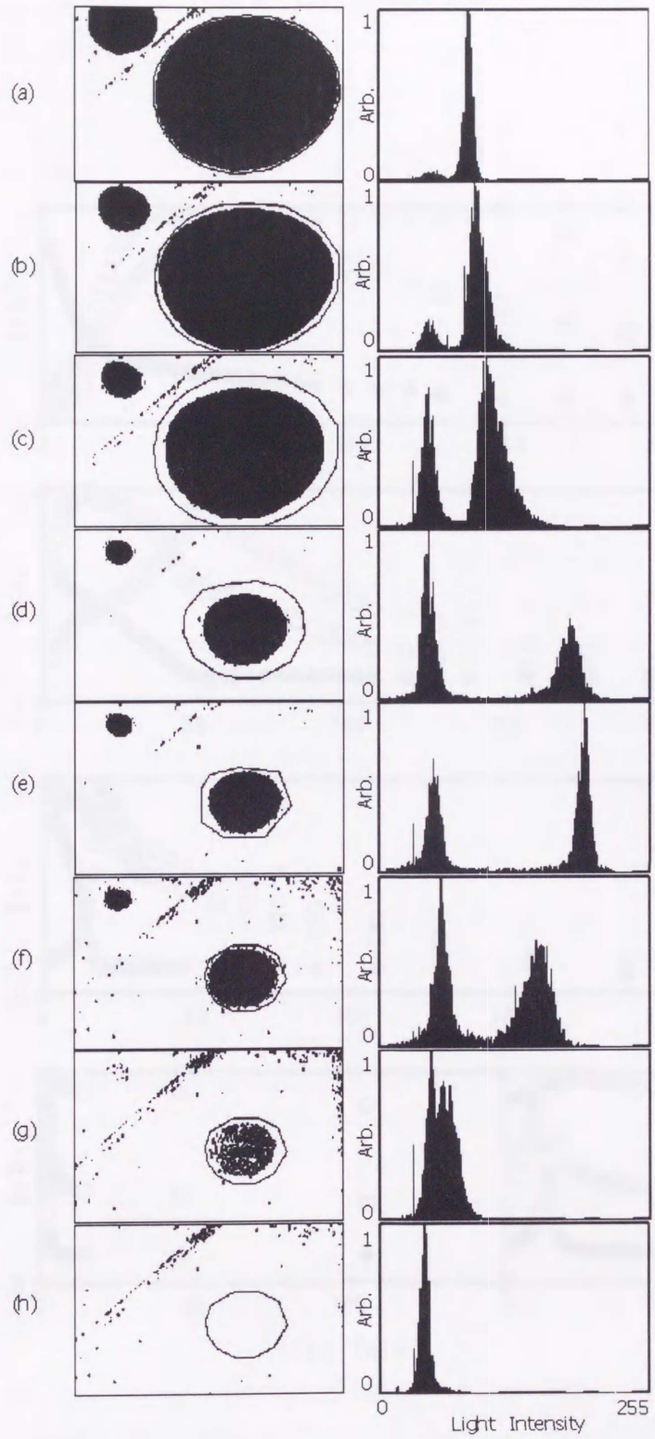

Figure 5. Temporal change in clipping images of PNIPA gels and light distribution. Time after jump at ΔT=1.0℃ is (a)3minutes (b)24minutes (c)30minutes (d)49minutes (e)60minutes (f)516minutes (g)1296minutes (h)2456minutes. Thickness and diameter of gels are about 0.4mm and 61mm, respectively.

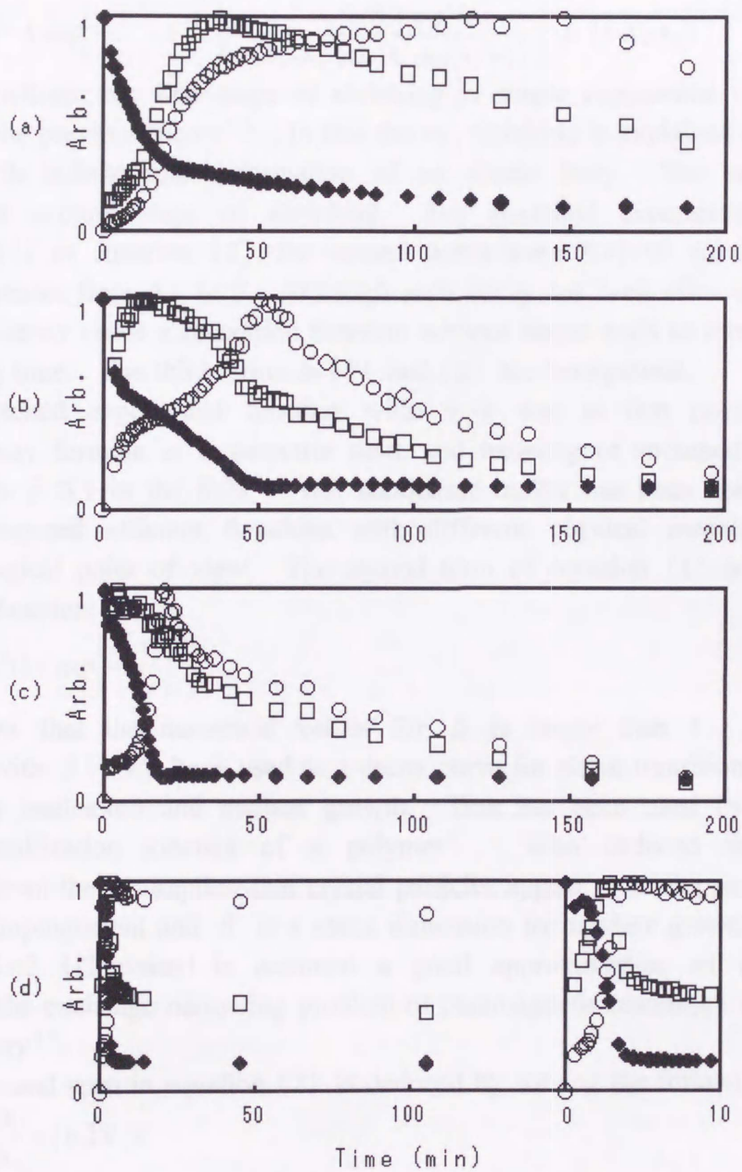

Figure 6. Graphs for normalized area of gels S(t)(●), normalized whitening of gels $W_1(t)$(□) and normalized whitening of gels per unit area $W_2(t)$(○). (a) ΔT=0.0℃, (b) ΔT=0.4℃, (c) ΔT=1.0℃, (d) ΔT=3.0℃.

3) Fitting Functions for S(t) in Shrinking of PNIPA Gels

Normalized areas of gels S(t) show two-step shrinking and we propose equations (1) and (2) as fitting functions of S(t).

$$S(t) = A_1 \exp\left(-\frac{t}{\tau_1}\right) + A_2 \exp\left(-\left(\frac{t}{\tau_2}\right)^{\beta}\right) + (1-A_1-A_2) \quad (1)$$

$$S(t) = A_1 \exp\left(-\frac{t}{\tau_1}\right) + \left(\frac{k}{\lambda} - \frac{(-A_2+k/\lambda)k\exp(kt)}{k+(-A_2+k/\lambda)\lambda(\exp(kt)-1)}\right) + (1-A_1-A_2) \quad (2)$$

For both functions, the first stage of shrinking is single exponential relaxation as deduced by the previous theory[14]. In this theory, shrinking is explained as collective diffusion with infinitesimal deformation of an elastic body. The second terms represent the second stage of shrinking. For stretched exponential with $\beta>1$ (equation (1)) or equation (2), the second terms keep $A_2(>0)$ for a while and abruptly decreases from A_2 to 0. Although such decay has been often observed, we consider the decay curve a relaxation function without stages such as incubation time or decreasing time. The third terms in (1) and (2) are background.

A stretched exponential function with $\beta<1$ was at first proposed as an empirical decay formula in a dielectric field, and meaning of stretched exponential function with $\beta \leqq 1$ in the field of soft condensed matter has been doscussed[26]. Here we proposed efficient functions with different physical meanings from a phenomenological point of view. The second term of equation (1) is a stretched exponential function:

$$X(t) = \exp\left(-\left(\frac{t}{\tau_2}\right)^{\beta}\right). \quad (3)$$

and we show that the numerical values for β is larger than 1. A stretched exponential with $\beta>1$ has been used as a decay curve for phase transition phenomena explained by nucleation and nuclear growth. This has been used by Avrami to explain crystallization kinetics of a polymer[27]. Who deduced the stretched exponential from the assumption that crystal particles appear as nuclei and grow with the particle impingement and β is a space dimension for nuclear growth. Equation (3) with $\beta=2$ (Gaussian) is assumed a good approximation, of a relaxation function for the exchange narrowing problem of paramagnetic resonance in Kubo and Tomita's theory[28].

The second term in equation (2) is deduced by solving the following equation,

$$\frac{dX}{dt} = (k-\lambda X)X \quad (4)$$

a nonlinear equation describing the growth of biological populations[29]. Population x (t) is determined by birth rate k and death rate λ and x(t) is controlled by x(t).

Which equation better explains the shrinking process of PNIPA gels, equation (1) or (2) ? It is clear that both equations show a strong interaction between elements. Some chemical reaction rates are affected strongly by amount of products.

4) Curve Fitting Analysis for S(t) in Shrinking Process of PNIPA Gels

Curve fittings for S(t) in temperature-induced shrinking processes of PNIPA gels at various ΔT are shown in Figure 7. Equations (1) and (2) fit S(t) quite well and fitting parameters in equations (1) and (2) at various ΔT are listed in Table I. Although equations (1) and (2) each have 5 parameters, the residual sum of squares χ^2 of equation (1) seems smaller than that of equation (2). But the difference is too small to be significant.

To discriminate between equations (1) and (2) as to better fit of data, we use the 'χ^2-map method'[30]. As shown in Figure 8, two parameters of a fitting function are selected as X and Y coordinate axes and calculated $1/\chi^2$ are plotted on the Z coordinate axis. Such a three dimensional graph is called an χ^2-map. Fitting parameters and χ^2 for the best fit are shown in Table I. One parameter increased or decreased. Minimum and maximum of the parameter are determined when χ^2 increases 10-fold. Minimum and maximum values of fitting parameters on a χ^2-map are shown in Table II. This method clarifies the uniqueness of the best fit variable parameters in a fitting function. χ^2-map fitted by equations (1) (Left side) and (2) (Right side) at $\Delta T = 1.0^{\circ}C$ is shown in Figure 8. A_2, τ_2, β, λ and k are important in order to discuss the properties of equations (1) and (2). Every χ^2-map on the left side shows a single peak, while that on the right side, a broad wall peak. Although the number of fitting parameters is the same in equations (1) and (2), A_2, τ_2 and β in equation (1) are more independent than A_2, λ and k in equation (2). So equation (1) is more adequate than equation (2) to fit S (t). To interpret the independency of fitting parameters quantitatively, clipping is used on a χ^2-map as shown in Figure 9. We count 0 if $1/\chi^2$ of the pixel is less than half maximum $1/\chi^2$ and 1 if more than half maximum $1/\chi^2$. We obtain black and white images of a peak in a χ^2-map depicted in Figure 9, and measure the lengths of the projection axes from the black area, X and Y. Two parameters R_1 and R_2 are introduced : R_1 obtained by dividing the number of black dots by (X × Y), and R_2 defined as X/Y or Y/X. R_1 and R_2 are smaller than 1. If a single peak is found on a χ^2-map, R_1 and R_2 are close to 1. If a broad wall is found, R_1 or R_2 are close to one. Various R_1 and R_2 at ΔT are shown in Figure 10. To compare fitting parameter independency of equations (1) and (2), R_1 and R_2 are A_2:τ_2, A_2:β, τ_2:β (equation (1)), A_2:λ, A_2:k, λ:k (equation (2)). R_1 of equation (1) is much smaller than that of equation (2) at various ΔT. Equation (1) is more adequate as a fitting function of S(t) from the viewpoint of statistical independency.

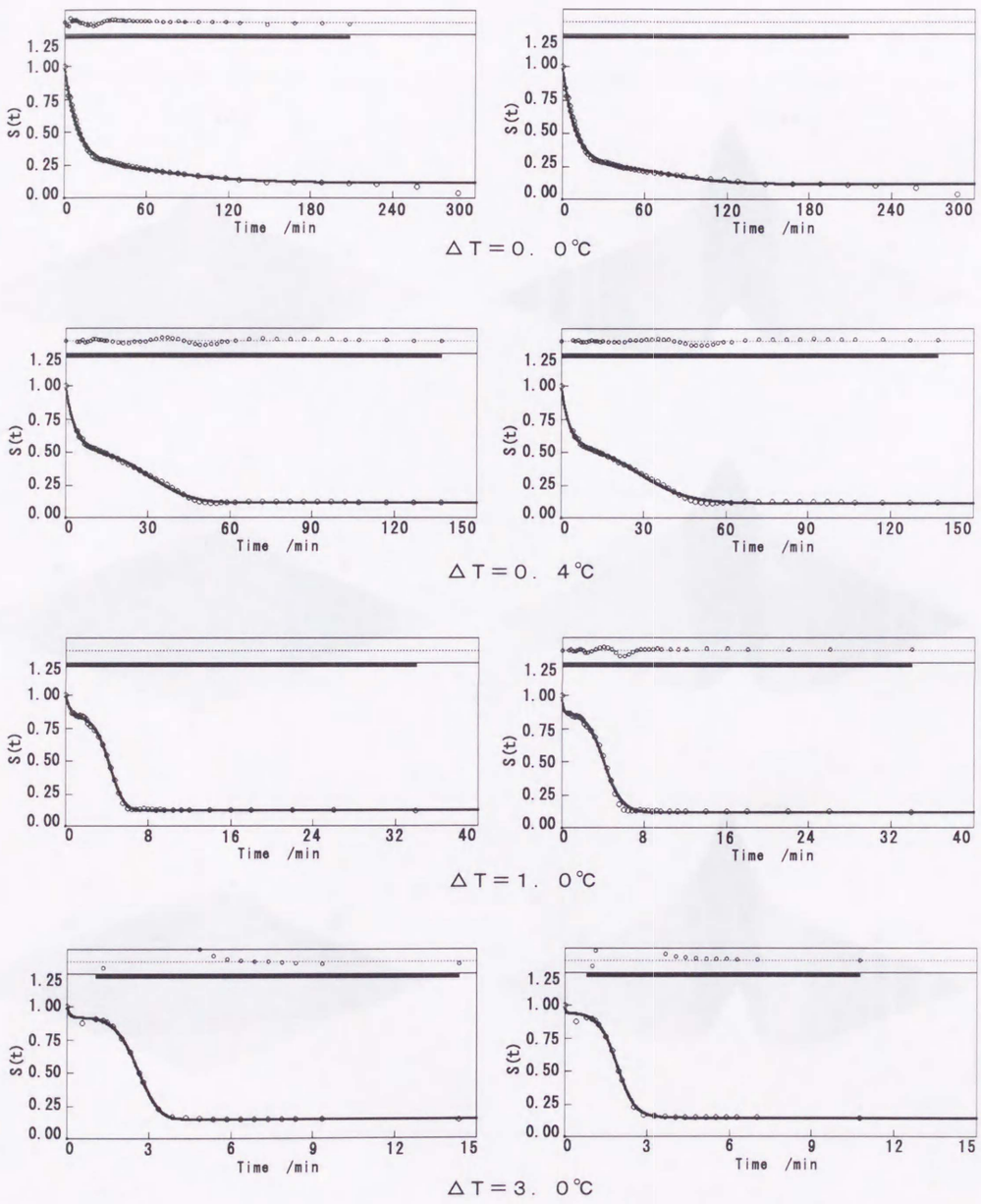

Figure 7. S(t) is plotted as a function of time at various Δ T. The solid line trough the data is a fit to equation (2). The residuals are shown above as a function of time. Left and right sides are equations (1) and (2), respectively.

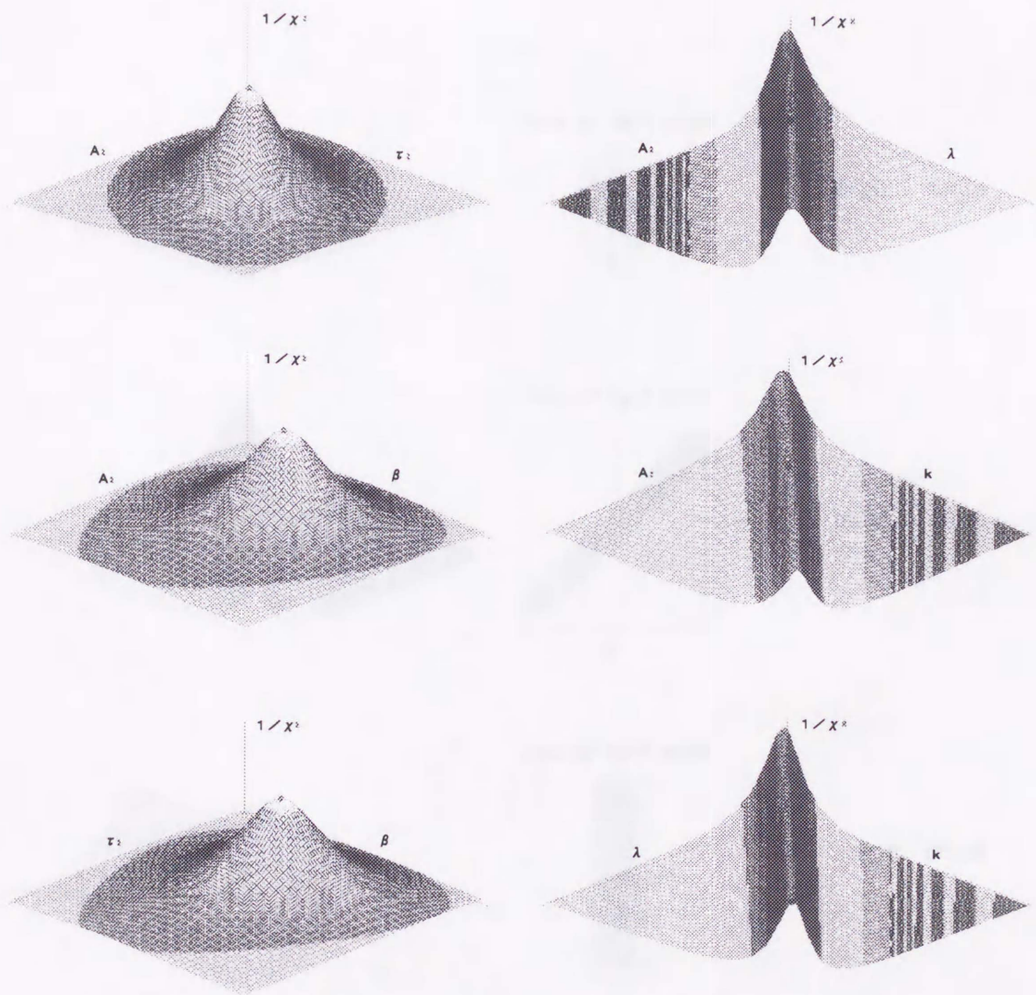

Figure 8. χ^2 maps of S(t) at volume phase transition of PNIPA gels. X, Y and Z axes are values of each parameter in equations (1)and (2) and $1/\chi^2$, respectively. Left and right side are equation (1) and (2), respectively.

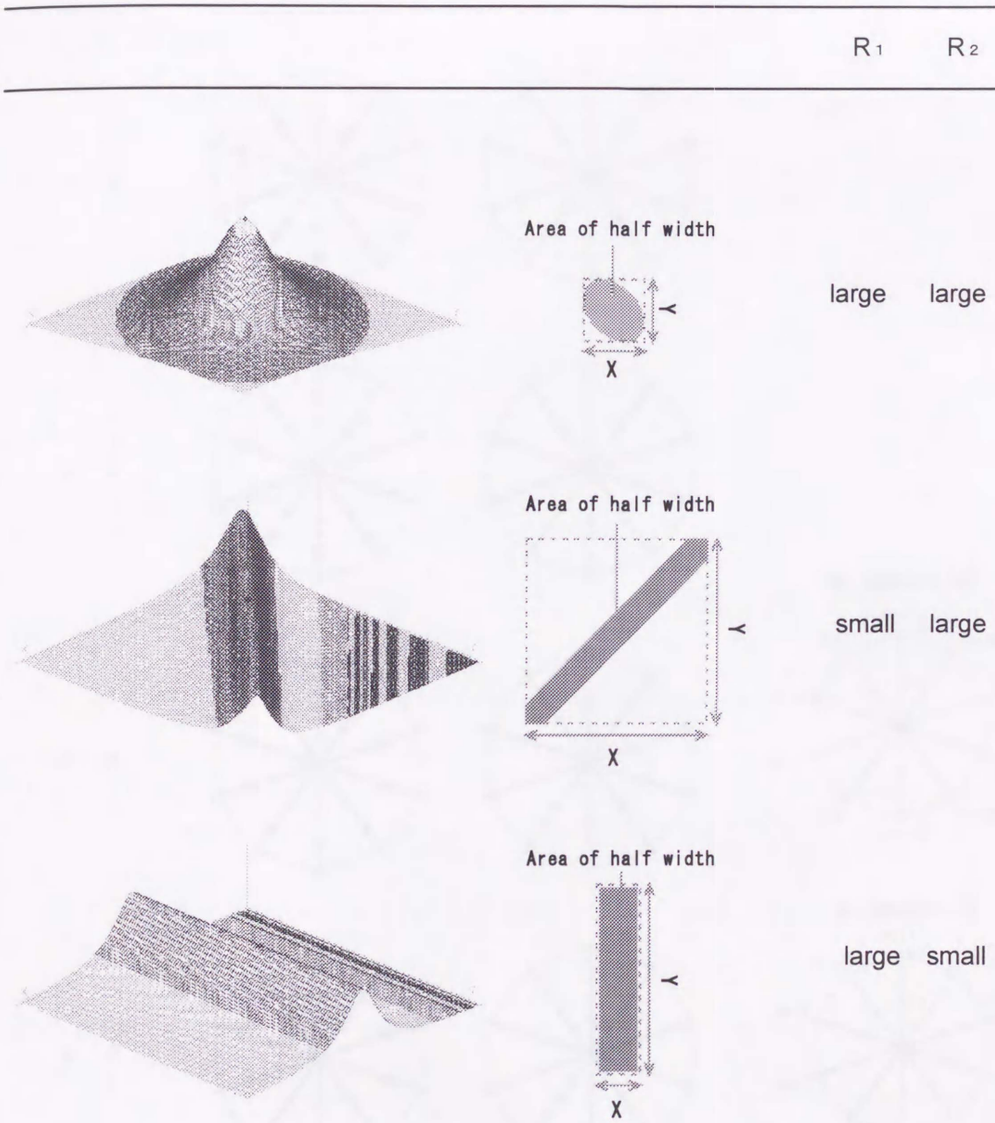

Figure 9. Introduction of parameters R_1 and R_2 to estimate independency of fitting parameters.

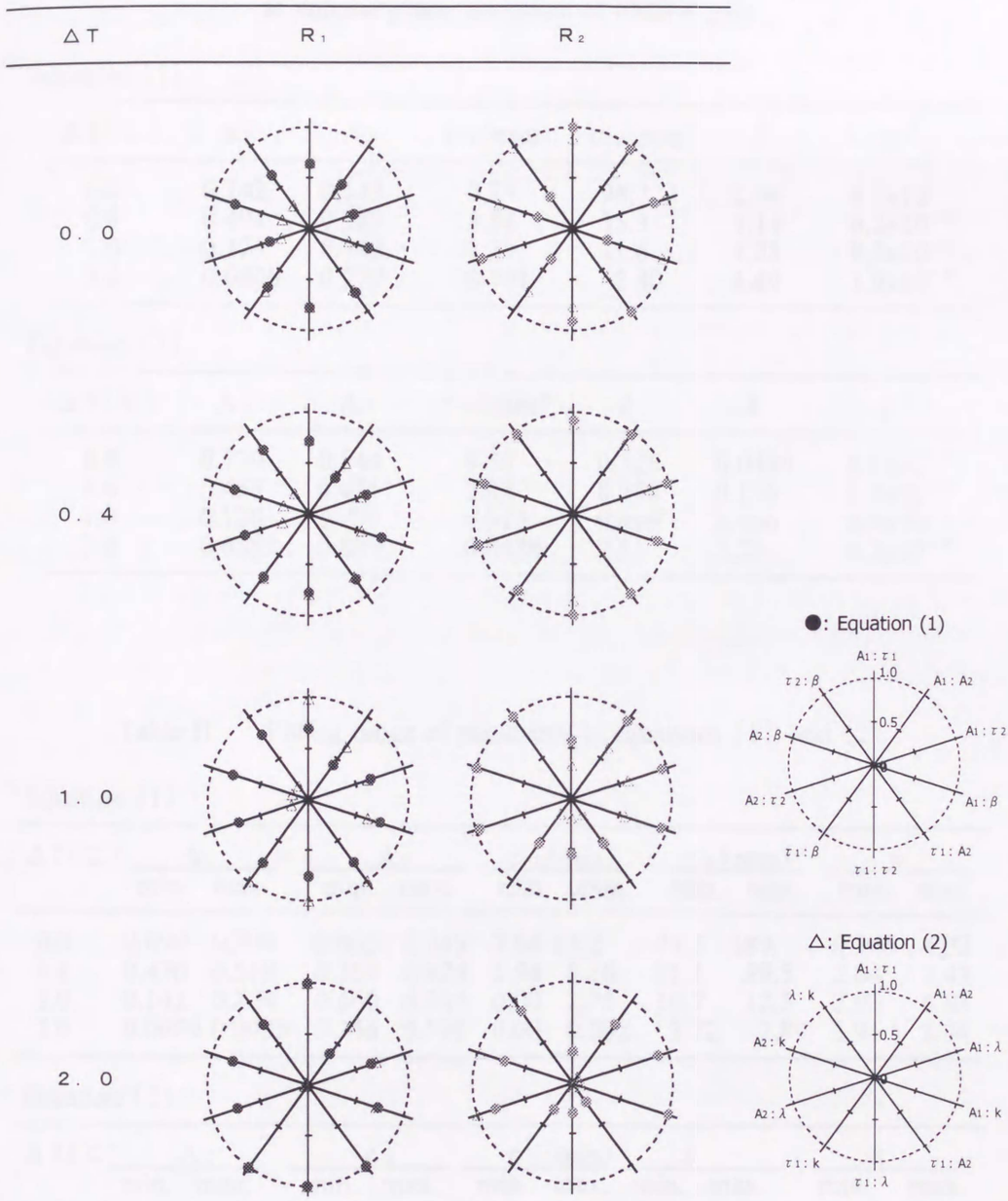

Figure 10. Independency of fitting parameters in equations (1) and (2).

Table I Parameters obtained by curve fitting of S(t) at volume phase transition of PNIPA gels

Equation (1)

ΔT(℃)	A_1	A_2	τ_1(min)	τ_2(min)	β	χ^2
0.0	0.742	0.145	9.77	94.7	2.04	8.7×10^{-5}
0.4	0.494	0.389	3.54	35.3	3.14	6.2×10^{-5}
1.0	0.173	0.702	1.36	11.6	4.28	9.2×10^{-5}
3.0	0.0806	0.770	0.101	2.80	4.49	1.9×10^{-5}

Equation (2)

ΔT(℃)	A_1	A_2	τ_1(min)	λ	k	χ^2
0.0	0.739	0.144	9.56	0.326	0.0480	8.6×10^{-5}
0.4	0.455	0.435	3.03	0.258	0.116	1.3×10^{-4}
1.0	0.126	0.759	0.313	0.609	0.466	2.9×10^{-4}
3.0	0.0555	0.800	0.0426	2.81	2.25	6.2×10^{-5}

Table II Fitting range of paramters in equations (1) and (2)

Equation (1)

ΔT(℃)	A_1		A_2		τ_1(min)		τ_2(min)		β	
	min.	max.	min.	max.	min.	max.	min.	max.	min.	max.
0.0	0.690	0.794	0.0351	0.249	7.04	13.2	44.5	189.	0.346	4.07
0.4	0.470	0.519	0.354	0.424	1.94	5.16	31.1	39.5	2.04	5.43
1.0	0.142	0.204	0.660	0.744	0.00	2.71	10.7	12.5	2.95	6.84
3.0	0.0669	0.0935	0.746	0.793	0.00	0.202	2.72	2.89	3.91	5.34

Equation (2)

ΔT(℃)	A_1		A_2		τ_1(min)		λ		k	
	min.	max.	min.	max.	min.	max.	min.	max.	min.	max.
0.0	0.702	0.776	0.125	0.148	7.84	11.8	0.300	0.336	0.0465	0.0513
0.4	0.418	0.491	0.417	0.443	0.00	5.57	0.248	0.263	0.114	0.119
1.0	0.0732	0.179	0.751	0.766	0.00	0.626	0.603	0.615	0.461	0.470
3.0	0.0317	0.0794	0.792	0.808	0.00	0.0851	2.78	2.84	2.23	2.28

5) Two-Step Mechanism in Temperature-Induced Volume Phase Transition Process of PNIPA Gels

Equation (1) is adequate as a fitting function of S(t) at various ΔT. We discuss the physical meaning of fitting parameters by taking account of skin layer. Images of volume phase transition of PNIPA gels are shown in Figure 11. Just above Tc, the coefficient A_2 is small, and shrinking can be described by a single exponential. The gels shrink monotonically and the skin layer does not appear. For larger temperature jump, A_2 increases, indicating greater contribution of the stretched exponential. PNIPA gels shrink at first, the skin layer is formed on the surface and gels stop shrinking. The skin layer breaks or changes and the inner part starts to shrink. β and τ_2 characterizing the stretched exponential in equation (1) represent respectively sharpness and average time for collapse of the skin layer. As shown in Table I, A_2/A_1 increases with ΔT. The first shrinking process is dominant near T_c. The second shrinking is important at larger ΔT. τ_1 and τ_2 decrease with increase in ΔT and first and second shrinkings of PNIPA gels become faster at larger ΔT. The relationship between τ's and ΔT is consistent with the theoretical model of skin layer developed by Tomari et al[20]. β increases with increase in ΔT and collapse of the skin layer is less with increasing ΔT.

The second term of equation (1) suggests that the second shrinking of PNIPA gels undergoes like nucleation and nuclear growth. Nuclei correspond to shrinking parts of PNIPA gels and nuclear growth can be shown as a network of shrinking parts. This is consistent with the visual observation. Although β is a spatial dimension when nuclei grow and usually smaller than 4 in Avrami's formula, β is a spatial strength of growth. As shown in Table I, nucleation and nuclear growth are faster with increase in ΔT.

The shrinking of PNIPA gels may be summarized as follows. Gels first shrink monotonically as collective diffusion with infinitesimal deformation. Gels stop shrinking with skin layer formation on the surface of gels. The skin layer may break or change, and the inner part starts to shrink. On increasing ΔT, the second shrinking becomes dominant and average time τ_2 to skin layer collapse decreases, and the degree of the collapse strength β increases. The general meaning of stretched exponential function with $\beta > 1$ will be explained in another article.

1-1-4. Conclusion

(1) The Present graphical analysis is effective to estimate temperature-induced volume phase transition of PNIPA gels.
(2) A two-step shrinking occurs in temperature-induced volume phase transition of PNIPA gels.
(3) The sum of exponential and stretched exponential functions (equation(1)) fits temperature-induced volume change of PNIPA gels using 'χ^2 map method'. On the assumption of collapse of skin layer, fitting parameters β and τ_2 in equation (1) represent sharpness and average time to collapse of skin layer,

respectively.

(4) Whitening is synchronized with shrinking in temperature-induced volume phase transition of PNIPA gels.

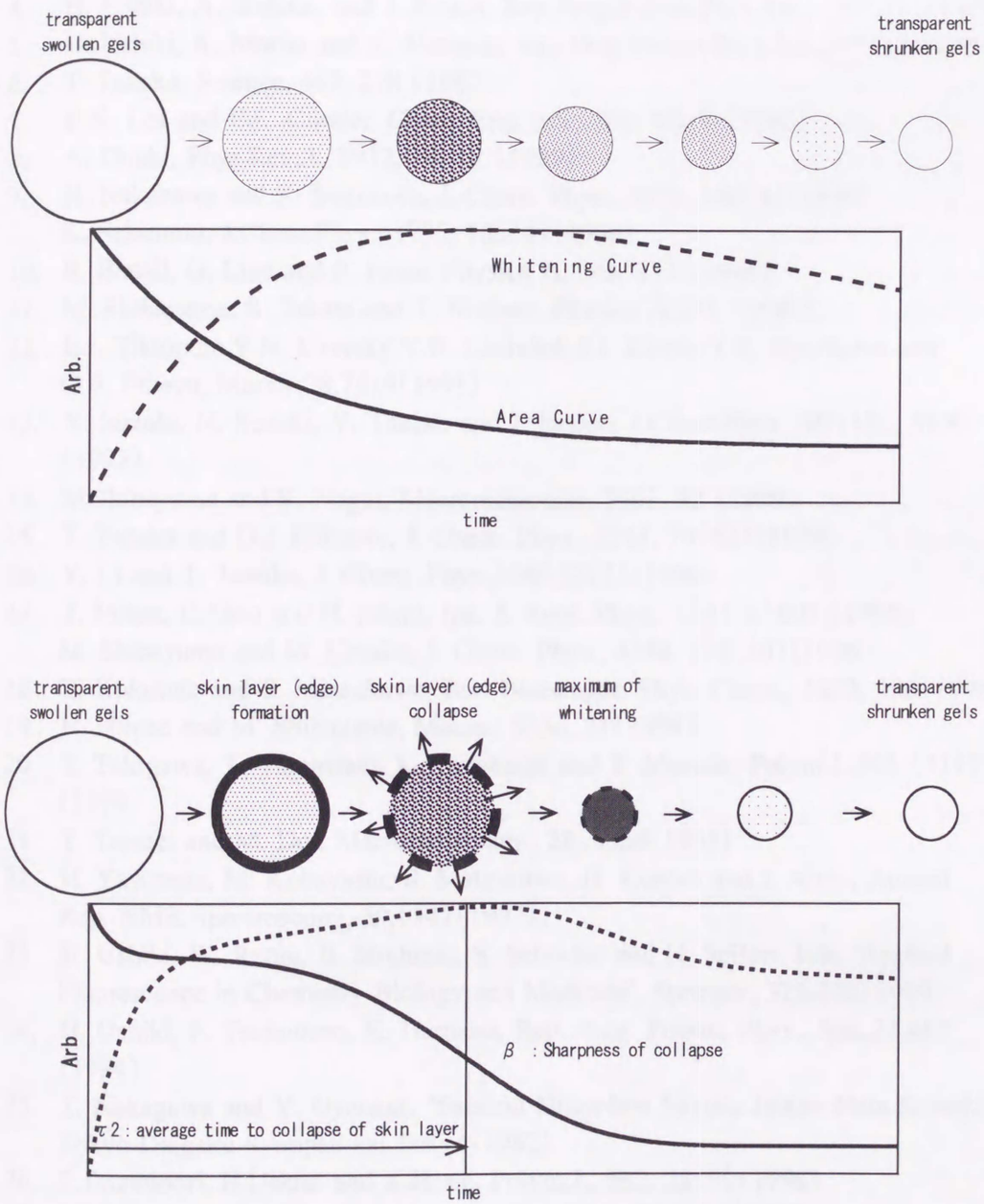

Figure 11. Shrinking of PNIPA gels.

References

1. E.S. Matsuo and T. Tanaka, J.Chem.Phys.,1695, 89(3)(1998)
2. T. Tanaka, S.T. Sun, Y. Hirokawa, S. Katayama, J. Kucera, Y. Hirose and T. Amiya, Nature,796, 325(26)(1987)
3. E.S. Matsuo and T. Tanaka, Nature,482,358(6)(1992)
4. H. Ushiki, A. Ikehata, and J. Rouch, Rep.Prog.Polym.Phys.Jpn., 169(41)(1998)
5. H. Ushiki, K. Morita and K. Hamano, Rep.Prog.Polym.Phys.Jpn., 97(37)(1994)
6. T. Tanaka, Science, 467, 218 (1982)
7. K.K. Lee and E.L. Cussler, Chem. Eng. Sci., 766, 45(3)(1990)
8. A. Onuki, Phys.Rev.A, 5932, 39, 11 (1989)
9. H. Nakazawa and K. Sekimoto, J. Chem. Phys., 1675, 104(4)(1996) K. Sekimoto, J.Chem.Phys., 1735, 105(4)(1996)
10. R. Bansil, G. Liao and P. Falus, Physica A, 346, 231 (1996)
11. M. Shibayama, S. Takata and T. Norisue, Physica A,245 (1998)
12. E.I. Tiktopulo,V.N. Uversky,V.B. Lushchik,S.I. Klenin,V.E. Bychkova and O.B. Ptitsyn, Macro.,28,7519(1995)
13. Y. Suzuki, N. Suzuki, Y. Takasu and I. Nishio, J.Chem.Phys.,107(15), 5890 (1997)
14. M.Shibayama and K. Nagai, Macromolecules, 7461, 32 (1999)
15. T. Tanaka and D.J. Fillmore, J. Chem. Phys., 1214, 70(03)(1979)
16. Y. Li and T. Tanaka, J. Chem. Phys.,1365,92(2)(1990)
17. T. Miura, E. Ono and H. Ichijo, Jpn. J. Appl. Phys., (34) L1603 (1995) M. Shibayama and M. Uesaka, J. Chem. Phys., 4350, 105(10)(1996)
18. E. Kokufuta and S. Matsukawa, Ber. Bunsenges. Phys. Chem., 1073, 100(1996)
19. H. Hirose and M. Shibayama, Macro., 5336, 31(1998)
20. T. Takigawa, T. Yamawaki, K. Takahashi and T .Masuda, Polym.J.,595 (31)7 (1999)
21. T. Tomari and M. Doi, Macromolecules., 28, 8334(1995)
22. H. Yasunaga, M. Kobayashi, S. Matsukawa, H. Kurosu and I. Ando, Annual Rep. NMR Spectroscopy, 39,(34)(1997)
23. H. Ushiki, W. Rettig, B. Strehmel, S. Schrader and H. Seifert, Eds. 'Applied Fluorescence in Chemistry Biology and Medicine', Springer, 325-370(1999)
24. H. Ushiki, F. Tsunomori, K. Hamano, Rep. Prog. Polym. Phys., Jpn.,37,463 (1994)
25. T. Nakagawa and Y. Oyanagi, "Saishou Nijou-hou Niyoru Jikken-Data Kaiseki", Tokyo Daigaku Syuppan-kai,Tokyo(1982)
26. F.Tsunomori, H.Ushiki and K.Horie, Polym.J., 582, 28(7)(1996)
27. M.Tomellini and M.Fanfoni, Phys.Rev.B, 14071, 55 (21)(1997)
28. R.Kubo and Tomita, J.Phys.Soc.Jpn.,888,9(1954)
29. R.May, Science, (186) 645(1974)
30. H.Ushiki and F.Tsunomori, Rep.Prog.Polym.Phys.Jpn., 36,373 (1993)

1-2. Analysis of Shrinking Process by Integral Transformation Method

1-2-1. Abstract

Kinetics of shrinking process of disk-like poly(N-isopropylacrylamide) gels (PNIPA) which show the temperature induced volume change was discussed in this report. PNIPA gels shrink and become opaque with their macroscopic deformation after temperature-jumping over the critical point. The shrinking process accompanied by whitening was measured and analyzed by our original apparatus and theoretical method. Temporal change of gels size after various temperature-jumping over the critical point were fitted by the sum of exponential and stretched exponential functions with $\beta>1$. In order to discuss the meaning of stretched exponential function with $\beta>1$, new theoretical concept using by distribution function was proposed. Applied this concept to secondary shrinking of PNIPA gels, assuming that there are a lot of parts in gels, each part shrinks step-like and the distribution function of the characteristic times was defined.

1-2-2. Introduction

In previous paper, the temporal change of area of disk-like PNIPA gels was measured after temperature-jumping over the critical point, and two-step shrinking of gels was observed at various destination temperature.[2] To fit the time-dependent shrinking process, the sum of exponential and stretched exponential functions was proposed. The shrinking curve at second stage was expressed very well by the following stretched exponential function with $\beta>1$

$$I(t) = \exp\left(-\left(\frac{t}{\tau_{SE}}\right)^{\beta}\right). \qquad (1)$$

When $\beta<1$, I(t) decreases monotonically. However when $\beta>1$, I(t) keeps 1 for a while and abruptly decreases from 1 to 0 as shown in Figure 1. Meaning of equation (1) was discussed in previous paper as follows. Stretched exponential function with $\beta \leqq 1$ was at first proposed as an empirical decay formula in a dielectric field[6] and has been very useful to express an experimental decay in the field of soft condensed matter.[7] The meanings of such decay curve and/or this function have been discussed by many researchers. In general, it is considered that such decay curve consists of many single exponential functions with various characteristic life times. This relationship means Laplace transform and there are attempts to deduce directly the distribution of characteristic times from the observed decay curve, for example CONTIN program[8] as explained below. And the meaning of β and/or the distribution of characteristic times has been discussed from the viewpoint of fractal structure and so on.[9, 10]

On the other hand, there are few discussion about stretched exponential with $\beta>1$ compared with $\beta<1$. However a stretched exponential analysis with $\beta>1$ has represented the kinetics of phase change such as isothermal crystallization of polymer,

which undergoes nucleation and nuclear growth. Equation (1) has been deduced by Avrami to explain crystallization kinetics of alloy and a polymer.[11] A stretched exponential analysis with $\beta>1$ was deduced from the assumption that crystal particles appear as nuclei and grow with the particle impingement, where β is a space dimension for nuclear growth. This is the most famous interpretation of equation (1), although equation (1) with $\beta=2$ (Gaussian) is assumed a good approximation, of a relaxation function for the exchange narrowing problem of paramagnetic resonance in Kubo and Tomita's theory.[12]

As shown in the case of stretched exponential function with $\beta<1$, the concept of distribution has been important more and more. Data are obtained as some distribution in various measurements, for example, dielectric relaxation, rheology, light scattering measurements, etc.. Attempts to interpret the observed phenomena using by distribution function can be considered to become getting important now. In this report we try to incorporate such thoughts of distribution function into the analysis of shrinking process of PNIPA gels and discuss the meaning of stretched function (equation (1)) with $\beta \geqq 1$.

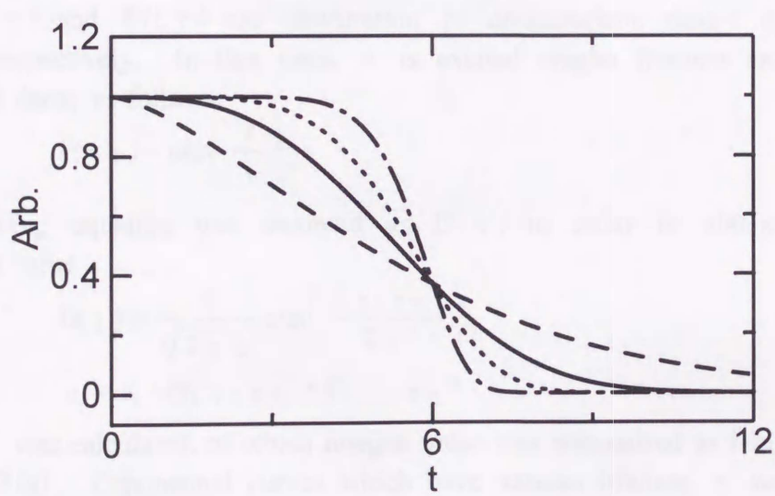

Figure 1. Curves of equation (1) with A=1.0 and τ_0=6.0. β values of solid, short-dashed, dash-dotted and long-dashed lines are 1.5, 3.0, 5.0 and 9.0, respectively.

1-2-3. Integral Transformation Method

1) Curve Fitting to Stretched Exponential Function

Normalized area of gels S(t) shows two-step shrinking and the following equation was proposed as a fitting function of S(t) in the previous article.[2]

$$S(t) = A_1 \exp\left(-\frac{t}{\tau_1}\right) + A_2 \exp\left(-\left(\frac{t}{\tau_2}\right)^{\beta}\right) + (1-A_1-A_2) \qquad (2)$$

The first stage of shrinking is single exponential relaxation as deduced by T.Tanaka et al.[14] In this theory, shrinking is explained as collective diffusion with infinitesimal deformation of an elastic body. The second term represents the second stage of shrinking and we showed that the numerical values for β is larger than 1 at various Δ T. The third term in equation (2) is fraction of shrunken gels.

Curve fitting for S(t) in temperature-induced shrinking processes of PNIPA gels at ΔT=0.4℃ is shown in Figure 5. Equation (2) fitted S(t) quite well and fitting parameters about the second term of equation (2) at various ΔT are listed in Table I.

2) Stretched Exponential Function with β<1 and Distribution Function

New analytical concept about the fluorescence intensity was presented by H.Ushiki.[15] The following concept is considerable to discuss the meaning of stretched exponential from the viewpoint of distribution. Assuming a distribution of excited singlet lifetime, the fluorescence intensity was given by

$$I(t) = \int_0^{\infty} D(\tau) F(t,\tau)\, d\tau , \qquad (3)$$

where $D(\tau)$ and $F(t,\tau)$ are distribution of characteristic time τ and elemental function, respectively. In this case, τ is excited singlet lifetime and F(t) is an exponential decay as follows

$$F(t,\tau) = \exp\left(-\frac{t}{\tau}\right). \qquad (4)$$

The following equation was assumed as $D(\tau)$ in order to obtain the various distribution value

$$D(\tau) = \frac{1}{\sqrt{2\pi}\,\sigma} \exp\left(-\frac{(\tau-\tau_0)^2}{2\sigma^2}\right) \qquad (5)$$

$$\sigma = A + B(\tau-\tau_0) + C(\tau-\tau_0)^2 \qquad (6)$$

and $D(\tau)$ was calculated, of which integral value was normalized to 1 in PC as shown in Figure 2(a). Exponential curves which have various lifetime τ were plotted in Figure 2(b). Each curve of which lifetime is τ has $D(\tau)$ at the initial value. The sum of these exponential curves are calculated and fitted very well by equation (1) with $0<\beta<1$ as shown in Figure 2(c). It was shown that a stretched exponential function with $0<\beta<1$ is analytically effective to express the sum of exponential functions of various lifetimes and discussed the relationship between β and $D(\tau)$. In the field of light scattering measurements, the intensity time correlation function has been well known to be represented by a stretched exponential function with $0<\beta\leqq 1$ and

recently D(τ) itself is deduced using by CONTIN program[16] etc. CONTIN program is justified to be one of the most faithful algorithms to solve equation (3) which means Laplace transform.

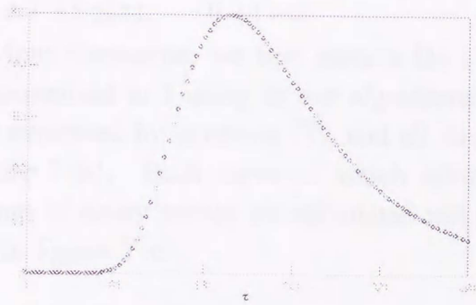

(a)

(b)

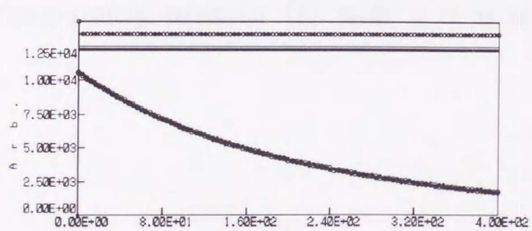

(c)

Figure 2. Calculation process of decay curve and its fitting result
(a) D(τ) deduced from equation (5) with τ_0=200, σ=20, ξ=1, t=0～400.
(b) Single exponential decay curves with various lifetimes of D(τ).
(c) Sum of various single exponential decay curves with D(τ) and its fitted graph by a stretched exponential function with $0<\beta<1$.

3) Relationship between Step Function and Stretched Exponential Function with $\beta > 1$

In this report, we try to incorporate such concept to a stretched exponential function with $\beta > 1$. In case that a stretched exponential function with $\beta > 1$ is observed as $I(t)$ phenomenologically, we assume that $I(t)$ is also represented by equation (3) which consists of $D(\tau)$ and $F(t, \tau)$. In case of $\beta > 1$, we propose that $F(t, \tau)$ can be expressed by step function as follows instead of equation (4).

$$F(t,\tau) = 1 \quad (t \leqq \tau), \qquad 0 \quad (t > \tau) \tag{7}$$

As same as the previous discussion, we first assume $D(\tau)$ as equation (5) of which integral value was normalized to 1 using by our algorithms in PC as shown in Figure 7 (a). Each decay is expressed by equation (7) and all decays which have various τ's were plotted in Figure 7(b). Each curve of which lifetime is τ has $D(\tau)$ at the initial value. The sum of decay curves are calculated and fitted well by equation (1) with $\beta > 1$ as shown in Figure 7(c).

4) Relationship between Distribution of Step Functions and Parameters in Stretched Exponential Function for $\beta > 1$

Assuming various $D(\tau)$ by changing parameters based on equation (5), the sum of decay curves was calculated and fitted by equation (1). The relationship between $D(\tau)$ and fitting parameters in equation (1) with $\beta > 1$ are obtained. As shown in Figure 8(a), left-side graph is various $D(\tau)$ changing by τ_0 in equation (5), and right-side is the relationship between τ_0 and fitting parameters τ_{SE} and/or β. τ_0 of $D(\tau)$ changes linearlly the value of not only τ_{SE} but also β. When σ increases as shown in Figure 8(b), τ_{SE} slightly increases and β decreases strongly. As shown in Figure 8(c), when σ increases only in one side containing the integrated value of $D(\tau)$ to 1, τ_{SE} slightly increases and β decreases strongly. These results show that the shape of $D(\tau)$ influences both τ_{SE} and β, and the relationship between τ_{SE} and β are not simple. Unfortunately equation (1) with $\beta > 1$ is not always very good as a fitting function.

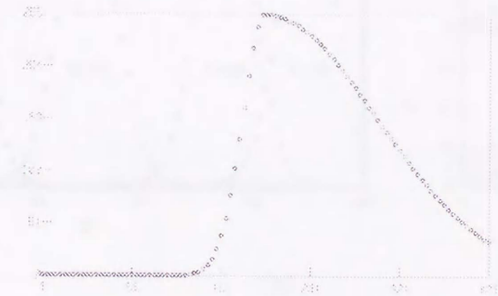

(a)

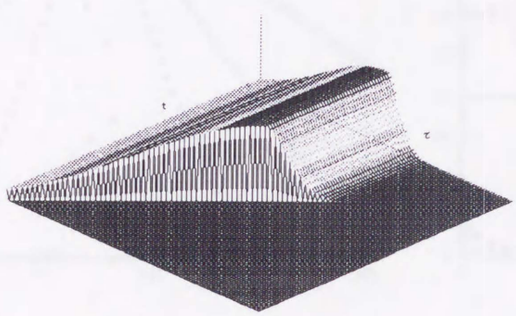

(b)

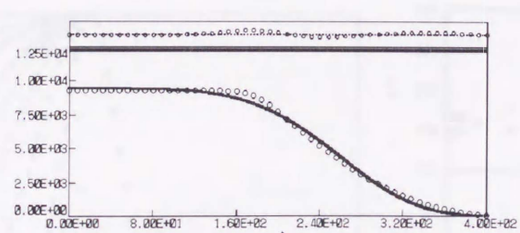

(c)

Figure 3. Calculation process of decay curve and its fitting result
(a) $D(\tau)$ deduced by equation (5) with τ_0=200, σ=20, ξ=1, t=0～400.
(b) Step functions with various lifetimes of $D(\tau)$. (c) Sum of various step functions and its fitted graph by a stretched exponential function.

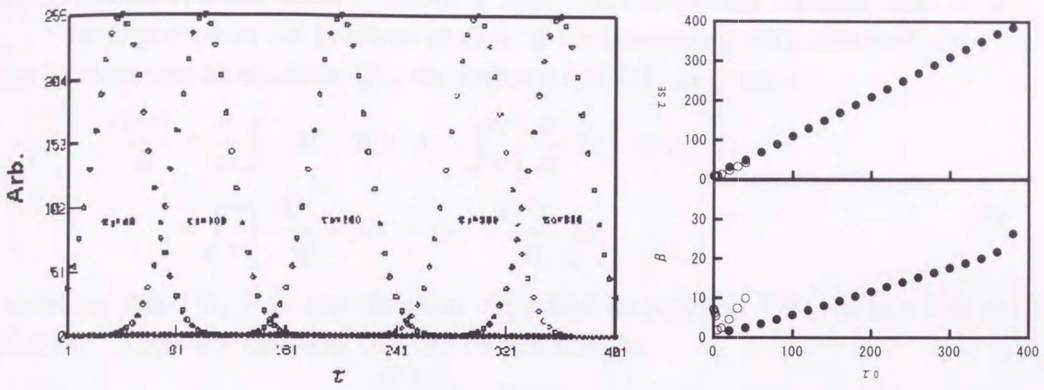

(a)

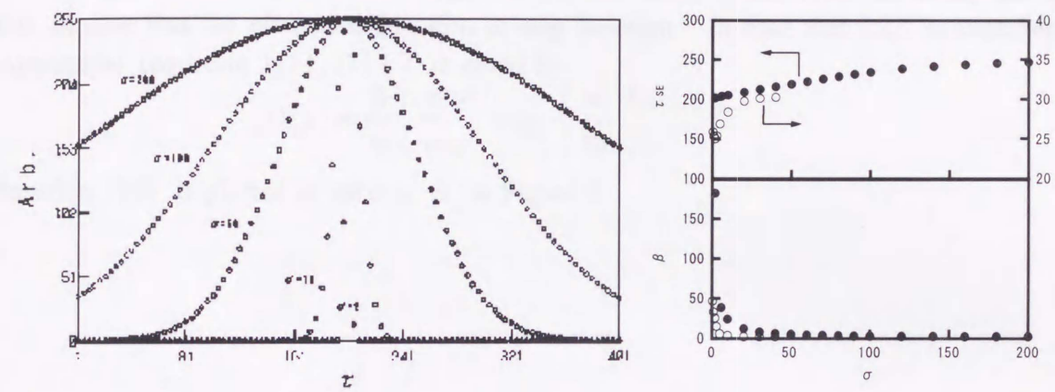

(b)

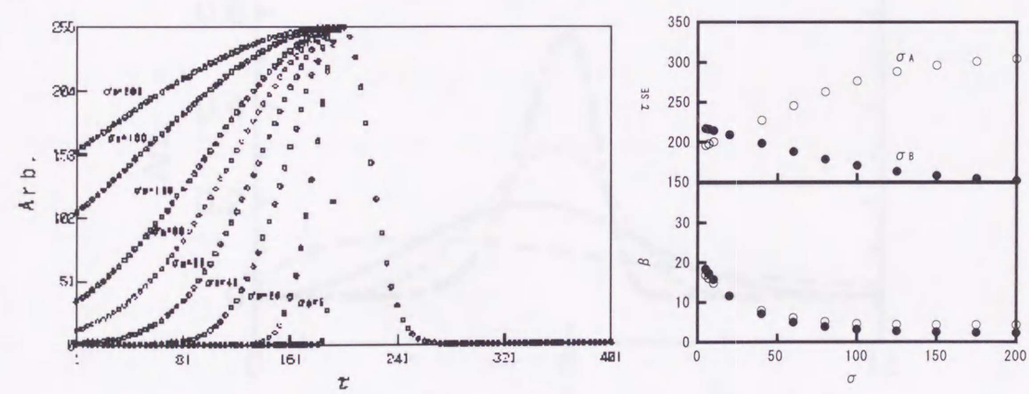

(c)

Figure 4. Fitting result to data based on various distribution D(τ).
Left-side images are various D(τ) of equation (5) changeing (a) τ_0 ,(b) σ, (c) σ_A and σ_B, where σ_A and σ_B are σ at smaller τ and at larger τ, respectively. Calculated data based on D(τ) were fitted by a stretched exponential function (equation (1)) with $\beta > 1$. Right-side images are plots of fitting parameters τ_{SE} and β vs. (a) τ_0, (b) σ, (c) σ_A and σ_B of D(τ).

5) Definition of Distribution Function in Stretched Exponential Function with $\beta > 1$

As explained in the previous section, if phenomenologically observed curve $I(t)$ can be expressed as equation (3), the derivative of $I(t)$ is given by

$$\frac{dI(t)}{dt} = \frac{d}{dt}\int_0^\infty D(\tau)F(t)\,d\tau = \int_0^\infty \left[\frac{d}{dt}(D(\tau)F(t))\right]d\tau$$

$$= \int_0^\infty \left[\frac{dD(\tau)}{dt}F(t) + D(\tau)\frac{dF(t)}{dt}\right]d\tau \qquad (8)$$

Assuming that $F(t,\tau)$ is step function expressed in equation (7), $-dF(t,\tau)/dt$ is δ function. Therefore equation (8) can be rewritten by

$$\frac{dI(t)}{dt} = -D(t) \qquad (9)$$

It shows that distribution $D(\tau)$ is equal to the derivative of the observed decay curve $I(t)$ in case that the elemental function is step function. In case that $I(t)$ is stretched exponential (equation (1)), $D(\tau)$ is given by

$$D(\tau) = \frac{\beta}{\tau_0}\left(\frac{\tau}{\tau_0}\right)^{\beta-1}\exp\left(-\left(\frac{\tau}{\tau_0}\right)^{\beta}\right) \qquad (10)$$

Equation (10) is plotted at various β in Figure 5.

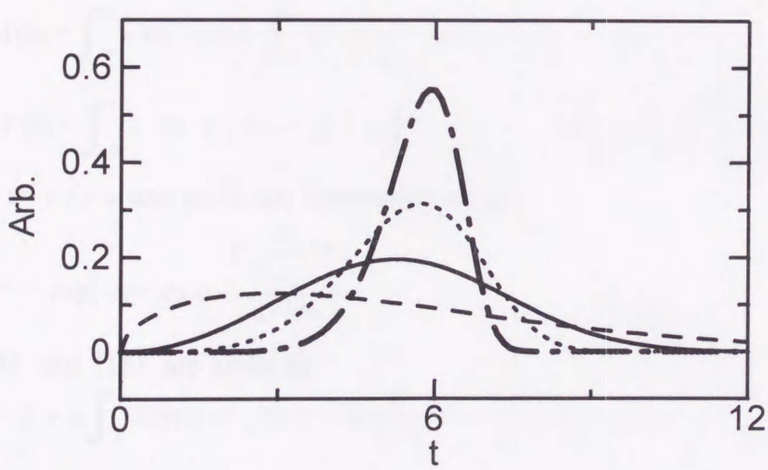

Figure 5. Curves of equation (10) with A=1.0 and τ_0=6.0. β values of solid, short-dashed, dash-dotted and long-dashed lines are 1.5, 3.0, 5.0 and 9.0, respectively.

6) Propaties of Distribution Function in Stretched Exponential Function for $\beta > 1$

In general, average E and distribution σ^2 of $D(\tau)$ were evaluated by following equations

$$E = \sum_{\tau=0}^{\infty} \tau D(\tau) \delta \tau \tag{11}$$

$$\sigma^2 = \sum_{\tau=0}^{\infty} (\tau - E)^2 D(\tau) \delta \tau \quad . \tag{12}$$

When $D(\tau)$ is equation (10), E and σ^2 of $D(\tau)$ are calculated like SCF method and plotted as a function of β in Figure 10. At that time the region for calculation of τ is 0 to 30. τ_0 and the step width $\delta \tau$ are 6 and 30/400=0.075, respectively. The integrated value $\sum_{\tau=0}^{\infty} D(\tau) \delta \tau$ was always fixed to 1.

On the other hand, is equation (10) a distribution function? If $D(\tau)$ is a distribution function, the following conditions are satisfied.

1. Integral value of $D(\tau)$ is equal to 1.
2. Average E and distribution σ^2 of $D(\tau)$ are expressed analytically.

First we will show the integral value of $D(\tau)$, $M(0)$ is 1 as follows.

$$M(0) = \int_{-\infty}^{\infty} D(\tau)\, d\tau = \left[\exp\left(-\left(\frac{\tau}{\tau_{SE}} \right)^{\beta} \right) \right]_{-\infty}^{\infty} = 1 \tag{13}$$

Then $M'(0)$ and $M''(0)$ are given by

$$M'(0) = \int_0^{\infty} \tau D(\tau)\, dt = \int_0^{\infty} \beta \left(\frac{\tau}{\tau_{SE}} \right)^{\beta} \exp\left(-\left(\frac{\tau}{\tau_{SE}} \right)^{\beta} \right) d\tau \tag{14}$$

$$M''(0) = \int_0^{\infty} \tau^2 D(\tau)\, d\tau = \beta\, \tau_{SE} \int_0^{\infty} \left(\frac{\tau}{\tau_{SE}} \right)^{\beta+1} \exp\left(-\left(\frac{\tau}{\tau_{SE}} \right)^{\beta} \right) d\tau \quad . \tag{15}$$

Substituting $z = \tau / \tau_{SE}$ and using the following formula

$$\int_0^{\infty} z^{b-1} \exp(-az^{\alpha}) dx = \frac{\Gamma\left(\frac{b}{\alpha} + 1 \right)}{a^{b/\alpha} b} \quad , \tag{16}$$

equation (14) and (15) are given as

$$M'(0) = \beta\, \tau_{SE} \int_0^{\infty} z^{\beta} \exp(-z^{\beta})\, dz = \tau_{SE} \frac{\beta}{\beta+1} \Gamma\left(\frac{\beta+1}{\beta} + 1 \right) = \tau_{SE} \Gamma\left(1 + \frac{1}{\beta} \right) \tag{17}$$

and

$$M''(0) = \beta\, \tau_0^2 \int_0^{\infty} z^{\beta+1} \exp(-z^{\beta})\, dz = \beta\, \tau_{SE}^2 \frac{\Gamma\left(\frac{\beta+2}{\beta} + 1 \right)}{\beta+2} = \tau_{SE}^2 \Gamma\left(1 + \frac{2}{\beta} \right) \quad , \tag{18}$$

respectively. Therefore, E was given by equation (17) and σ^2 is written by

$$\sigma^2 = M''(0) - \{M'(0)\}^2 = \tau_{SE}^2 \left\{ \Gamma\left[1+\frac{2}{\beta}\right] - \Gamma\left[1+\frac{1}{\beta}\right]^2 \right\}. \quad (19)$$

As a result, equation (10) is proved as distribution function in general. In addition, the time which shows the maximum $D(\tau)$, τ_{Max} was calculated as a function of β as follows.

$$\tau_{Max} = \tau_{SE} \exp(\ln(1-1/\beta)/\beta) \quad (20)$$

Analytically deduced E, σ^2 and τ_{Max} were also plotted as a function of β in Figure 10 using by the following formula

$$\Gamma(1+x) \sim 1-0.5748646x+0.9512363x^2-0.6998588x^3+0.4245549x^4-0.1010678x^5, \quad (21)$$

where the error inherent is below 2.2E-7. As shown in Figure 10, there are very good agreements between evaluated values like SCF method and analytically.

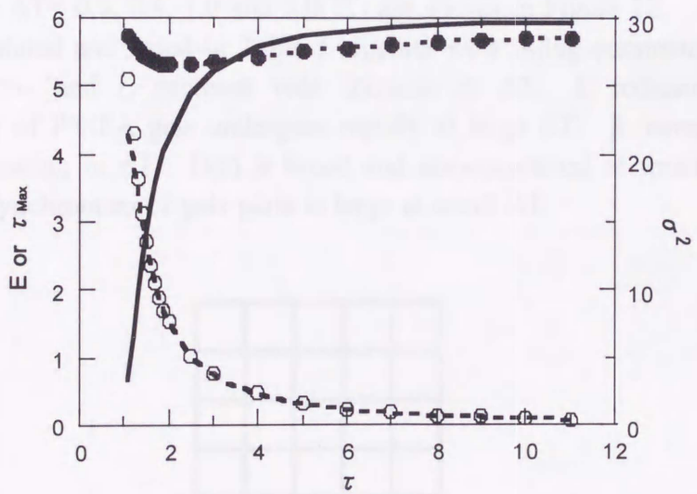

Figure 6. Average E, dispersion σ^2 and τ_{Max} of distribution function $D(\tau)$ (equation (10)) are plotted as a function of β. Solid, broken and dotted lines are analitically evaluated ones τ_{Max}, E and σ^2, while solid and round circle are E and σ^2 evaluated like SCF, respecrively

7) Shrinking Phenomenon of PNIPA Gels from the viewpoint of Distribution Function

Stretched exponential function(equation (1)) with $\beta>1$ was proposed as a part of fitting function of S(t), that is, the second shrinking process of PNIPA gels. When a stretched exponential function (equation (1)) with $\beta>1$ is observed phenomenologically, if elemental function is step-like, the distribution function of τ $D(\tau)$ is expressed by equation (10). Here let us imagine that PNIPA gels consist of a lot of parts as shown in Figure 11. Each part of gels undergoes step-like shrinking at $t=\tau$ and $D(\tau)$ is expressed by equation (10). In the previous report, we assumed that skin layer which is formed on the surface of gels collapse or change its nature on the secondary shrinkage. τ_2 and β in equation (2) are average time to collapse skin layer and the strength of collapse of skin layer, respectively. Assuming that skin layer shows a step-like collapse in each part of gels at $t=\tau$, average E and dispersion σ^2 of $D(\tau)$ are given instead of τ_2 and β. That is, E and σ^2 are average time to collapse skin layer and the degree of asynchronous collapse of skin layer, respectively.

Although PNIPA gels show two-step shrinking, a single exponential expresses the first shrinking process of PNIPA gels and there is no distribution of characteristic time of shrinking τ. On the other hand, a lot of parts in gels shrink on the second stage and the distribution of τ $D(\tau)$ is explained by equation (10). Various $D(\tau)$ of secondary shrinking process at ΔT= 0.0, 0.4, 1.0 and 3.0(℃) are shown in Figure 12. τ_{Max} , E and σ^2 of $D(\tau)$ are calculated and listed in Table I together with fitting parameter values of equation (2). τ_2, τ_{Max} and E decrease with increase in ΔT. It indicates that the secondary shrinking of PNIPA gels undergoes rapidly at large ΔT. β increases and σ^2 decreases with increasing in ΔT. $D(\tau)$ is broad and unsymmetrical at small ΔT and it indicates that the asynchronism of gels parts is large at small ΔT.

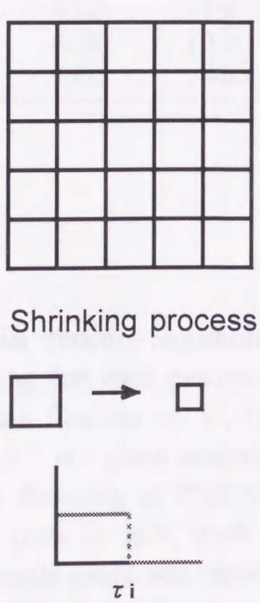

Figure 7. Secondary shrinking process of PNIPA gels

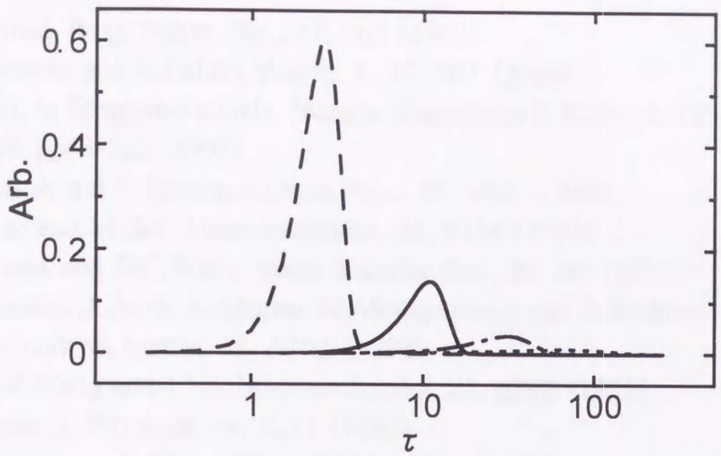

Figure 8. $D(\tau)$ in second shrinking process of PNIPA gels at ΔT=0.0℃ (dotted), 0.4℃ (□), 1.0℃ (solid) and 3.0℃ (broken).

Table I. Fitting parameters of S(t) (equation (2)) A_2, τ_2 and β and the characteristic parameters of $D(\tau)$ (equation (10)) τ_{Max}, E and σ^2. E and σ^2 correspond to τ_2 and β, respectively.

ΔT(℃)	A_2	τ_2 (min)	β	τ_{Max} (min)	E	σ^2
0.0	0.145	94.7	2.04	68.2	83.9	1.86×10^{3}
0.4	0.389	35.3	3.14	31.4	31.6	1.21×10^{2}
1.0	0.702	11.6	4.28	10.9	10.6	7.76×10^{0}
2.0	0.770	2.80	4.49	2.63	2.56	4.17×10^{-1}

1-2-4. Conclusion

When a stretched exponential function (equation (1)) with $\beta>1$ is observed phenomenologically as I(t), assuming that each process undergoes like step function as $F(t,\tau)$ in each part, the distribution function of τ, $D(\tau)$ is expressed by equation (10). The average E, distribution σ^2 are given analytically in this discussion. If this concept is applied to the secondary shrinking of PNIPA gels, it can be considered that, assuming that there are a lot of parts in gels, each part shrinks step-like and the distribution function of the characteristic times was represented as $D(\tau)$

References

1. H.G.Schild, Prog. Polym. Sci., 17, 163 (1992)
2. C.Hashimoto and H.Ushiki, Polym. J., 32, 807 (2000)
3. A.Onuki, in 'Responsive Gels: Volume Transitions I' K.Dusek Eds., Adv. Polym. Sci., 109, pp63-122 (1993)
4. E.S.Matsuo and T.Tanaka, J.Chem.Phys., 89,1695 (1988)
5. T.Tomari and M.Doi, Macromolecules, 28, 8334 (1995)
6. G.Williams and D.C.Watts, Trans. Faraday Soc., 66, 80 (1970)
7. J.Colmenero, A.Arbe, A.Alegria, M.Monkenbusch and D.Richter, J.Phys.:Condens. Matter, 11, A363 (1999)
8. B.Chu, Z.Wang and J.Yu, Macromolecules, 24, 6832 (1991)
9. U.Evesque, J. Physique, 44, 1217 (1983)
10. P.G. de Gennes, J. Chem. Phys., 76(6), 3316 (1982)
11. Avrami, J. Chem. Phys., 7, 1103 (1939); 8, 212 (1940); 9, 177 (1941)
12. R.Kubo and T.Tomita, J. Phys. Soc. Jpn., 9, 888 (1954)
13. H.Ushiki, in 'Applied Fluorescence in Chemistry Biology and Medicine', W. Rettig, B. Strehmel, S. Schrader and H. Seifert, Eds., Springer, Heidelberg, p325-370(1999)
14. Y.Li and T.Tanaka, J. Chem. Phys., 92(2), 1365 (1990)
15. H.Ushiki, J.Rouch, J.Lachaise and A.Gracia, Rep. Prog. Polym. Phys. Jpn., 41, 497 (1998)
16. S.W.Provencher, Makromol. Chem., 180, 201 (1979)

Chapter 2. Whitening Process of PNIPA Gels

2-1. Abstract

Kinetics of whitening process of disk-like poly (N-isopropylacrylamide) (PNIPA) gels which show the temperature induced volume change was discussed in this report. Just after PNIPA gels are immersed into thermostat apparatus over the critical point, they shrink and become opaque, then the whitening slowly disappears. The whitening process accompanied with shrinking one was measured and analyzed by our original apparatus and analytical method. A fitting function for the temporal change of whitening of gels is proposed as double differential stretched exponential functions. It indicates that whitening occurs like δ function in each part when gels shrink in each part, assuming that there are a lot of parts from the viewpoints of mesoscopic level.

2-2. Introduction

All materials are formed by their elements-in-theirselves and the relationship between dynamics of their elements. Their elements are divided into various classes of nature, and there is an especial movement in each class. The concept of class organization in nature connects with the recent research theme of 'complex system', 'complex fluid', 'supermolecules', 'cluster', etc. It is very important to discuss the fundamental principle of the relationship between each class of nature in order to clarify the mechanism of structural formation processes in condensed matter. Especially it is necessary to discuss from the viewpoint of dynamics in order to understand the following vector development, reaction→relaxation→transition→structural formation. According to the optical spectroscopic techniques, measurement images of five class organizations in macromolecules are shown in Figure 1. In naked eye and microscope levels, a typical measurement technique is CCD video graphical analysis. In light scattering level, it is static and dynamic two-dimensional light scattering analysis. In molecular level, it is fluorescence molecular probe analysis. In functional group level, it is two-dimensional image raman microscope. The effective length scale for measurement are approximately $\sim 1\,\mu$m, $10\,\mu$m$\sim$10 nm, 100 nm$\sim$1 nm, 10 nm$\sim$ in naked eye and microscope levels, in light scattering level, in molecular level and in functional group level, respectively. Two dimensional images were discussed in both real and wave-number space from a different point of view[1]. Two-dimensional light scattering images are obtained in wave-number space, while image in real space can be transferred to two-dimensional Fourier transformation image in wavenumber space. Till now we were making a new apparatus named PLASMA (Perfective Laboratory Automation System for Macromolecular Analysis) based on the concept mentioned above[2].

The concept of PLASMA will be effective to clarify the mechanism of volume phase transition processes of gels. Volume phase transition of gels has so far been

Naked Eye and Microscope Levels

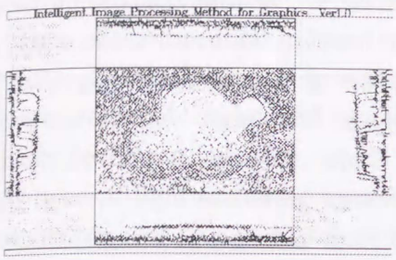

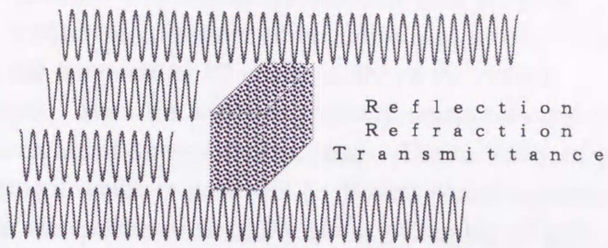

Example: Two Dimensional Graphics Analysis for Shape, Light and Shade, and Pattern of Gels

Light Scattering Level

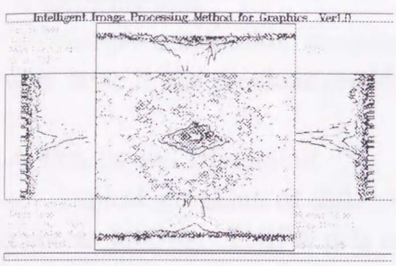

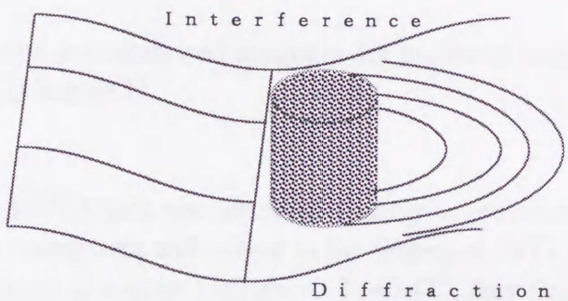

Example: Static and Dynamic Two Dimensional Light Scattering Analysis for Mesoscopic Domain Structure in Gels

Molecular Level

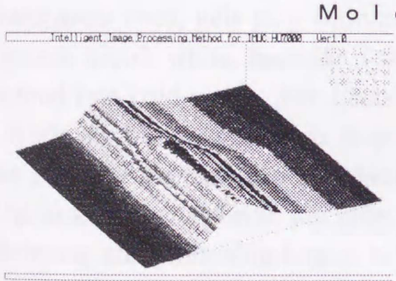

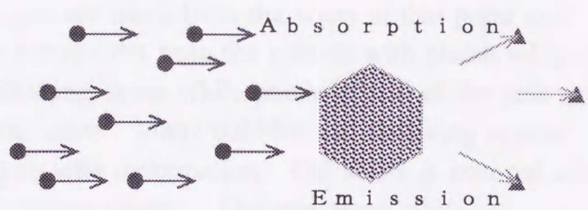

Example: Molecular Probe Analysis for Microenveronment, Motional Behaviour, and Microstructure in Gels

Functional Group Level

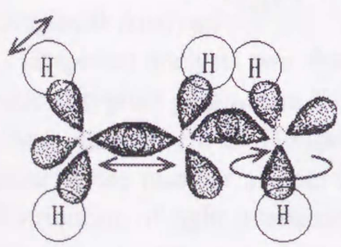

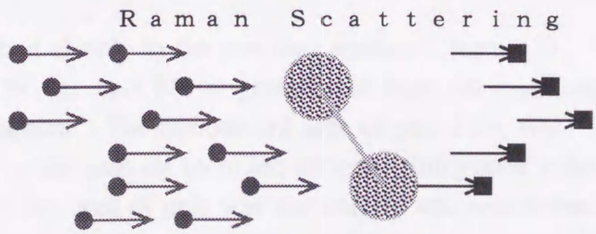

Example: Two Dimensional Raman Scope Analysis for Distribution of Various Functional Groups in Gels

Figure 1. Schematic diagram of optical spectroscopic techniques for each class organization in Gels.

investigated by various measurements ··· microscope[3], light scattering[4], neutron scattering[4], NMR spectroscopy[5], fluorescence spectroscopy[6] and so on. Poly (N-isopropylacrylamide) (PNIPA) gels are well known as nonionic gels showing volume phase transition induced by temperature, solvent composition and so on. When PNIPA gels are immersed in water, the temperature of which is above the critical temperature, gels shrink and be opaque. Then the whitening slowly disappears and gels finally become transparent, which is regarded as equilibrium state. The turbidity of gels has rejected light scattering measurement which is powerful to discuss phase separation mechanism and few studies from the viewpoints of turbidity about whitening of gels have been carried out[7, 8, 9]. They showed an initial increase in turbidity of PNIPA gels and tried to discuss the whitening from the viewpoint of phase separation.

2-3. Experimental

Sample preparation, experimental procedure and programs for graphical analysis were same in the previous section (Chapter 1).

2-4. Results and Discussion

Typical shrinking of disk-like PNIPA gels was observed visually in previous section as follows. PNIPA gels are transparent and adhere to the fingers at 20℃ before shrinking. When the gels are immersed in a water bath above T_c+0.4℃, they first shrink monotonically. If lighted from above by a white light source, they become bluish white due to intense multiple scattering. Bluish white gels are less adhesive than transparent ones, gels stop shrinking for a while. During this first step, and the gels become bluish white, because if the gels are taken from the water at that point and poured into cold water, then become transparent from the outside with bluish white core. While the bluish white gels stop shrinking, some white points appear in the gels and the edges of the disk-like gels become white. Many bubbles and shrinking appear. The disk-like gels shrink abruptly again with deformation. Gel shape is restored after shrinking and whitening begins to disappear slowly. The gels show white and transparent spots randomly. With time the white spots slowly disappear and finally the gels become completely transparent.

1) Graphical Analysis

Graphical analysis was described closely in the previous section (Chapter 1). We introduced typical parameters $S(t)$, $W_1(t)$ and $W_2(t)$ transferred from the monitored graphical images by a CCD video camera. The normalized area of gels $S(t)$ was obtained by the number of dots due to the gels on recorded images. Integrated value of the distribution of light intensities within area of gels was normalized and was named the normalized whitening amount of gels $W_1(t)$. Normalized whitening amount of gels per unit area $W_2(t)$ was obtained by $W_1(t)/S(t)$. Plots of $S(t)$, $W_1(t)$ and $W_2(t)$ as a function of time at various ΔT are shown in Figure 2. Calculated $\Delta S(t)/\Delta t$ was also plotted. $S(t)$ first decreases monotonically and stop shrinking for a while, then

decreases drastically and keeps a certain constant value. $W_1(t)$ and $W_2(t)$ first increase sharply and decrease gradually, reaching 0 at the final stage. A synchronization between shrinking and whitening processes of PNIPA gels is found out intuitively. $W_2(t)$ shows a maximum when $S(t)$ reaches a minimum. The sample gels sometimes stuck to glass plates, and probably due to the adhesiveness of transparent PNIPA gels. In most cases, these gels did not shrink more and never became white. If the fixed part was taken off, gels started to shrink and became white. This indicates that gels will not be white without shrinking. It is also interesting that $\Delta S(t)/\Delta t$ is accordance with $W_1(t)$ in the initial stage at $\Delta T=3.0℃$ as shown in Figure 2(d). It indicates the fact that the temperature-induced shrinking process of PNIPA gels clearly undergo together with whitening one.

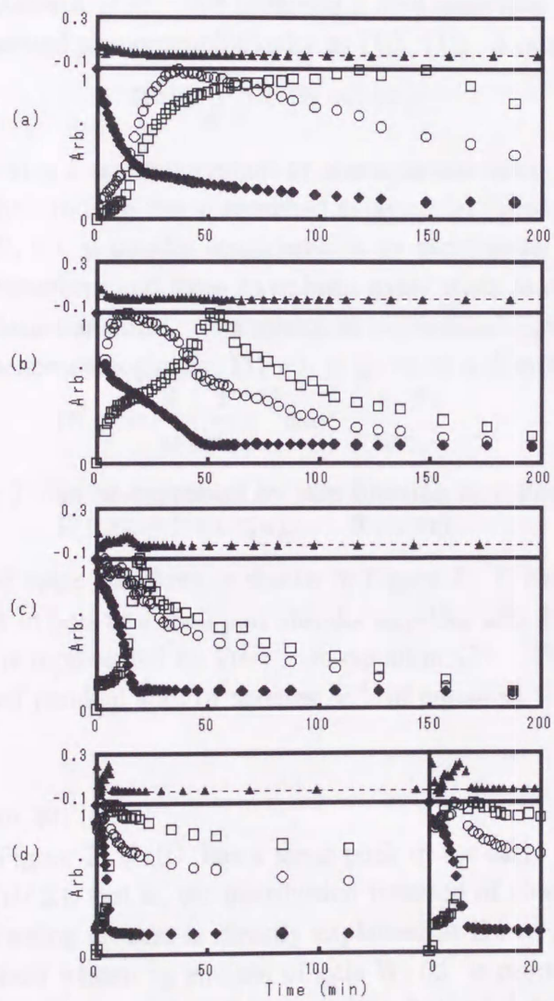

Figure 2. Graphs for normalized area of gels $S(t)$ (●), normalized whitening amount of gels $W_1(t)$ (□), normalized whitening amount of gels per unit area $W_2(t)$ (○) and $\Delta S(t)/\Delta t$ (▲). Thickness of gels is about 0.3mm. ΔT is (a) 0.0℃, (b) 0.4℃, (c) 1.0℃, (d) 3.0℃, respectively.

2) Curve Fittings for S(t)

As shown in previous section (Chapter 1), PNIPA gels show a two-step shrinking after jumping temperature and the fitting function of normalized area of gels S(t) was proposed as follows

$$S(t) = A_1 \exp\left(-\frac{t}{\tau_1}\right) + A_2 \exp\left(-\left(\frac{t}{\tau_2}\right)^{\beta}\right) + (1-A_1-A_2) \quad (1)$$

The first and second terms represent first and second stage of shrinking, respectively. The first term is a usual relaxation function deduced by T.Tanaka et al and they showed that the shrinking of gels is explained as collective diffusion with infinitesimal deformation of an elastic body. The second term is a stretched exponential function and the third one is fraction of shrunken gels.

The second stage of shrinking was always expressed by a stretched exponential function with the exponent $\beta > 1$. We proposed a new analytical concept as follows. If some process is observed phenomenologically as I(t), I(t) is represented by

$$I(t) = \int_0^{\infty} D(\tau) F(t,\tau)\, d\tau , \quad (2)$$

where $D(\tau)$ and $F(t, \tau)$ are distribution of characteristic time τ and element function, respectively. In case that a stretched exponential function with $\beta < 1$ is observed as I(t), $F(t, \tau)$ is usually considered as an exponential function. This relation is Laplace transform and there have been many trials to obtain $D(\tau)$ by solving inverse-Laplace transform. If a stretched exponential function with $\beta > 1$ is observed as I(t) phenomenologically, $D(\tau)$ is given as a distribution function by

$$D(\tau) = \frac{\beta}{\tau_0}\left(\frac{\tau}{\tau_0}\right)^{\beta-1} \exp\left(-\left(\frac{\tau}{\tau_0}\right)^{\beta}\right) \quad (3)$$

assuming that $F(t, \tau)$ can be expressed by step function as follows

$$F(t,\tau) = 1 \ (t \leqq \tau), \qquad 0 \ (t > \tau) \quad (4)$$

The image of second stage shrinking is shown in Figure 3. It can be considered that there are many parts in gels and each part shrinks step-like and the distribution of the characteristic times is represented by $D(\tau)$ in equation (3). The values of various fitting parameters and residual sum of squares χ^2 of equation (1) at various ΔT are listed in Table I.

3) Curve Fittings for $W_1(t)$

As shown in Figure 2, $W_1(t)$ has a steep peak in the early stage at large ΔT and it is similar to $\Delta S(t)/\Delta t$, that is, the distribution function of characteristic time $D(\tau)$. Assuming that whitening process is directly explained as $D(\tau)$, the following fitting functions of normalized whitening amount of gels $W_1(t)$ is proposed as

$$W_1(t) = B_1\left[B_2\left(\frac{t}{\tau_a}\right)^{\beta_a-1} \exp\left(-\left(\frac{t}{\tau_a}\right)^{\beta_a}\right) + (1-B_2)\left(\frac{t}{\tau_b}\right)^{\beta_b-1} \exp\left(-\left(\frac{t}{\tau_b}\right)^{\beta_b}\right)\right] \quad (5)$$

Equation (5) consists of two terms and it indicates that two whitening processes undergo independently. PNIPA gels show a two-step shrinking and whitening process

such as transparency → whitening → transparency is accompanied with each shrinking one. Each whitening process is directly explained by $D(\tau)$ and the idea of whitening one is shown in Figure 3. Assuming that there are a lot of parts from the viewpoints of mesoscopic level, whitening occurs like δ function in each part when gels shrink in each part. Whitening occurs in the instance when gels shrink at $t=\tau$ and the distribution of characteristic times $D(\tau)$ is represented by equation (3). Curve fittings for $W_1(t)$ at various ΔT are shown in Figure 3. Equation (5) can be found to be in good agreement with data, especially a peak in the initial stage at $\Delta T=3.0℃$. Values of various fitting parameters and the residual sum of squares χ^2 of equation (5) at various ΔT are listed in Table II.

Normalized whitening amount of gels per unit area $W_2(t)$ was obtained by

$$W_2(t) = W_1(t)/S(t) \quad (6)$$

Curve fittings for $W_2(t)$ by equation (6) substituted equation (1) and (5) are also shown in Figure 3 at various ΔT. $W_2(t)$ is in good agreement with equation (6). Values of fitting parameters of equation (6) were basically same as ones of equation (5). and they are listed in Table II. The strong synchronization of $S(t)$ and $W_2(t)$ indicates the fact that macroscopic phenomenon is coupled with mesoscopic one in volume phase transition of PNIPA gels.

4) Whitening of Gels

Shrinking process of gels has been considered as fluctuation of phase separation between polymer chain and solvents. Although whitening behavior on shrinking process of PNIPA gels show the formation of domains over wavelength of visible light, whitening itself is considered as fluctuation of phase separation. $W_1(t)$ is the integrated scattering light intensities due to whitening of gels and an initial steep increase in $W_1(t)$ was observed at every ΔT. Y.Li et al. observed the temporal change in transmitted light intensities of PNIPA gels and showed that the turbidity increases xponentially and remains constant when PNIPA gels are immersed into hot water which of temperature is above the critical temperature[8]. R.Bansil et al. showed a ring by two-dimensional light scattering of PNIPA gels and described that the time evolution of the scattered light in the same condition is represented by single exponential function[9]. According to the theory of spinodal decomposition[15], the scattered light intensity I_s is related to the fluctuation growth rate $R(q)$ as follows

$$I_s(q,t) \sim \exp[2R(q)t] \quad (7)$$

where q is the scattering wavevector and t is time. However disappearance of whitening has not been considered in discussion of PNIPA gelsphase separation mechanism. Dynamics of gels on the basis of phase diagram is not still clear, although determination of spinodal line of gels was discussed with the structure factor by T.Tanaka[16] and A.Onuki[17]. Increasing and decreasing of scattered light was also observed on phase separating process of polymer solution, but scattered light has been usually studied from the viewpoint of q, not t[18, 19]. At that point, equation (5) is a new approach to discuss the appearance and disappearance of whitening.

As listed in Table II, τ_a and τ_b are separated well on whitening processes of $W_1(t)$. Although fitting parameters of $S(t)$ is listed in Table I, every τ_i(i=a,b) of $W_1(t)$ was larger than corresponding τ_i(i=1,2) of $S(t)$. It accordance the fact that PNIPA gels will not be white without shrinking above mentioned[11], so τ_a decreases with increasing ΔT and it indicates that the early whitening process corresponds to the first shrinking. On the other hand, τ_b shows the minimum value at ΔT=0.4℃. It will be due to the the elastic effect of polymer chain.

2-5. Conclusion

In closing, we would like to sum some new knowledge in this report as follows;

(1) The synchronization of shrinking and whitening indicates the fact that macroscopic phenomena is coupled with mesoscopic one in volume phase transition of PNIPA gels.

(2) Equation (3) is adequate to explain $W_i(t)$. It indicates that, assuming that there are a lot of parts in gels from the viewpoints of mesoscopic level, whitening occurs like δ function in each part when gels shrink in each part.

(3) A fitting function of $W_2(t)$ is proposed as $W_1(t)/S(t)$.

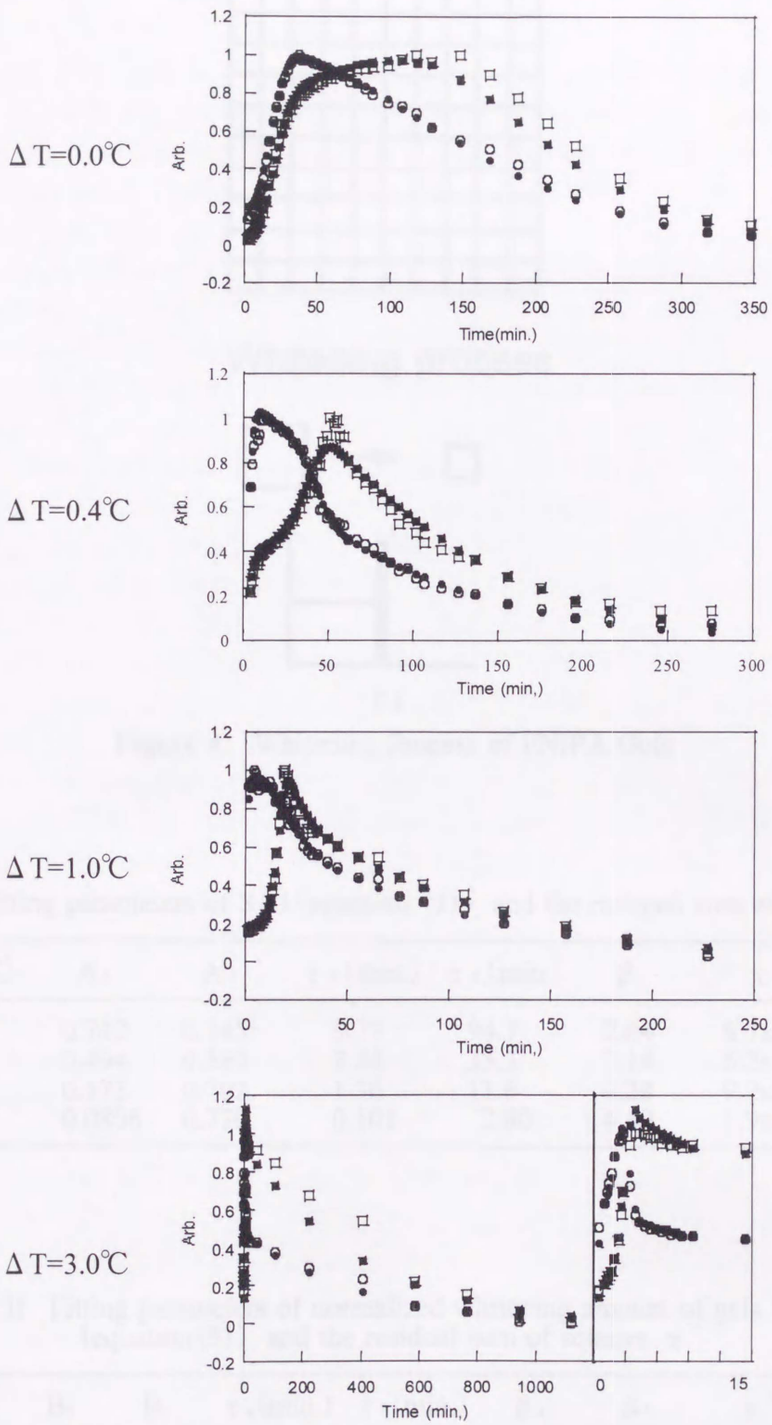

Figure 3. $W_1(t)$ and $W_2(t)$ are plotted as a function of time at various ΔT. $W_1(t)$ (○) and $W_2(t)$ (□) are fitted by equation (1) (●) and equation (2) (■), respectively.

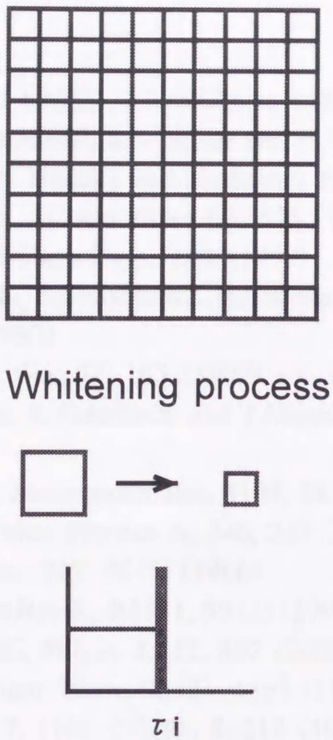

Figure 4. Whitening Process of PNIPA Gels

Table I. Fitting parameters of S(t) (equation (1)) and the residual sum of squares χ^2

ΔT(℃)	A_1	A_2	τ_1 (min.)	τ_2 (min.)	β	χ^2
0.0	0.742	0.145	9.77	94.7	2.04	8.7×10^{-5}
0.4	0.494	0.389	3.54	35.3	3.14	6.2×10^{-5}
1.0	0.173	0.702	1.36	11.6	4.28	9.2×10^{-5}
3.0	0.0806	0.770	0.101	2.80	4.49	1.9×10^{-5}

Table II Fitting parameters of normalized whitening amount of gels W_1 (t) (equation (5)) and the residual sum of squares χ^2

△T(℃)	B_1	B_2	τ_a (min.)	τ_b (min.)	β_a	β_b	χ^2
0.0	170	138	42.2	140	2.63	1.77	1.4×10^{-3}
0.4	27.0	40.0	28.8	90.0	1.45	1.60	8.3×10^{-4}
1.0	7.72	134	12.9	169	1.46	1.16	1.1×10^{-3}
3.0	0.988	191	2.74	404	3.67	0.990	5.4×10^{-4}

References

1. H.Tanaka, T.Hayashi and T.Nishi, J.Appl.Phys., 4480, 65(12) (1989)
2. Ushiki,H., W.Rettig, B.Strehmel, S.Schrader and H.Seifert, Eds. 'Applied Fluorescence in Chemistry Biology and Medicine', Springer, 325-370 (1999)
3. E.S.Matsuo and T.Tanaka, J.Chem.Phys., 89,1695 (1988)
4. M.Shibayama, Macromol.Chem.Phys., 198 (1997)
5. H.Yasunaga, M.Kobayashi, S.Matsukawa, H.Kurosu and I.Ando, Annual Rep. NMR Spectroscopy, 39 (34) (1997)
6. H.G.Schild, Prog. Polym. Sci., 17, 163 (1992)
7. T.Takigawa, T.Yamawaki, K.Takahashi and T.Matsuda, Polym. J., 595, 31(7) (1999)
8. Y.Li, G.Wang and Z.Hu, Macromolecules, 4194, 28 (1995)
9. R.Bansil, G.Liao and P.Falus, Physica A, 346, 231 (1996)
10. H.Tanaka, Phys. Rev. Lett., 787, 76(5) (1996)
11. A.Onuki and S.Puri, Phys.Rev.E, R1331, 59(2) (1999)
12. C.Hashimoto and H.Ushiki, Polym. J., 32, 807 (2000)
13. Y.Li and T.Tanaka, J. Chem. Phys., 92(2), 1365 (1990)
14. Avrami, J. Chem. Phys., 7, 1103 (1939); 8, 212 (1940); 9, 177 (1941)
15. J.W.Cahn and J.E.Hilliard, J.Chem.Phys., 688, 31(3) (1959)
    J.W.Cahn, J.Chem.Phys., 93, 42(1) (1965)
16. A.Hochberg, T.Tanaka and D.Nicoli, Phys.Rev.Lett., 217, 43(3) (1979)
17. A.Onuki, in 'Responsive Gels: Volume Transitions I' K.Dusek Eds., Adv. Polym. Sci., 109, pp63-122 (1993)
18. K.Kuwahara, K.Hamano, N.Aoyama and T.Nomura, Phys.Rev.A, 27(3), 1724 (1983)
19. H.Furukawa, Adv.Phys., 703, 34(6) (1986)
20. A.T.Bharucha-Reid, "Elements of the Theory of Markov Processes and their Applications", McGraw-Hill, New York (1960)
21. H.Ushiki and H.Obata, Seibutsukagaku, 69, 29(2) 1977: 158, 29(3) (1977)
22. V.K.LaMer and R.H.Dineger, J.Ame.Chem.Soc., 4847, 72(11) (1950)

Chapter 3. Size of Gels and Temperature Effects on Shrinking and Whitening Processes

3-1. Abstract

Our digital image analysis was applied to investigate the shrinking and whitening processes of disk-like Poly(N-isopropylacrylamide) (PNIPA) gels after temperature jump above the critical temperature. PNIPA gels show two-step shrinking accompanied with intense multiple scattering and the whitening of gels slowly disappear after shrinking. Size of disk-like gels and jumping temperature were changed and the effects on both shrinking and whitening processes was discussed. Diameter of disk-like gels gives no change, while the time scale of shrinking and whitening processes is elongated with increasing thickness of gels. The relationship between shrinking(whitening) process and thickness of gels suggests that PNIPA gels shrink as collective diffusion with infinitesimal deformation. Critical slowing down is observed in shrinking and whitening processes and shrinking process in macroscopic level is always strongly related to whitening one in mesoscopic level. However disappearance of whitening is slow when temperature gap is large and it will be due to the effect of strong elastic effects of gels chain. When gels are thick and jumping temperature is high, 3 step shrinking was shown and the possibility of multi-step shrinking was proposed.

3-2. Introduction

T.Tanaka et. al. proposed that the swelling and shrinking processes of gels are explained by diffusion equation, assuming that gels shrink infinitesimally and isotropically as an elastic body. A sum of single exponential functions was obtained to express the volume change of gels[1] and the characteristic relaxation time τ was represented by

$$\tau \propto R^2/D , \qquad (1)$$

where R and D are the characteristic length of gels and the cooperative diffusion coefficient between polymer chain and solvents, respectively. In case of disk-like gels, R is thickness of gels. Since the thickness of disk-like gels is much smaller than the diameter, the time to diffuse along thickness of gels is dominant. In case of PNIPA gels, volume change in shrinking process was expressed by a sum of a single exponential and a stretched exponential functions in previous section (Chapter 1). The first and second shrinkings are expressed by a single exponential and a stretched exponential functions, respectively. It was considered that the two-step shrinking is due to the skin layer was formed on the surface of gels in the final stage of first shrinking. PNIPA gels become turbid when gels shrink and then the turbidity disappears slowly. Such whitening process is accompanied with shrinking process

and represented by a distribution function and the meaning of a fitting function was discussed in Chapter 2..

3-3. Experimental

1) Sample Preparation

Details of sample preparation were completely same in previous section (Chapter 1). PNIPA gels were synthesized between glass plates with a spacer, the thickness of which was about 0.1, 0.2, 0.3 and 0.4mm. The synthesized sheet-like gels was taken out from the glass plates and washed several times with a large amount of distilled water for about a week. Thicknesses of gels were measured under a microscope at room temperature. The gels swell after taking out from the cell for synthesis and thickness of gels changes from 0.1, 0.2, 0.3 and 0.4 to 0.5, 0.7, 1.5 and 2.0mm, respectively. Disk-like gels were prepared by cutting out the sheet-like gels with a cookie cutter, the diameter of which was about 28, 34 and 48mm. The sample gels were put into a cell of 0.7, 1.0 and 2.0mm thickness filled with distilled water and sealed with epoxy resin. The crosslinkage density of the sample gels was about 8.8×10^{-3}. The critical temperature (Tc) was about 33.7℃ assigned based on cloud point measurements and did not depend on size of gels.

2) Experimental Procedure

Details of experimental measurement was written in previous section (Chapter 1). The sample cell was set up in a water bath, which was thermostated at $Tc+\Delta T$ ($\Delta T=0.0 \sim 5.0$℃) with the accuracy of about 50mK. The shrinking and whitening processes of the sample gels are observed by a digital video CCD camera.

3-4. Size Effects

1) Graphical Analysis

Details of graphical analysis were described in previous section (Chapter 1). In order to evaluate the shrinking and whitening processes of PNIPA gels, the following parameters $S(t)$, $W_1(t)$ and $W_2(t)$ were calculated from the time-resolved recorded images by a CCD video camera. The normalized area of gels $S(t)$ was obtained by the number of dots due to the gels on recorded images. Integrated value of the distribution of light intensities within area of gels was normalized and was named the normalized whitening amount of gels $W_1(t)$. Normalized whitening amount of gels per unit area $W_2(t)$ was obtained by $W_1(t)/S(t)$.

When disk-like gels shrink, the edge part of the gels tends to turn over. Therefore the thickness of the cell was changed in order to estimate the effect of the edge's turning over. Plots of $S(t)$, $W_1(t)$ and $W_2(t)$ at various thickness of cell at $\Delta T=1.0$℃ are shown in Figure 1. In temperature-induced volume phase transition process of PNIPA gels, $S(t)$ first decreases monotonically and keeps a certain constant value. $W_1(t)$ and $W_2(t)$ first increase sharply and decrease gradually.

Thickness of cell gives no change of $S(t)$, $W_1(t)$ and $W_2(t)$. It can be concluded that the effect of the edge's turning over is little in our experiments.

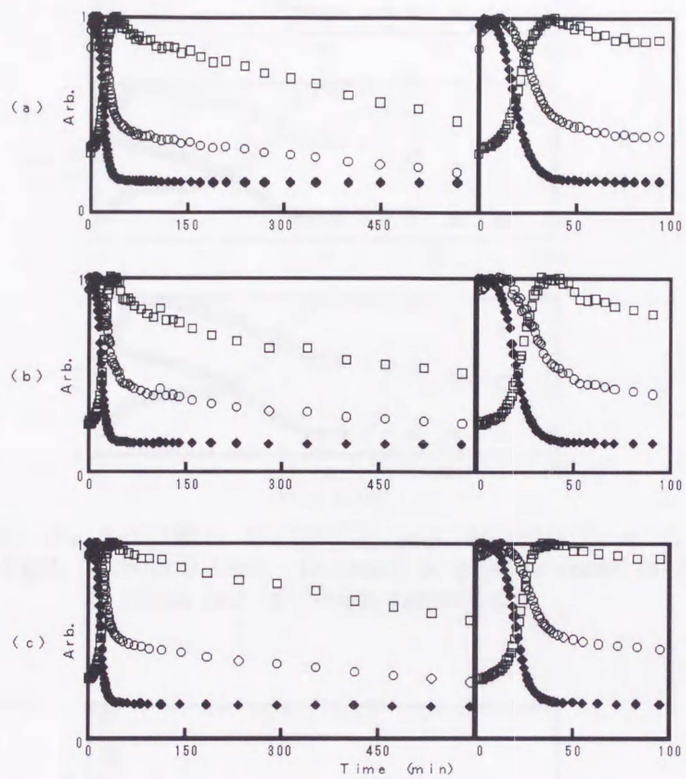

Figure 1. Graphs for normalized area of gels $S(t)$ (●), normalized whitening amount of gels $W_1(t)$ (□) and normalized whitening amount of gels per unit area $W_2(t)$ (○) at $\Delta T=0.4℃$. Thickness of gels is about 0.4mm. Thickness of cell are about (a) 0.7mm, (b) 1.0mm and (c) 2.0mm, respectively.

Thickness of cell was fixed to 2.0mm and size of gels was changed. Figure 2 shows the plots of $S(t)$, $W_1(t)$ and $W_2(t)$ at various diameter of disk-like gels at $\Delta T=0.4℃$. $S(t)$ clearly shows a two-step shrinking. $W_1(t)$ increases abruptly and decreases gradually. $W_2(t)$ is synchronized with $S(t)$ well till the gels shrink. The diameter of the gels gives no change of $S(t)$, $W_1(t)$ and $W_2(t)$ at all. On the other hand, the plots of $S(t)$, $W_1(t)$ and $W_2(t)$ at various thickness of gels are shown in Figure 3. Only the time scale of $S(t)$, $W_1(t)$ and $W_2(t)$ is elongated with increasing thickness of gels and the shapes of curves are not changed by thickness of gels. Figure 2 and 3 show that the synchronism of $S(t)$ and $W_2(t)$ holds over the size range of gels.

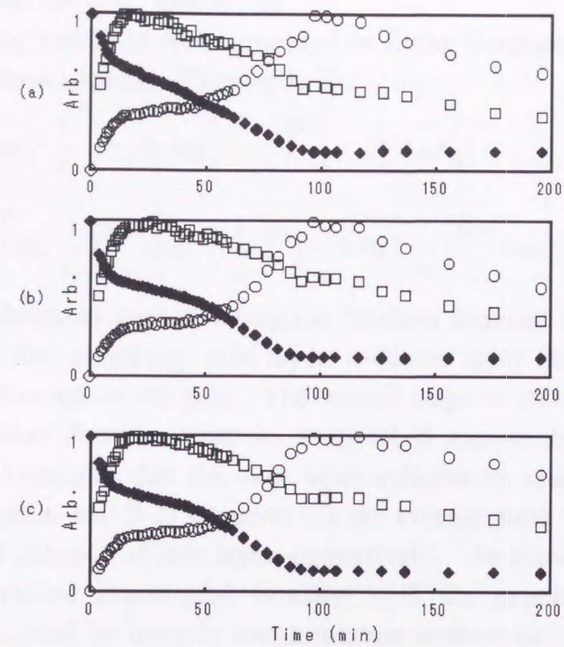

Figure 2. Graphs for S(t) (●), W_1(t) (□) and W_2(t) (○) at ΔT=0.4℃. Thickness of gels is about 0.3mm. Diameter of gels are about (a) 28mm, (b) 38mm and (c) 46mm, respectively.

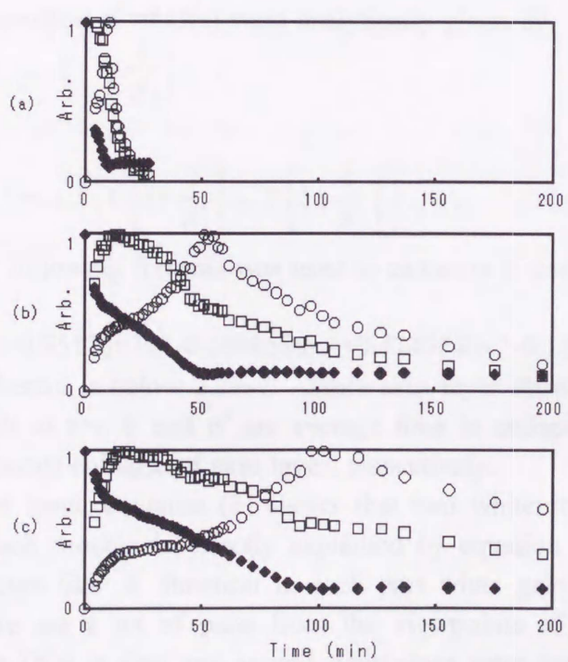

Figure 3. Graphs for S(t) (●), W_1(t) (□) and W_2(t) (○) at ΔT=0.4℃. Diameter of gels is about 28mm. Thickness of gels are about (a) 0.1mm, (b) 0.3mm and (c) 0.4mm, respectively.

2) Fitting Functions for $S(t)$ and $W_1(t)$

The following equations were proposed as fitting functions of $S(t)$ and $W_1(t)$ as shown in previous sections (Chapter 1, 2).

$$S(t) = A_1 \exp\left(-\frac{t}{\tau_1}\right) + A_2 \exp\left(-\left(\frac{t}{\tau_2}\right)^{\beta_2}\right) + (1-A_1-A_2) \tag{2}$$

$$W_1(t) = B_1\left[B_2\left(\frac{t}{\tau_a}\right)^{\beta_a-1}\exp\left(-\left(\frac{t}{\tau_a}\right)^{\beta_a}\right)+(1-B_2)\left(\frac{t}{\tau_b}\right)^{\beta_b-1}\exp\left(-\left(\frac{t}{\tau_b}\right)\right)^{\beta_b}\right] \tag{3}$$

PNIPA gels first shrink as a usual relaxation function deduced by diffusion equation. In final stage of first shrinking, skin layer, a denser layer due to the existence of surface tension is formed on the gels. The second stage of shrinking is expressed by an unusual relaxation function, that is, a stretched exponential function with the exponent $\beta > 1$. Assuming that the skin layer collapse or change its nature in the secondary shrinkage, τ_2 and β in equation (2) are average time to collapse skin layer and the strength of collapse of skin layer, respectively. As shown in Chapter 1-2, the meaning of a stretched exponential function with the exponent $\beta > 1$ in second shrinkage was described by integral transformation method as follows. Assuming a lot of parts in PNIPA gels, each part shrinks step-like at $t=\tau$ and the distribution of τ is represented by $D(\tau)$ as follows

$$D(\tau) = \frac{\beta_i}{\tau_i}\left(\frac{\tau}{\tau_i}\right)^{\beta_i-1}\exp\left(-\left(\frac{\tau}{\tau_i}\right)^{\beta_i}\right) . \tag{4}$$

Average E and dispersion σ^2 of $D(\tau)$ were analytically given by

$$E = \tau_i \Gamma\left(1+\frac{1}{\beta_i}\right) \tag{5}$$

and

$$\sigma^2 = \tau_i^2\left\{\Gamma\left[1+\frac{2}{\beta_i}\right]-\Gamma\left[1+\frac{1}{\beta_i}\right]^2\right\} \tag{6}$$

respectively. The following formula was used to calculate E and σ^2 in this report.

$$\Gamma(1+x) \sim$$
$$1-0.5748646x+0.9512363x^2-0.6998588x^3+0.4245549x^4-0.1010678x^5, \tag{7}$$

where the error inherent is below 2.2E-7. Since skin layer shows a step-like collapse in each part of gels at $t=\tau$, E and σ^2 are average time to collapse skin layer and the degree of asynchronous collapse of skin layer, respectively.

On the other hand, equation (3) shows that two whitening processes undergo independently. Each process is directly explained by equation (4) and it indicates that whitening occurs like δ function in each part when gels shrink in each part, assuming that there are a lot of parts from the viewpoints of mesoscopic level. Average E of each $D(\tau)$ in first and second whitenings were evaluated as E_a and E_b, respectively. σ_a^2 and σ_b^2 were also evaluated as dispersion of $D(\tau)$ in first and second whitenings. E_i and σ_i^2 (i=a,b) represent average time of appearance of whitening and the degree of asynchronous appearance of whitening, respectively.

3) Size of Gels Dependence on S(t)

Our experimental data in various diameters and thicknesses of gels agreed with equations (2) very well. The plots of fitting parameters of equation (2) as a function of diameter or thickness of gels at various ΔT are shown in Figure 4. Diameter of gels gives no change on any fitting parameter. Since diameter of gels is so long compared with thickness of gels in our experiments, the exhaust of solvents along the thickness of gels will be dominant. The fraction of first shrinking A_1 is large and independent on thickness of gels at $\Delta T=0.0℃$, while A_1 is relatively small and decreases with increasing thickness of gels at large ΔT. Considering A_1 as the fraction of skin layer, the thickness of skin layer is proportional to product of A_1 and thickness of gels as shown in Figure 5. Thickness of skin layer is proportional to thickness of gels at small ΔT, while thickness of skin layer becomes to costant at large ΔT. The effect of ΔT is large and the thickness of gels effects is not so obvious. As shown in Figure 4, characteristic times of shrinking τ_1 and τ_2 increase with an increase in thickness of gels. According to T.Tanaka's theory mentioned above, the relationship between characteristic time of first shrinking τ_1 and thickness of gels d is represented by equation (1) with R=d as follows. The log-log plot of τ_1 vs. d^2 is shown in Figure 6 and it agrees with equation (1) with R=d. Characteristic time of secondary shrinking τ_2 and average of $D(\tau)$ in secondary shrinking E are also plotted as a function of d in Figure 6 and the following equations hold.

$$\tau_i (i=1,2) \sim d^{-2} \qquad (8)$$

$$E \sim d^{-2} \qquad (9)$$

There is no obvious difference between τ_2 and E. τ_2 and E are characteristic time and average time to collapse skin layer, respectively. Equations (8) and (9) are same as equation (1) and it suggests that the PNIPA gels shrink in secondary shrinking as collective diffusion with infinitesimal deformation. As shown in Figure 4, the strength of skin layer collapse β_2 decreases with increasing thickness of gels. It indicates that not only the average time of collapse of skin layer but also the strength of collapse of skin layer become small when gels are thick. σ^2 is the degree of asynchronous collapse of skin layer and the log-log plot of σ^2 vs. d^2 is shown in Figure 7. The following equation holds.

$$\sigma^2 \sim d^{-4} \qquad (10)$$

It is reasonable that the exponent of equation (10) is two times that of equation (9). It indicates the asynchronous collapse of skin layer is observed when average time of collapse is large, that is, gels are thick. Not only the average time of collapse of skin layer but also the degree of synchronous collapse of skin layer become small when gels are thick.

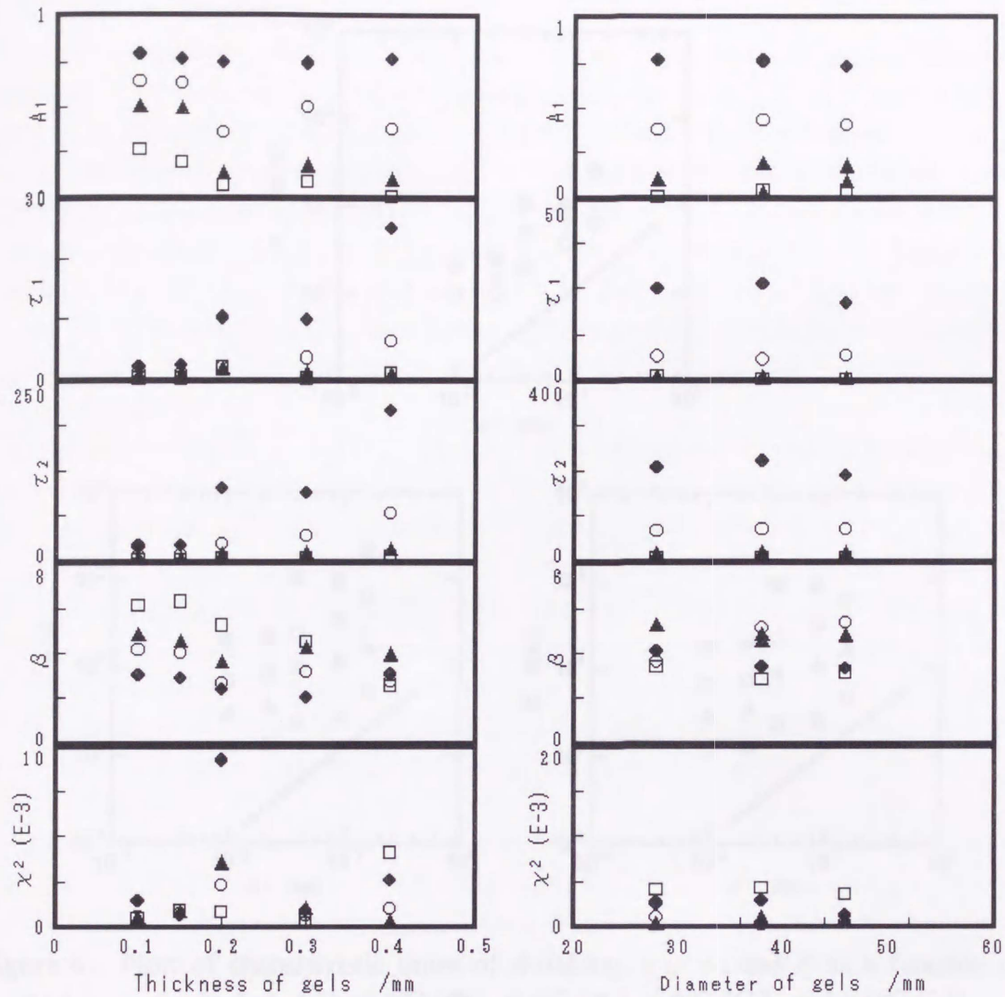

Figure 4. Relationship between size of disk-like gels and fitting parameters of equation (2) at ΔT=0.0℃(●), 0.4℃(○), 1.0℃(▲) and 3.0℃(□).

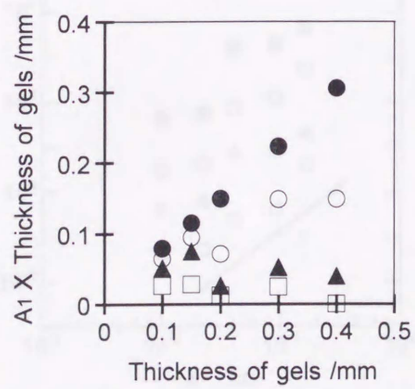

Figure 5. Plots of the fraction of first shrinking A_1 as a function of thickness of gels when at ΔT= 0.0℃●), 0.4℃(○), 1.0℃(▲) and 3.0℃(□).

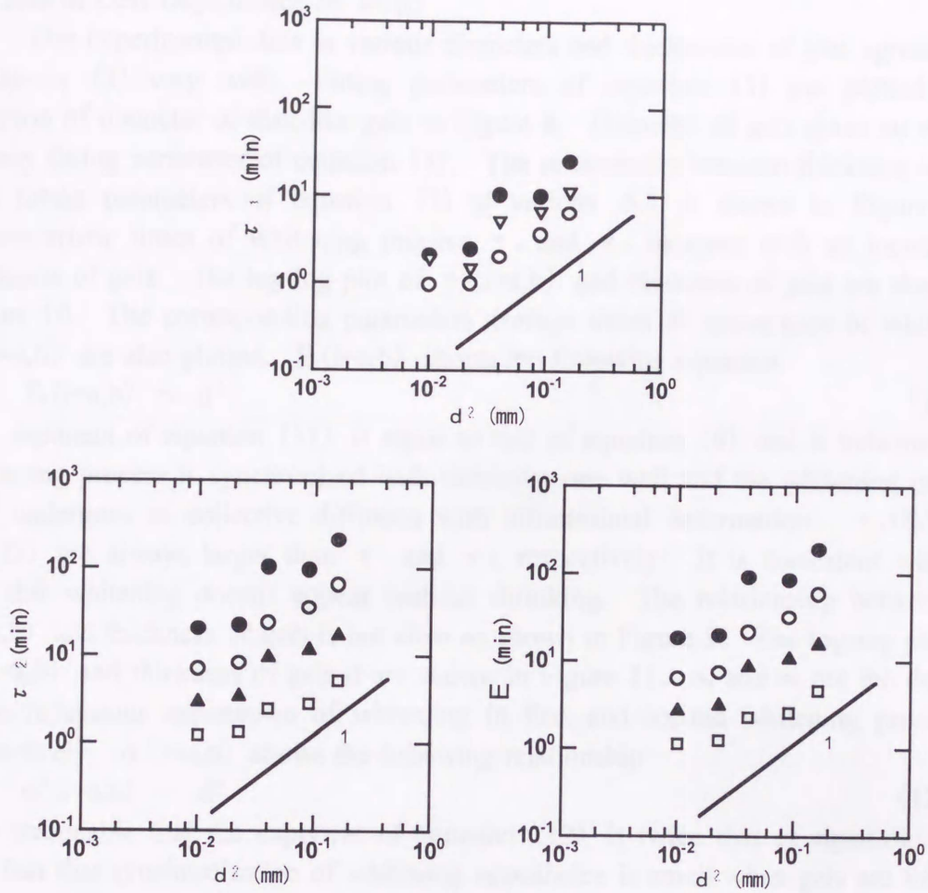

Figure 6. Plots of characteristic times of shrinking τ_1, τ_2 and E as a function of thickness of gels d at ΔT= 0.0℃ (●), 0.4℃ (▲), 1.0℃ (○) and 2.0℃ (□).

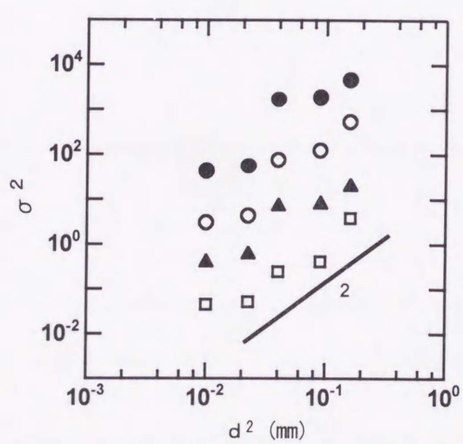

Figure 7. Plots of characteristic times of shrinking σ^2 vs. square of thickness of gels d^2 at ΔT= 0.0℃ (●), 0.4℃ (▲), 1.0℃ (○) and 2.0℃ (□).

4) Size of Gels Dependence on $W_1(t)$

Our experimental data in various diameters and thicknesses of gels agreed with equations (3) very well. Fitting parameters of equation (3) are plotted as a function of diameter of disk-like gels in Figure 8. Diameter of gels gives no change on any fitting parameter of equation (3). The relationship between thickness of gels and fitting parameters of equation (3) at various ΔT is shown in Figure 9. Characteristic times of whitening process τ_a and τ_b increase with an increase in thickness of gels. The log-log plot of τ_i (i=a,b) and thickness of gels are shown in Figure 10. The corresponding parameters average times of appearance of whitening E_i (i=a,b) are also plotted. E_i (i=a,b) shows the following equation.

$$E_i \text{ (i=a,b)} \sim d^{-2} \qquad (11)$$

The exponent of equation (11) is equal to that of equation (9) and it indicates that whitening process is synchronized with shrinking one well and the whitening process also undergoes as collective diffusion with infinitesimal deformation. $\tau_a(E_a)$ and $\tau_b(E_b)$ are always larger than τ_1 and τ_2, respectively. It is consistent with the fact that whitening doesn't appear without shrinking. The relationship between β_i (i=a,b) and thickness of gels is not clear as shown in Figure 9. The log-log plots of σ_i (i=a,b) and thickness of gels d are shown in Figure 11. σ_a and σ_b are the degrees of asynchronous appearance of whitening in first and second whitening processes, respectively. σ_i (i=a,b) shows the following relationship

$$\sigma_i^2 \text{ (i=a,b)} \sim d^{-4} \qquad (12)$$

It is reasonable that the exponent of equation (12) is twice that of equation (11). The fact that synchronization of whitening appearance is small when gels are thick is same as that of collapse of skin layer. Since $W_1(t)$ is synchronized with $S(t)$ well, size of gels dependence on $W_1(t)$ is very similar to that of $S(t)$ mentioned above.

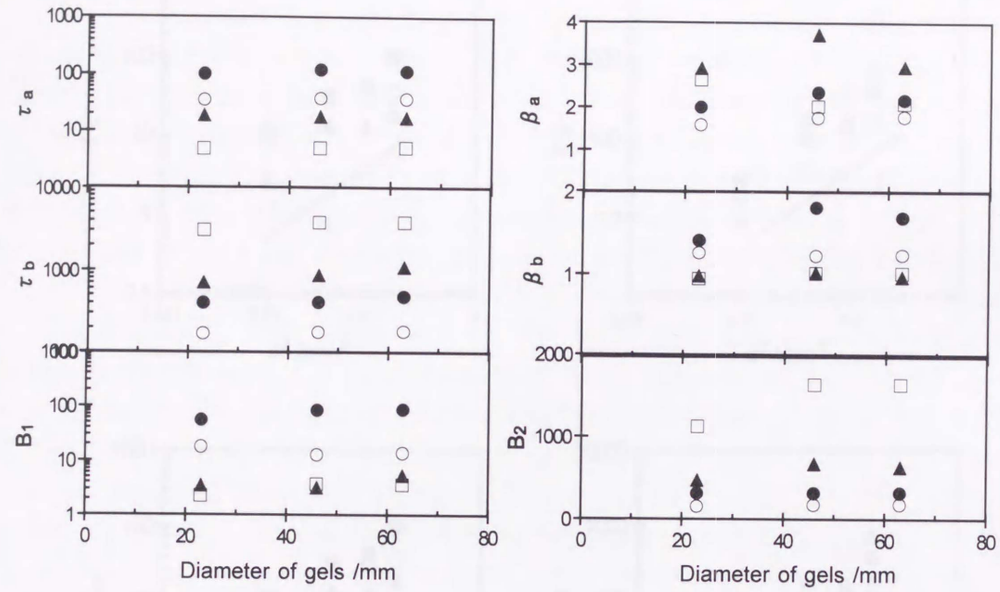

Figure 8. Relationship between diameter of gels and fitting parameters of equation (2) when ΔT is 0.0℃ (●), 0.4℃ (○), 1.0℃ (▲) and 3.0℃ (□).

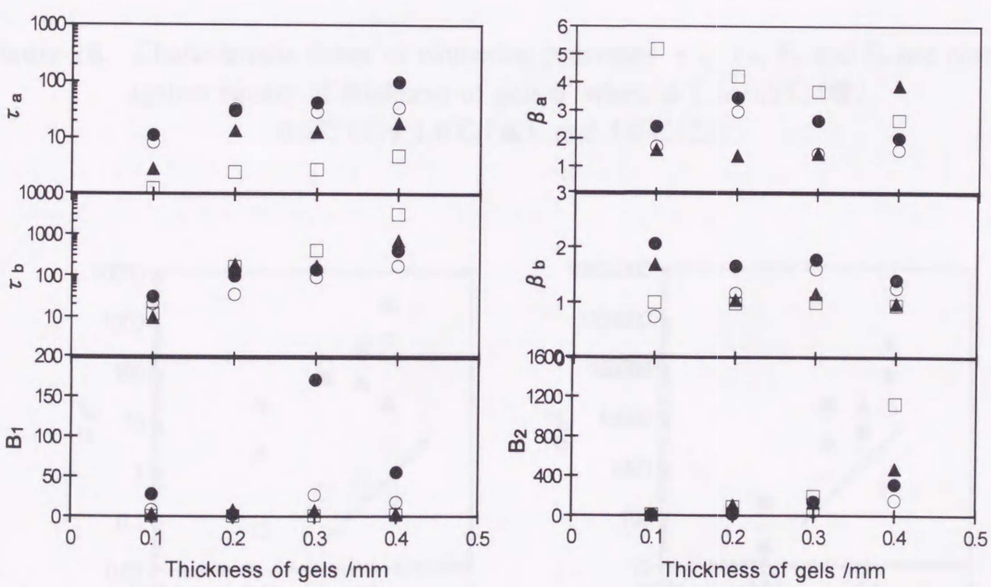

Figure 9. Relationship between thickness of gels and fitting parameters of equation (2) when ΔT is 0.0℃ (●), 0.4℃ (○), 1.0℃ (▲) and 3.0℃ (□).

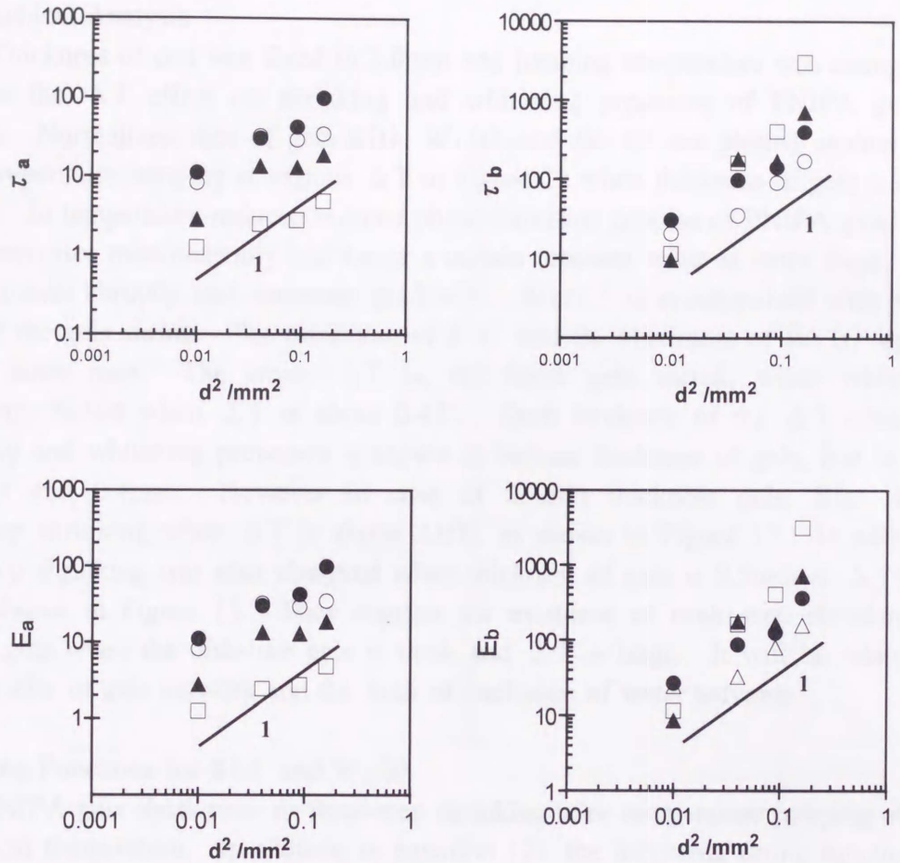

Figure 10. Characteristic times of whitening processes τ_a, τ_b, E_a and E_b are plotted against square of thickness of gels d^2 when ΔT is 0.0℃ (●), 0.4℃ (○), 1.0℃ (▲) and 3.0℃ (□).

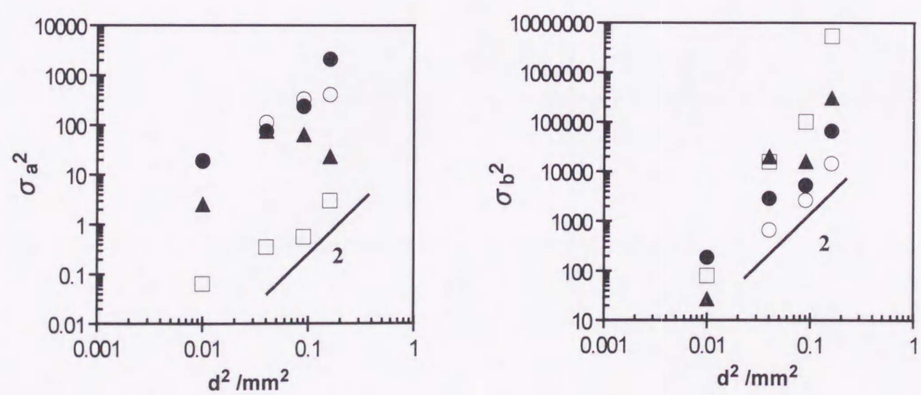

Figure 11. σ_a^2 and σ_b^2 are plotted against square of thickness of gels d^2 when ΔT is 0.0℃ (●), 0.4℃ (○), 1.0℃ (▲) and 3.0℃ (□).

3-5. Jumping Temperature Effects

1) Graphical Analysis

Thickness of cell was fixed to 2.0mm and jumping temperature was changed to evaluate the ΔT effect on shrinking and whitening processes of PNIPA gels as follows. Normalized area of gels $S(t)$, $W_1(t)$ and $W_2(t)$ are plotted against time after temperature-jumping at various ΔT in Figure 12 when thickness of gels is about 0.4mm. In temperature-induced volume phase transition process of PNIPA gels, $S(t)$ first decreases monotonically and keeps a certain constant value at latter stage. $W_1(t)$ increases abruptly and decreases gradually. $W_2(t)$ is synchronized with $S(t)$ well till the gels shrink. The minimum of $S(t)$ and the maximum of $W_2(t)$ appear at the same time. The larger ΔT is, the faster gels shrink, while whitening disappears fastest when ΔT is about 0.4℃. Such tendency of the ΔT effect on shrinking and whitening processes is shown in various thickness of gels, that is, 0.1, 0.2, 0.3 and 0.4mm. However in case of 0.4mm thickness gels, $S(t)$ shows three-step shrinking when ΔT is above 2.0℃ as shown in Figure 12. In addition, three-step shrinking was also observed when thickness of gels is 0.5mm at ΔT= 0.4 ℃ as shown in Figure 13. They suggest the existence of multi-step shrinking of PNIPA gels when the disk-like gels is thick and ΔT is large. It will be related to the elasticity of gels network and the limit of exclusion of water solvents.

2) Fitting Functions for $S(t)$ and $W_1(t)$

PNIPA gels show two- or three-step shrinking after temperature jumping above the critical temperature. In addition to equation (2) the following fitting function of normalized area of gels $S(t)$ was explained by

$$S(t) = A_1\exp\left(-\frac{t}{\tau_1}\right) + A_2\exp\left(-\left(\frac{t}{\tau_2}\right)^{\beta_2}\right) + A_3\exp\left(-\left(\frac{t}{\tau_3}\right)^{\beta_3}\right) + (1-A_1-A_2-A_3) \qquad (13)$$

The second and third terms are unusual relaxation functions, stretched exponential functions with the exponents β_i (i=2,3)>1. Shrinking mechanism of third shrinking is same as that of second shrinking. Equation (3) was used as a fitting function for $W_1(t)$.

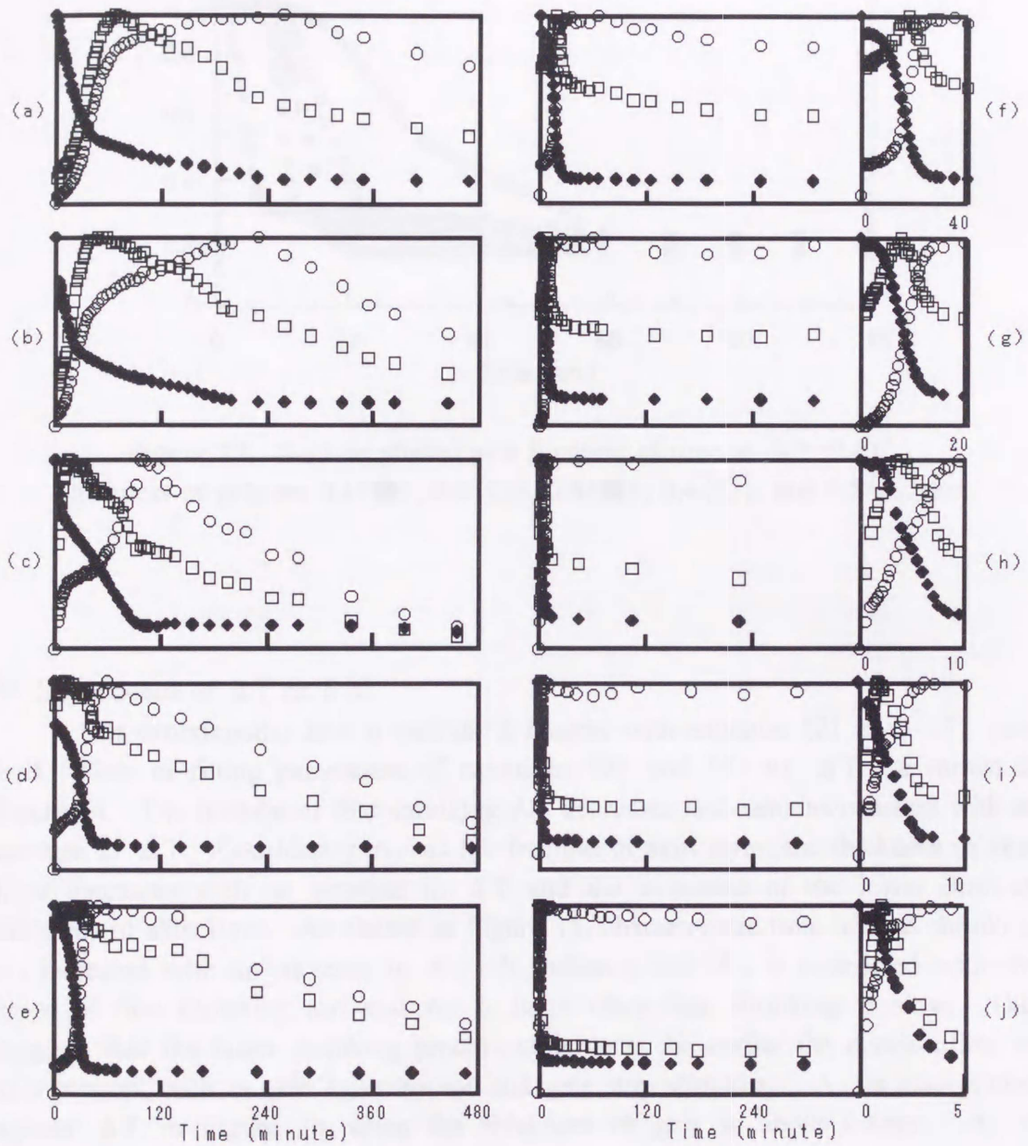

Figure 12. Graph for jumping temperature-dependence on S(t), $W_1(t)$ and $W_2(t)$. ΔT is (a) 0.0℃, (b) 0.2℃, (c) 0.4℃, (d) 0.6℃, (e) 0.8℃, (f) 1.0℃, (g) 2.0℃, (h) 3.0℃, (i) 4.0℃ and (j) 5.0℃.

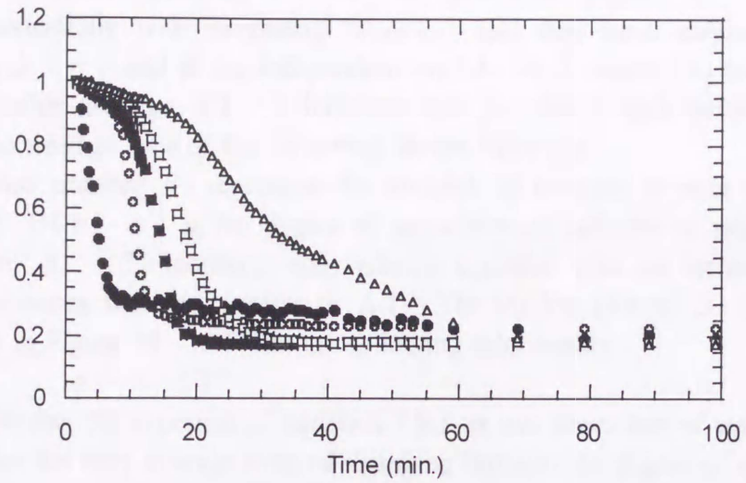

Figure 13. S(t) is plotted as a function of time at ΔT=0.4℃.
Thickness of gels are 0.1(●), 0.2(○), 0.3(■), 0.4(□) and 0.5(□)mm.

3) Dependence of ΔT on S(t)

Our experimental data in various ΔT agree with equation (2) and (13) very well. Plots of fitting parameters of equations (2) and (5) vs. ΔT are shown in Figure 14. The fraction of first shrinking A_1 decreases and remains constant with an increase in ΔT. Considering A_1 as the fraction of skin layer, the thickness of skin layer decreases with an increase in ΔT and the existence of the lower limit of thickness of skin layer. As shown in Figure 15, characteristic time of first shrinking τ_1 increases with an increase in A_1. It indicates that A_1 is connected with the speed of first shrinking and that A_1 is large when first shrinking is slow. This suggests that the faster shrinking process undergoes, the earlier the elastic effect of gels network such as skin layer appear and gels stop shrinking. A_3 is also plotted against ΔT in Figure 14 when the thickness of gels is about 0.4mm. A_3 is independent on ΔT and A_2 decreases with ΔT instead of the appearance of A_3.

τ_1 is characteristic time of first shrinking. τ_2 is characteristic time of second shrinking and corresponds to average of $D(\tau)$ E, while E is average time of second shrinking and collapse of skin layer. As shown in Figure 15 and 16, each τ_1, τ_2 and E has scaling behaviour as follows

$$\tau_i \text{ (i=1,2 and 3)} \propto \Delta T^{-1} \quad (14)$$

$$E \propto \Delta T^{-1}, \quad (15)$$

Since vigorous motion of solvents and gels network will be observed when ΔT is large, shrinking process will be faster at larger ΔT. There is no obvious difference

between τ_2 and E. τ_2 and E are also plotted as a function of the fraction of gels size before secondary shrinking (A_2+A_3) as shown in Figure 17. τ_2 and E decrease exponentially with increasing (A_2+A_3) and they have various values at large (A_2+A_3). τ_2 and E are independent on (A_2+A_3) when (A_2+A_3) reaches a maximum value at large ΔT. It indicates that the size of gels before shrinking determines the average time of the following abrupt shrinking.

The index number β_2 represents the strength of collapse of skin layer, while dispersion of $D(\tau)$ σ^2 is the degree of asynchronous collapse of skin layer and corresponds to β_2. β_2 increases and remains constant with an increase in ΔT, while σ^2 decreases with an increase in ΔT. The log-log plot of β_2 and σ^2 vs. ΔT is shown in Figure 18. σ^2 has the following relationship

$$\sigma^2 \propto \Delta T^{-2} \qquad (16)$$

It is reasonable that the exponent of equation (16) is two times that of equation (15). It indicates that not only average time of shrinking but also the degree of synchronous shrinking appearance become small at large ΔT. β_2 remains constant at large ΔT and it seemes that dispersion σ^2 is not reflected on β_2 well. The strength and the synchronous degree of collapse of skin layer increase with an increase in ΔT. β_2 and σ^2 are plotted against (A_2+A_3) in Figure 19. β_2 increases almost lineally and σ^2 decreases with an increase in (A_2+A_3). It indicates that the size of gels before shrinking determines the strength of the following abrupt shrinking. That is, the larger size of gels is, the stronger shrinking of gels is. However an upper limit of (A_2+A_3) exists.

The third stage of shrinking process is characterized by A_3, τ_3 and β_3. Characteristic time of third shrinking τ_3 decreases with increasing ΔT, while both β_3 and A_3 are almost independent on ΔT. The plots of τ_3 and β_3 as a function of A_3 are shown in Figure 20 and data are almost concentrated at one point. It indicates that the size of gels before shrinking is independent on the characteristic time of the following abrupt shrinking.

The schematic diagram of shrinking process of PNIPA gels is summarized in Figure 21. Just above Tc, the fraction of first shrinking A_1 is large and temporal change of disk-like gels area can be described by a single exponential. Gels shrink monotonically as collective diffusion with infinitesimal deformation. The skin layer will not be formed. On increasing ΔT, the fraction of second shrinking A_2 increases and skin layer becomes to be formed after first shrinking. Considering the fraction of first shrinking A_1 as the fraction of skin layer, thickness of skin layer decreases with increasing ΔT. Average time τ_2 to skin layer collapse decreases, and the degree of the collapse strength β increases. The skin layer may break or change its nature, and the inner part starts to shrink. For large ΔT, three-step shrinking undergoes. PNIPA gels shrink at first, the skin layer is formed on the surface of gels and gels stop shrinking. The skin layer breaks or changes its nature and the inner part starts to shrink. However the evacuate of solvent is not enough and the skin layer is formed again. The possibility of multi-shrinking is high when

ΔT is large or gels are thick.

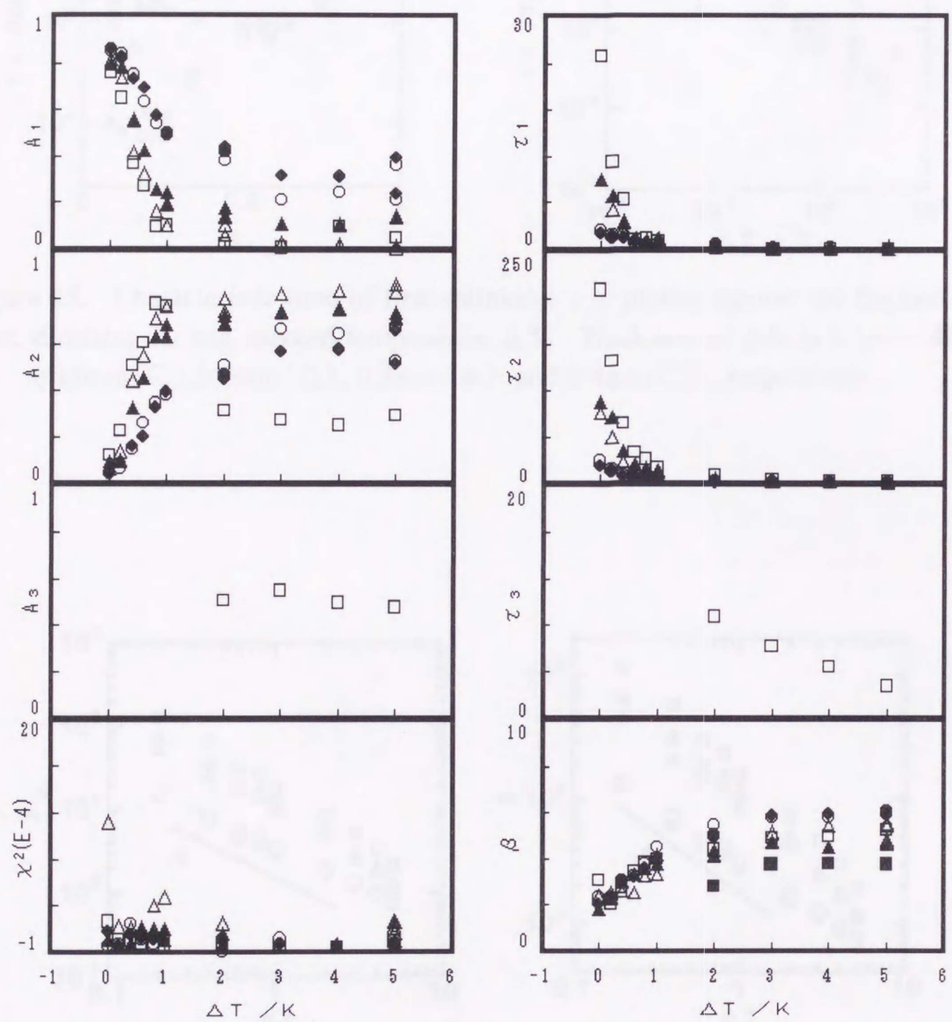

Figure 14. Relationship between ΔT and fitting parameter of S(t)
Thickness of gels is 0.1mm(●), 0.15mm(○), 0.2mm(△), 0.3mm(▲) and 0.4mm(□), respectively. β_3(■) is plotted for 0.4mm thickness of gels.

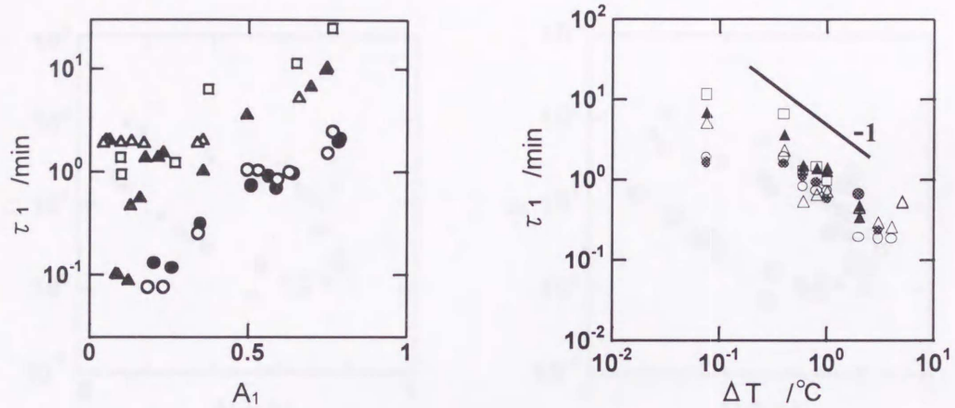

Figure 15. Characteristic time of first shrinking τ_1 plotted against the fraction of first shrinking A_1 and reduced temperature ΔT. Thickness of gels is 0.1mm (●), 0.15mm (○), 0.2mm (△), 0.3mm (▲) and 0.4mm (□), respectively.

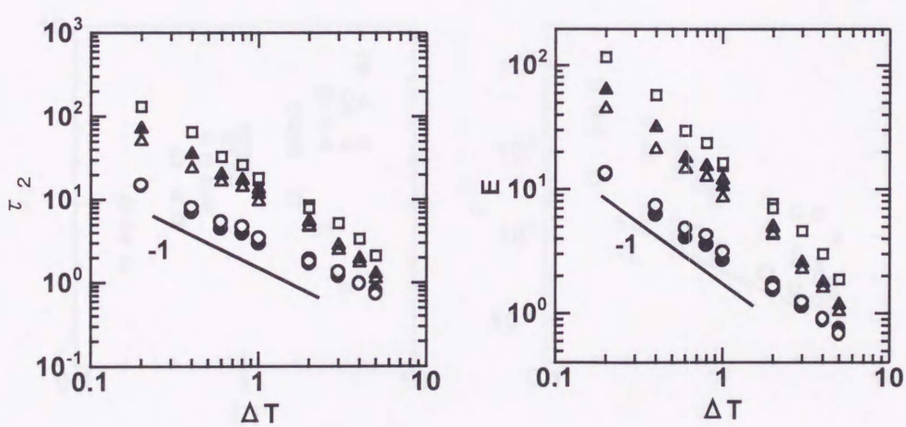

Figure 16. Log-log plot of characteristic times of second shrinking τ_2 and E as a function of reduced temperature ΔT. Thickness of gels is 0.1mm (●), 0.15mm (○), 0.2mm (△), 0.3mm (▲) and 0.4mm (□), respectively. The slope is -1.0.

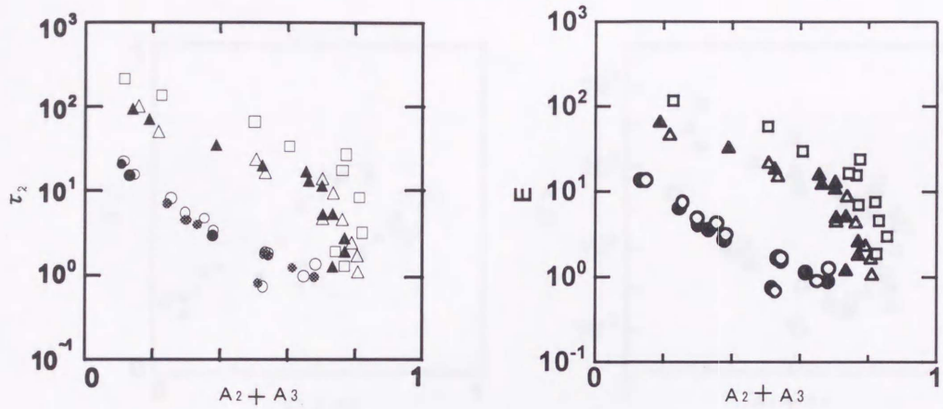

Figure 17. Plots of τ_2 and E as a function of (A_2+A_3). Thickness of gels is 0.1mm(●), 0.15mm(○), 0.2mm(△), 0.3mm(▲) and 0.4mm(□), respectively.

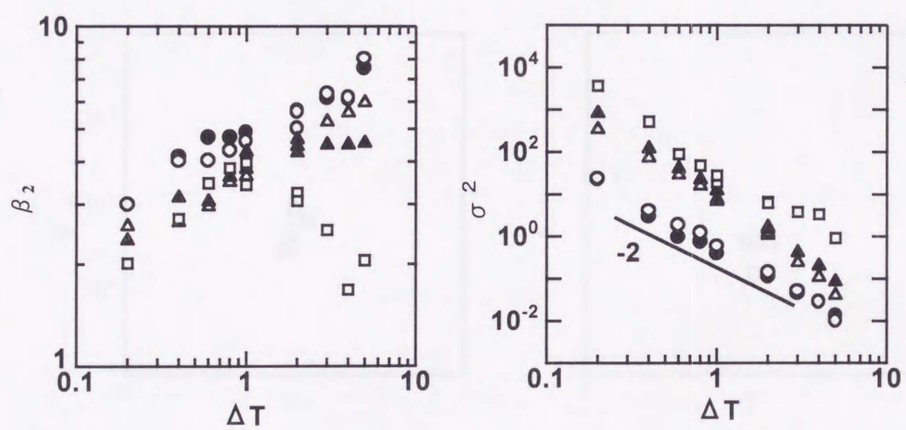

Figure 18. The log-log plot of β_2 and σ^2 as a function of △T. Thickness of gels is 0.1mm(●), 0.15mm(○),0.2mm(△), 0.3mm(▲) and 0.4mm(□), respectively.

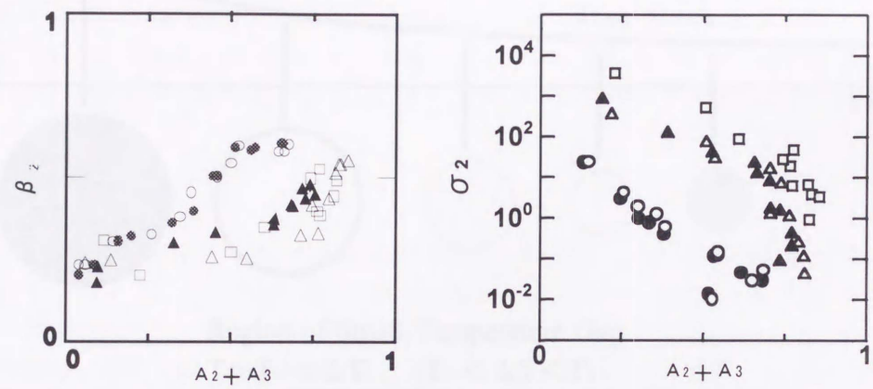

Figure 19. Plots of β_2 and σ^2 against (A_2+A_3). Thickness of gels is 0.1mm(●), 0.15mm(○), 0.2mm(△), 0.3mm(▲) and 0.4mm(□), respectively.

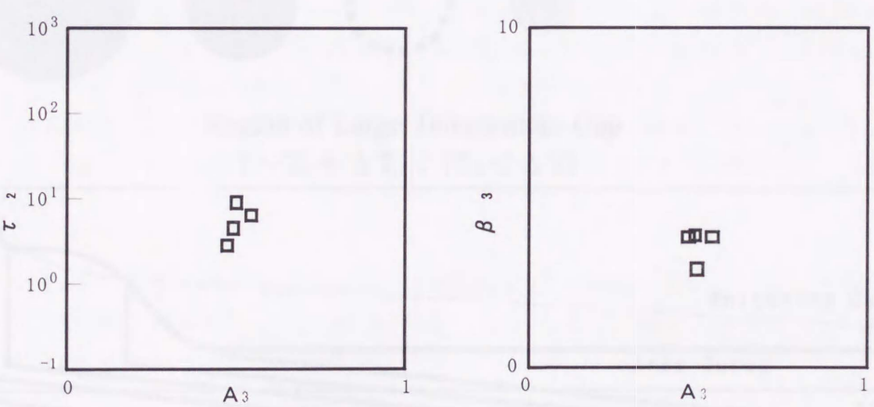

Figure 20. Relationship between third shrinking parameters τ_3 and β_3 as a function of A_3. Thickness of gels is 0.4mm.

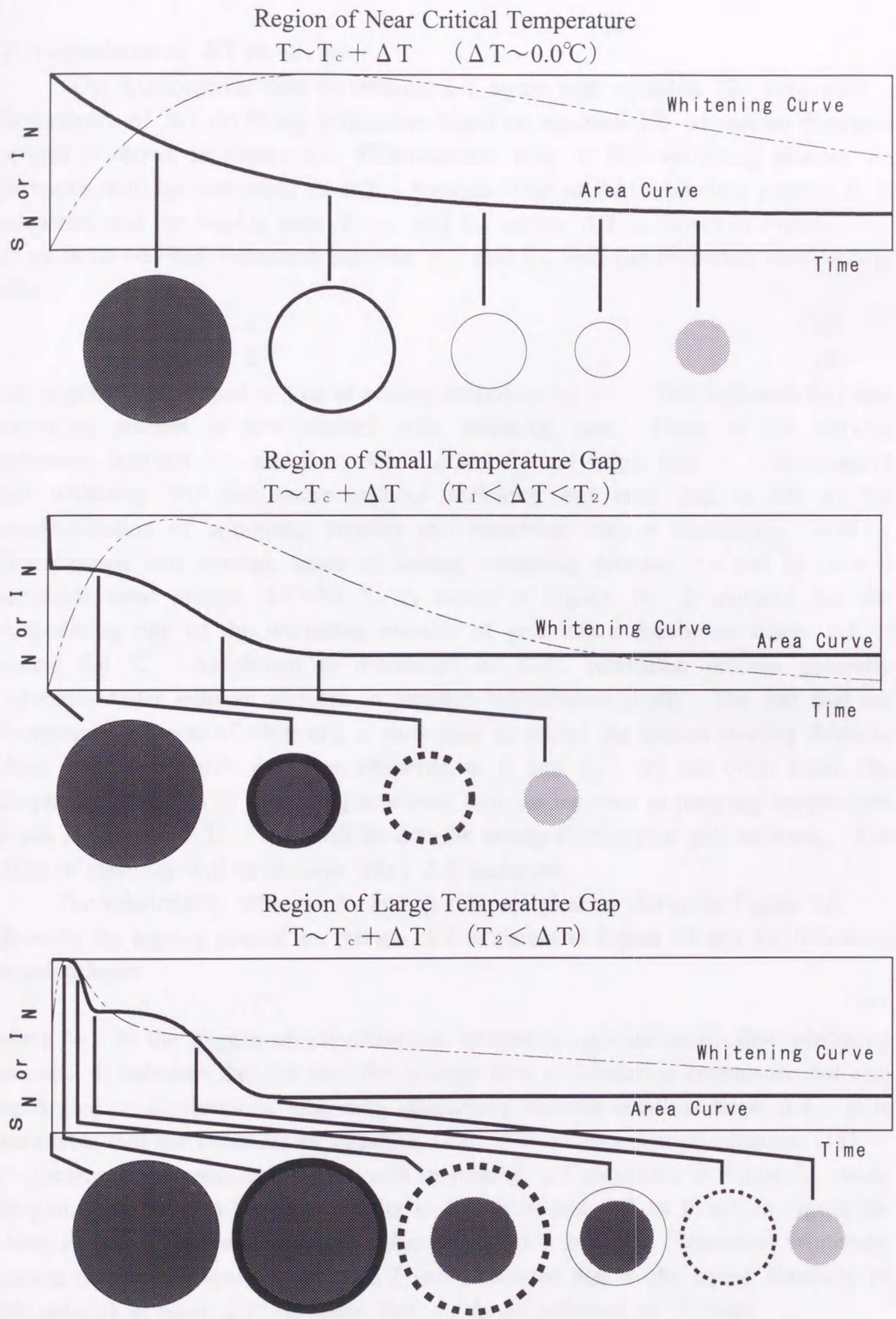

Figure 21. Schematic diagram of shrinking process of PNIPA gels

4) Dependence of ΔT on $W_1(t)$

Our experimental data in various ΔT agree with equation (3) very well. Dependence of ΔT on fitting parameters based on equation (3) at various thickness of gels is shown in Figure 22. Characteristic time of first whitening process τ_a decreases with an increasing in ΔT. Average time of first whitening process E_a is calculeted and the log-log plot of τ_a and E_a versus ΔT is shown in Figure 23. There is no obvious difference between τ_a and E_a, and the following relationships hold.

$$\tau_a \propto \Delta T^{-1} \quad (17)$$

$$E_a \propto \Delta T^{-1} \quad (18)$$

The exponents are equal to that of scaling behaviour of τ_1. This indicates that first whitening process is synchronized with shrinking one. There is not obvious difference between τ_a and E_a. All τ_a and E_a are larger than τ_1, so it agrees that whitening will not occur without shrinking and time gap is due to the synchronization of whitening process and shrinking one in mesoscopic level. Characteristic and average times of second whitening process τ_b and E_b have a minimum value around ΔT=0.4 ℃ as shown in Figure 24. It explains that the disappearing rate of the whitening amount of gels has a maximum when ΔT is around 0.4 ℃. As shown in discussion of $S(t)$, relaxation process generally undergoes faster with an increase in jumping temperature depth. The fact that the disappearing process of whitening is slow near Tc shows the critical slowing down in phase transition which was also observed in E and E_a. On the other hand, the disappearing process of whitening is slower with an increase in jumping temperature which is above 0.4 ℃. This will be due the strong elasticity of gels network. The effect of elasticity will be obvious when ΔT increases.

The relationship between β_a and ΔT is not clear as shown in Figure 22. However the log-log plot of σ_a^2 versus ΔT is shown in Figure 23 and the following equation holds

$$\sigma_a^2 \sim \Delta T^{-4}, \quad (19)$$

where σ_a^2 is the degree of asynchronous whitening appearance of first whitening process. It indicates that not only the average time of whitening appearance but also the degree of synchronous whitening appearance become small at large ΔT. It is reasonable that the exponent of equation (19) is two times that of equation (18). β_b decreases and remains constant with increasing ΔT as shown in Figure 22, while the plot of σ_b^2 and ΔT is very similar to that of E_b and ΔT as shown in Figure 24. Both E_b and σ_b^2 have a minimum value around ΔT is 0.4℃. Secondary whitening process undergoes slowly at large ΔT and it will be due to the strong elasticity of gels network at large ΔT. It seems that σ_b^2 is not reflected on β_b well.

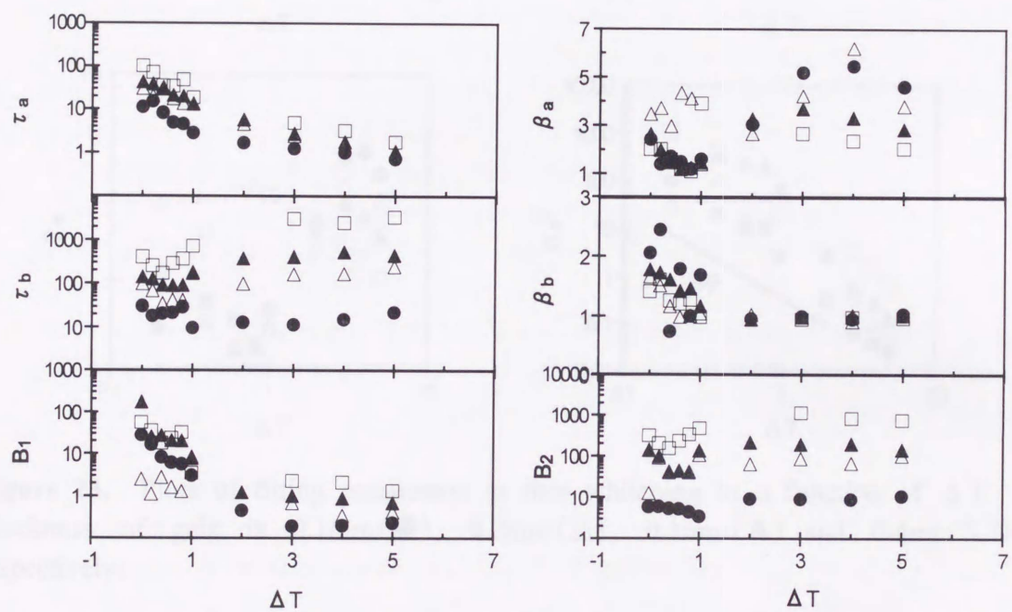

Figure 22. Relationship between fitting parameters of $W_1(t)$ and ΔT. Thickness of gels is 0.1mm (●), 0.15mm (○), 0.2mm (△), 0.3mm (▲) and 0.4mm (□), respectively.

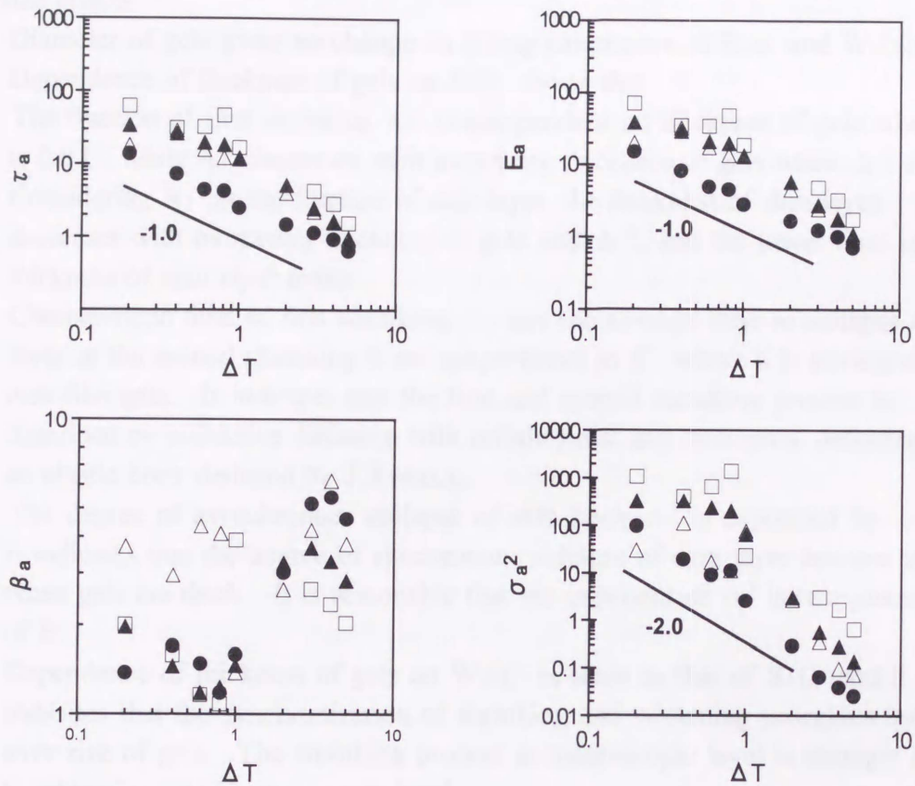

Figure 23. Plots of fitting parameters in first whitening as a function of ΔT. Thickness of gels is 0.1mm(●), 0.2mm(△), 0.3mm(▲) and 0.4mm(□), respectively.

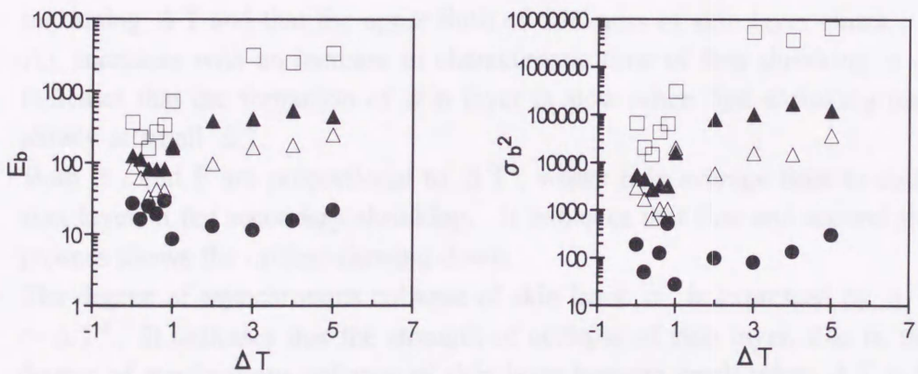

Figure 24. Plots of E_b and σ_b^2 as a function of ΔT. Thickness of gels is 0.1mm (●), 0.2mm(△), 0.3mm(▲) and 0.4mm(□), respectively.

3-6. Conclusion

1) Size effects

(1) Diameter of gels gives no change on fitting parameters of $S(t)$ and $W_1(t)$.

(2) Dependence of thickness of gels on $S(t)$ shows that

1. The fraction of first shrinking A_1 is independent on thickness of gels when ΔT is 0.0℃, while A_1 decreases with increasing thickness of gels when ΔT is large. Considering A_1 as the fraction of skin layer, the thickness of skin layer decreases with increasing thickness of gels and ΔT, and the lower limit of thickness of skin layer exists.
2. Characteristic time of first shrinking τ_1 and the average time to collapse of skin layer in the second shrinking E are proportional to d^{-2}, where d is thickness of disk-like gels. It indicates that the first and second shrinking process is described by collective diffusion with infinitesimal and isotropical deformation as an elastic body deduced by T.Tanaka.
3. The degree of asynchronous collapse of skin layer σ^2 is expressed by $\sigma^2 \sim d^{-4}$. It indicates that the degree of synchronous collapse of skin layer become small when gels are thick. It is reasonable that the exponent of σ^2 is two times that of E.

(3) Dependence of thickness of gels on $W_1(t)$ is same as that of $S(t)$ and it indicates that the synchronization of shrinking and whitening processes holds over size of gels. The shrinking process in macroscopic level is strongly related to whitening one in mesoscopic level.

2) Jumping temperature effects

(1) Dependence of jumping temperature on $S(t)$ shows that

1. The fraction of first shrinking A_1 decreases and remains constant with increasing ΔT. It indicates that the thickness of skin layer increases with increasing ΔT and that the upper limit of thickness of skin layer exists.
2. A_1 increases with an increase in characteristic time of first shrinking τ_1. It indicates that the formation of skin layer is slow when first shrinking undergoes slowly at small ΔT.
3. Both τ_1 and E are proportional to ΔT^{-2}, where E is average time to collapse of skin layer in the secondary shrinking. It indicates that first and second shrinking process shows the critical slowing down.
4. The degree of asynchronous collapse of skin layer σ^2 is expressed by $\sigma^2 \sim \Delta T^{-2}$. It indicates that the strength of collapse of skin layer, that is, the degree of synchronous collapse of skin layer become small when ΔT is large. It is reasonable that the exponent of σ^2 is two times that of E.
5. E and σ^2 are closely related to the size of gels before shrinking (A_2+A_3).

(2) Dependence of jumping temperature on $W_1(t)$ shows that

1. The average time of first whitening process E_a is expressed by $E_a \sim \Delta T^{-1}$. It

indicates that first whitening process shows the critical slowing down.

2. The degree of asynchronous whitening appearance in first whitening process σ_a^2 is expressed by $\sigma_a^2 \sim \Delta T^{-2}$. It indicates that the degree of synchronous whitening appearance become small at large ΔT. It is reasonable that the exponent of σ_a^2 is two times that of E_a.
3. Average time E_b and the degree of asynchronous whitening appearance σ_b^2 in second whitening process are synchronized over ΔT and have a minimum value at $\Delta T=0.4℃$. The fact that the secondary whitening occurs slower and broader at large ΔT will be due to the elasticity of gels network.

(3) Dependence of ΔT on $W_1(t)$ is same as that of $S(t)$ and it indicates that the synchronization of shrinking and whitening processes holds over ΔT. The shrinking process in macroscopic level is strongly related to whitening one in mesoscopic level.

(4) $S(t)$ shows three-step shrinking when gels are thick and ΔT is large. It suggests the possibility of multi-step shrinking of PNIPA gels.

Reference

1. Y.Li and T.Tanaka, J.Chem.Phys., 92(2),1365 (1990)

indicates that first whitening process shows the critical slowing down.

2. The degree of asynchronous whitening appearance in first whitening process σ_a^2 is expressed by $\sigma_a^2 \sim \Delta T^{-2}$. It indicates that the degree of synchronous whitening appearance become small at large ΔT. It is reasonable that the exponent of σ_a^2 is two times that of E_a.
3. Average time E_b and the degree of asynchronous whitening appearance σ_b^2 in second whitening process are synchronized over ΔT and have a minimum value at ΔT=0.4℃. The fact that the secondary whitening occurs slower and broader at large ΔT will be due to the elasticity of gels network.
4. Dependence of ΔT on first whitening is same as that of first shrinking and it indicates that the synchronization of shrinking and whitening processes holds over ΔT. The shrinking process in macroscopic level is strongly related to whitening one in mesoscopic level.

(3) S(t) shows three-step shrinking when gels are thick and ΔT is large. It suggests the possibility of multi-step shrinking of PNIPA gels.

Reference

1. Y.Li and T.Tanaka, J.Chem.Phys., 92(2),1365 (1990)

Chapter 4. Shape of Gels Effects

4-1. Abstract

Poly N-(isopropyleacrylamide) (PNIPA) gels show two-step shrinking accompanied with a multiple scattering after temperature-jump above the critical temperature. Sample gels were prepared by cutting out the synthesized sheet-like PNIPA gels with a cookie cutter, the shape of which was clover, diamond, heart and spade, respectively. Shape of gels dependence on the shrinking and whitening processes was not observed, but all the gels show that the convexoconcave of the shape disappear in second shrinking and the shape is restored after shrinking. This deformation corresponds to the three-dimensional deformation of gels like Japanese original pouch 'Kinchaku'. The edge part of disk-like gels tends to turn over after first shrinking and it is due to the edge part's shrinking. Skin layer is formed as shrunken layer on the surface of gels after first shrinking process and the edge part exactly corresponds to skin layer itself.

4-2. Introduction

Some polymer gels show enormous volume change by solvent composition and temperature etc.[1] Poly N-(isopropyleacrylamide) (PNIPA) gels are well known as nonionic polymer gels which show a large volume change by temperature. When PNIPA gels are put into hot water above the critical temperature, the transparent gels become opaque and show two-step shrinking accompanied with some morphological change on the second stage of shrinking. However if you put the gels at same temperature, the very high degree of multiple scattering and the morphological change of gels finally disappear.[2] These interesting characteristics of PNIPA gels mean the relationship between macroscopic morphological change and some structure change at the mesoscopic level. Volume phase transition of gels has so far been discussed from the viewpoint of phase separation accompanied by strong elastic effect[3] and the mechanism of macroscopic morphological change has been discussed on the assumption of skin layer[2,4,5] which is believed to be formed on the surface of gels as shrunken phase when gels shrink. A lot of paper about phase diagram of gels involved the fluctuation of gels as an viscoelastic body and it is very important for the treatment of volume phase transition of gels as phase transition[6]. Recently inhomogenity of gels is divided to static imhomoginiety and thermal fluctuation by M.Shibayama et al[7]. Morphological changes which appear while shrinking[1] are very interesting and such dynamical phenomena of gels will be explained as combined effects of thermodynamic instability and nonlinear elasticity.

4-2. Experimental

Details of sample preparation, measurement and calculation were same in the

previous section (Chapter 1 and 2). Here sample gels were prepared by cutting out the synthesized sheet-like gels with a cookie cutter, the shape of which was clover, diamond, heart and spade, respectively. The thickness of gels is about 0.4mm and the length of gels is about 60mm. The sample gels were put into a cell of 2.0mm thickness filled with distilled water and sealed with epoxy resin. The crosslinkage density of the sample gels was about 8.8×10^{-3} and critical temperature (Tc) was about 33.7℃ assigned based on cloud point measurements.

The sample cell was set up in a water bath, which was thermostated at $Tc + \Delta T$ (ΔT=0,0.6,1.0 and 3.0K) with the accuracy of about 50mK. The shrinking and whitening processes of PNIPA gels after the temperature jump were observed intermittently by a digital video camera (Sony Co.). The recorded video pictures were converted into V-RAM system on MS-DOS personal computer. The light intensities on V-RAM(RGB: 320x200dots) were divided into 0-255 based on the imaginary V-RAM System exploited using our original programs.

4-3. Results and Discussions

1) Graphical Analysis

Details of graphical analysis were described in previous section (Chapter 1 and 2). On increasing scattered light on the gels, the disk-like gels become white and can be observed clearly against a black background. In our graphical analysis, the resolution of light was from 0 up to 255. Using a clipping procedure, we obtain black and white images of the disk-like gels as shown on the upper-right side of Figure 1(a). In these images, the black dot area due to whitening of gels in upper-right side picture is smaller gradually with increasing time. The temporal change in the graphical analysis image of clover-type PNIPA gels at ΔT=0.6℃ is shown in Figure 1. In these images, the black dot area due to white gels in upper-right side picture is smaller gradually with increasing time. It is also shown that the gels deform its shape in the course of shrinking process. It will be due to the buckling of gels when disk-like gels shrink. 3-dimensional buckling of disk-like gels cut by star-shaped cookie cutter is shown in Figure 2. The edge part of PNIPA gels tends to turn over. We name this buckling phenomena 'Kinchaku Transition', because the shape is very similar to the Japanese original pouch 'Kinchaku'. In our experiments, the buckling was suppressed by putting sample gels between glass plates, so the convexoconcave of gels disappears as shown in Figure 3. Such disappearance of convexoconcave of gels in shrinking process was also observed in other shape-types of gels, diamond, heart and spade type of gels. In the final stage of shrinking of gels, the convexococcave of clover appears again and PNIPA gels return to the original shape.

In order to evaluate the shrinking process of PNIPA gels, the following parameters $S(t)$, $W_1(t)$ and $W_2(t)$ were calculated from the time-resolved recorded images. The normalized area of gels $S(t)$ was obtained by the number of dots due to the gels on recorded images. Integrated value of the distribution of light

intensities within area of gels was normalized and was named the normalized whitening amount of gels $W_1(t)$. Normalized whitening amount of gels per unit area $W_2(t)$ was also obtained by $W_1(t)/S(t)$.

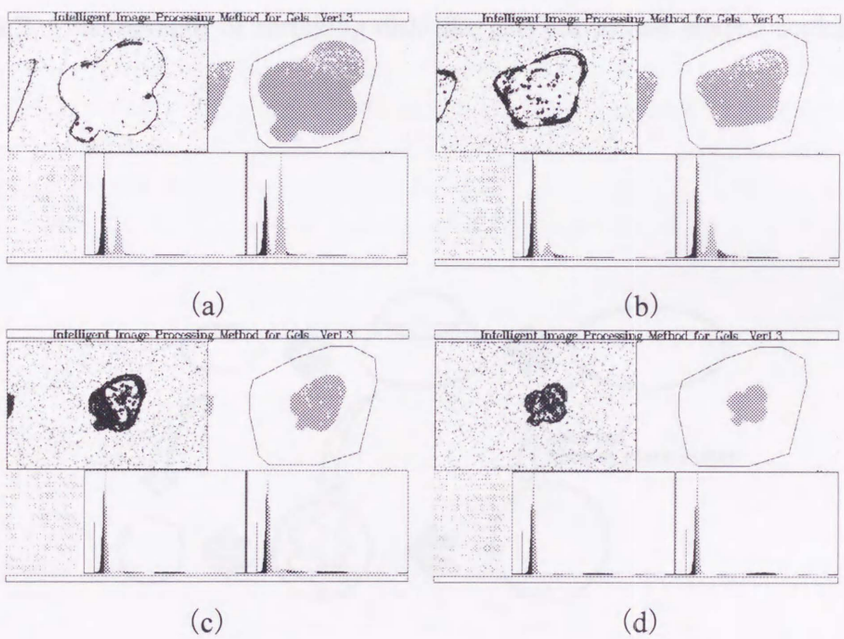

Figure 1. Shrinking process of clover type disk-like PNIPA gels using by graphical analysis. Time after jumping temperature at Tc+0.6℃ is (a) 11minutes (b) 53minutes (c) 67minutes (d) 87minutes.

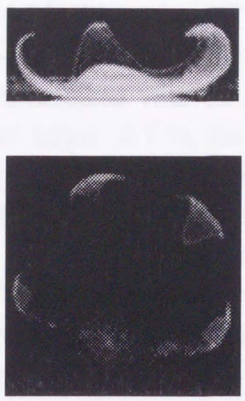

Figure 2. Photographs of shrinking disk-like gels cut by star-shaped cookie cutter.

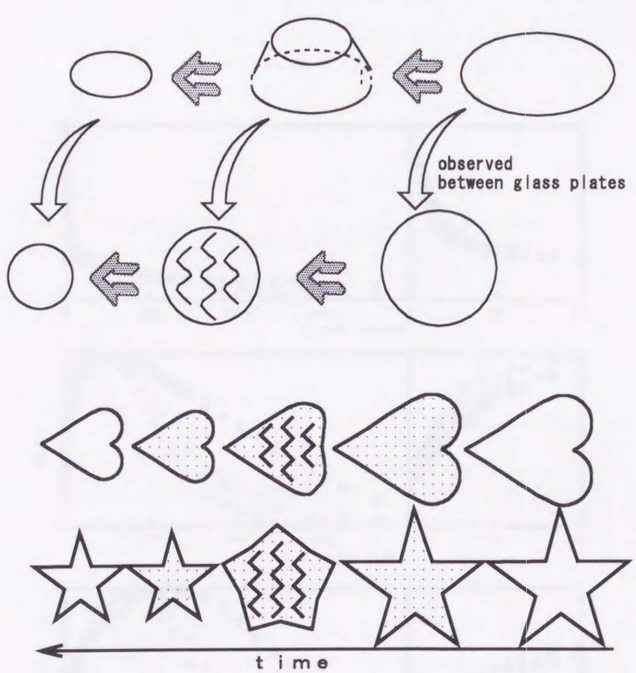

Figure 3. Shrinking image of disk-like PNIPA gels between glass plates

2) Dependence of Gels Shape and ΔT on $S(t)$, $W_1(t)$ and $W_2(t)$

The plots of $S(t)$, $W_1(t)$ and $W_2(t)$ at various ΔT are shown in Figure 4-7 for clover-type(●), diamond-type(▲), heart-type(○) and spade-type(△) PNIPA gels. Every $S(t)$ shows a two-step shrinking. $W_1(t)$ increases abruptly and decreases gradually. $W_2(t)$ is synchronized with $S(t)$ well till the gels shrink, and decreases as $W_1(t)$ decreases. The larger ΔT is, the faster gels shrink. Whitening disappears fastest when ΔT is about 0.6℃. The smaller and the larger ΔT is from about 0.4℃, the longer whitening disappear. The shape of gels gives no change of $S(t)$, $W_1(t)$ and $W_2(t)$ at all. The synchronism of $S(t)$ and $W_2(t)$ was independent on shape of gels. It indicates that the synchronism of macroscopic shrinking phenomena and mesoscopic phase separation one holds over the shape range in our experiments. The behaviour of $S(t)$, $W_1(t)$ and $W_2(t)$ is same as that of disk-like gels which was shown in previous section at various ΔT. According to that, Motions of solvents and gels network are more vigorous with an increase in jumping temperature, so shrinking process will be faster at larger ΔT. And the fact that the disappearing process of whitening is slow near Tc shows the critical slowing down in phase transition which was observed in $S(t)$. And the fact that the disappearing process of whitening is slower with an increase in jumping temperature which is above Tc+0.4 ℃ will be due the effect of elasticity of gels network.

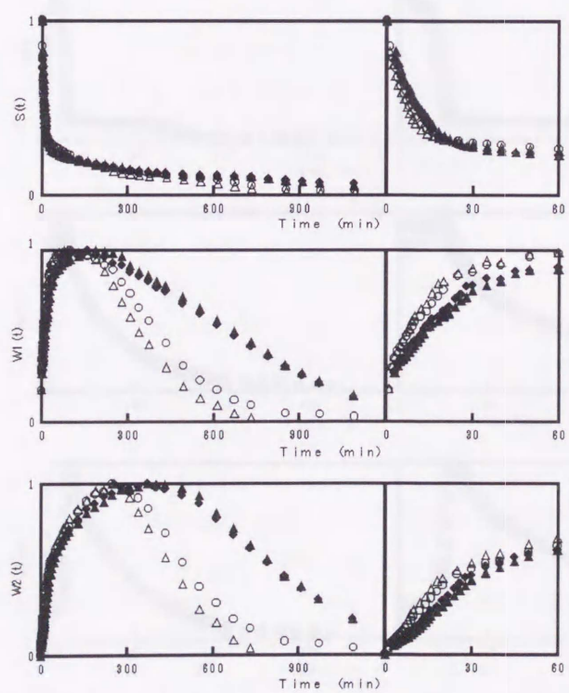

Figure 4. Graph for shape of gels-dependence on $S(t)$, $W_1(t)$ and $W_2(t)$ at ΔT=0.0℃. The shape of gels is clover(●), diamond(▲), heart(○) and spade(△).

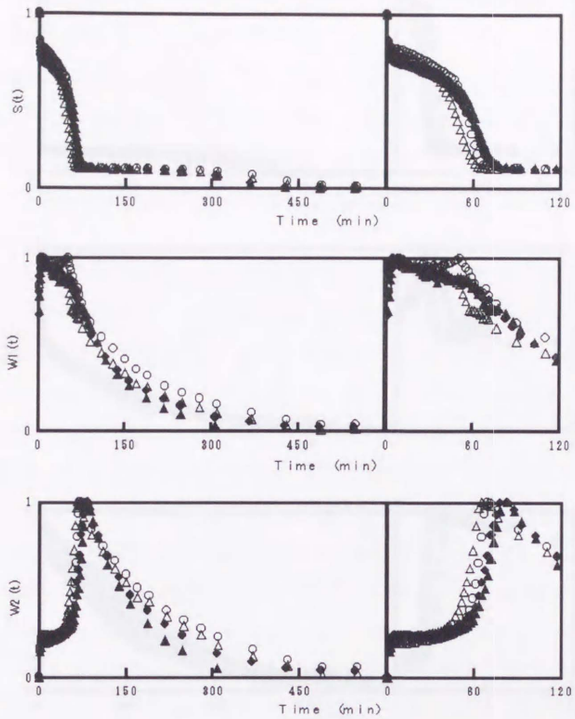

Figure 5. Graph for shape of gels-dependence on S(t), W_1(t) and W_2(t) at Δ T=0.6℃. The shape of gels is clover(●), diamond(▲), heart(○) and spade(△).

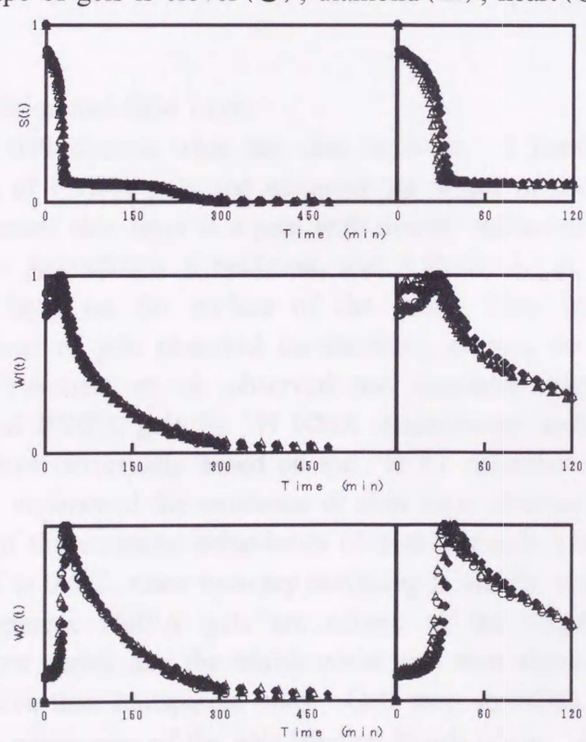

Figure 6. Graph for shape of gels-dependence on S(t), W_1(t) and W_2(t) at Δ T=1.0℃. The shape of gels is clover(●), diamond(▲), heart(○) and spade(△).

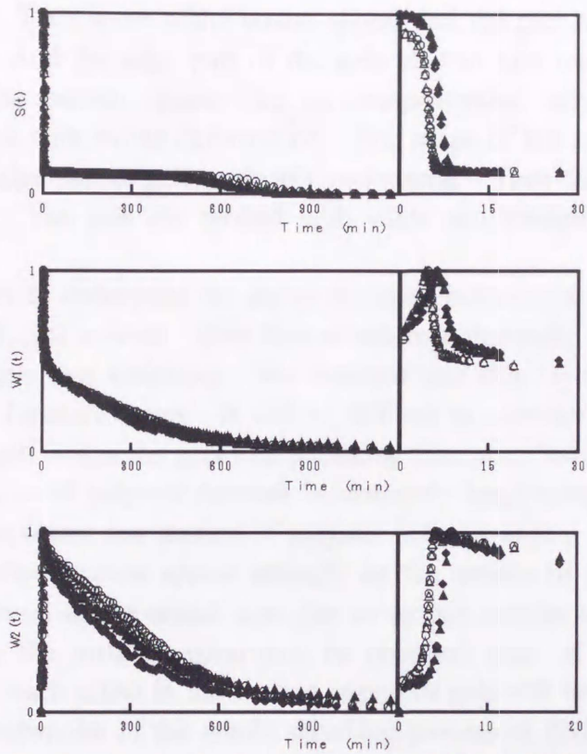

Figure 7. Graph for shape of gels-dependence on S(t), $W_1(t)$ and $W_2(t)$ at ΔT=2.0℃. The shape of gels is clover(●), diamond(▲), heart(○) and spade(△).

3) Kinchaku Transition and Skin Layer

At first we will discuss what the skin layer is. T.Tanaka et al. observed two-step shrinking of PNIPA gels and assumed the origin as the formation of skin layer[1]. He represented skin layer is a peel with density sufficient for impermeability to the inner fluid. Accordingly K.Sekimoto and A.Onuki et. al. also assumed skin layer is a dense layer on the surface of the gels. They tried to explain the morphological change of gels observed on shrinking process on the assumption of skin layer[102]. H.Yasunaga et. al. observed two spin-spin relaxation time T_2 on shrinking process of PNIPA gels by ^1H NMR spectroscopy and they indicated the existence of skin layer structually based on the ^1H T_2 enhanced image[3]. But some people still clearly understand the existence of skin layer structurally. First we will give a full detail of the shrinkng behavioues of disk-like gels which is observed by our eyes when ΔT is 0.6℃, since two-step shrinking is clearly observed when ΔT is 0.6℃. The transparent PNIPA gels are adhere to the fingers at 20℃ before shrinking. Gels first shrink and the bluish white gels stop shrinking. Bluish white gels are less adhesive than transparent ones. Gels stop shrinking for a while. It is considered that the whole part of the gels become bluish white. Because if you take out the cylindrical bluish white gels from the water bath at that point and pour the gels by cold distilled water, the gels become transparent from the outside with the

core bluish white. Then some white points appear and the part of the edge become apparently white. And the edge part of the gels tend to turn over. Many bubbles and shrinking white pattern appear like an interpenetrated network and gels are crumpled and shrink with strong deformation. The shape of the gels is restored after shrinking and the edge part of gels is already transparent. Then the whitening of gels disappears slowly. The gels are spotted with white and transparency and become transparent finally.

It will be easy to understand the above shrinking behaviours from the viewpoint of polymer network, not solvent. Gels first shrink monotonically due to coil-globule transition. Then gels stop shrinking. We assumed that skin layer is formed at that point as shown in Tanaka's report. It will be difficult to consider that the formation of the skin layer itself makes the gels stop shrinking from the viewpoint of solvents. Because the pore size of polymer network is extremely large compared with solvent molecules. It is important that tension of polymer network appear all over the gels at that point. So surface tension appear strongly on the surface of gels. So a denser outside may be formed as the actual state due to surface tension as a result, and the different motion in the surface region may be observed like ^{1}H T_2 measurements when gels shrink. Such effect in the surface region of gels will be explained as 'skin layer'. From the viewpoint of the whole shrinking process of PNIPA gels, it can be regarded that skin layer prevent solvents permiative outer in a sense. Because shrinking of the gels actually stop.

When gels first shrink monotonically, the skin is formed on the surface of gels as shrunken layer. At that time shrunken layer is structually concentrated in the edge part as shown in Figure 8, so the edge part easily shrink compared with other part. The edge part shrink and 'Kinchaku transition' is due to the edge part. Other part consist of shrunken layer and the attached swollen inner part. K.Sekimoto shows that the bukling occuars due to the shear between shrunken layer and swollen layer. In secondary shrinking, all gels are crumpled and 'Kinchaku' shape is deformed .

4) Dependence of ΔT on Deformation of Gels Shape

The temporal change in the graphical analysis image of clover-type PNIPA gels at various ΔT is shown in Figure 1, 9, 10 and 11. The convexoconcave of clover disappears strongly at $\Delta T=0.6℃$ as shown in Figure 1(c). Gels shrink isotropically in first shrinking at $\Delta T=0.0℃$ as shown in Figure 9. The fraction of second shrinking is to small to show kinchaku shape. Kinchaku transition is not also clear at $\Delta T=3.0℃$. The strength of shrinking is stronger at large ΔT and the difference between edge's part and other part will be evident at large ΔT. The secondary shrinking process undergoes fast and the difference between edge's part and other part become evident. The convexoconcave observed while gels stop shrinking is due to 'Kinchaku' shape and the needed.

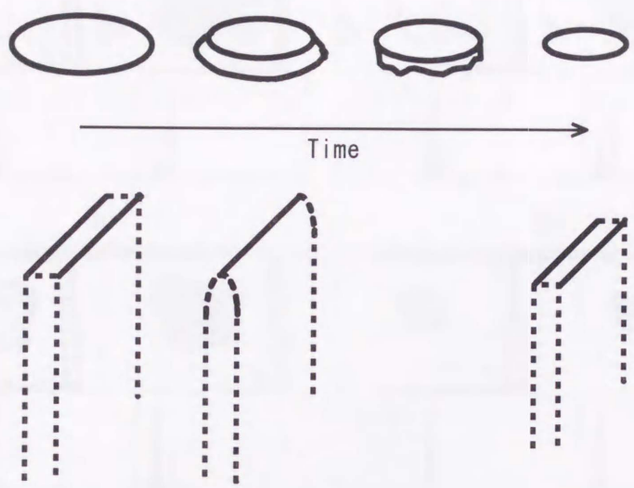

Figure 8. Schematic diagram of edge's effect in second shrinking stage

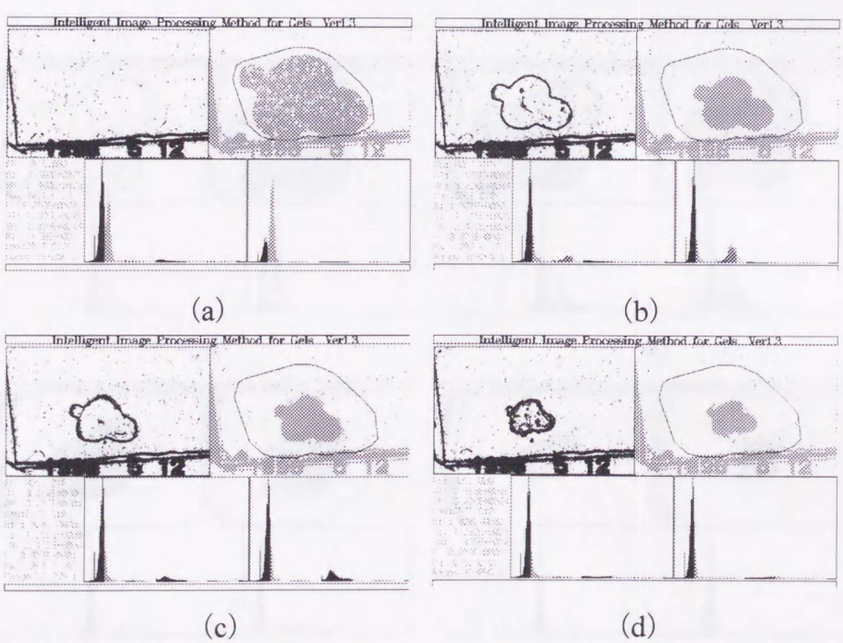

Figure 9. Shrinking process of clover type disk-like PNIPA gels using by graphical analysis. Time after jumping temperature at Tc+0.0℃ is (a) 5minutes (b) 30minutes (c) 130minutes (d) 553minutes.

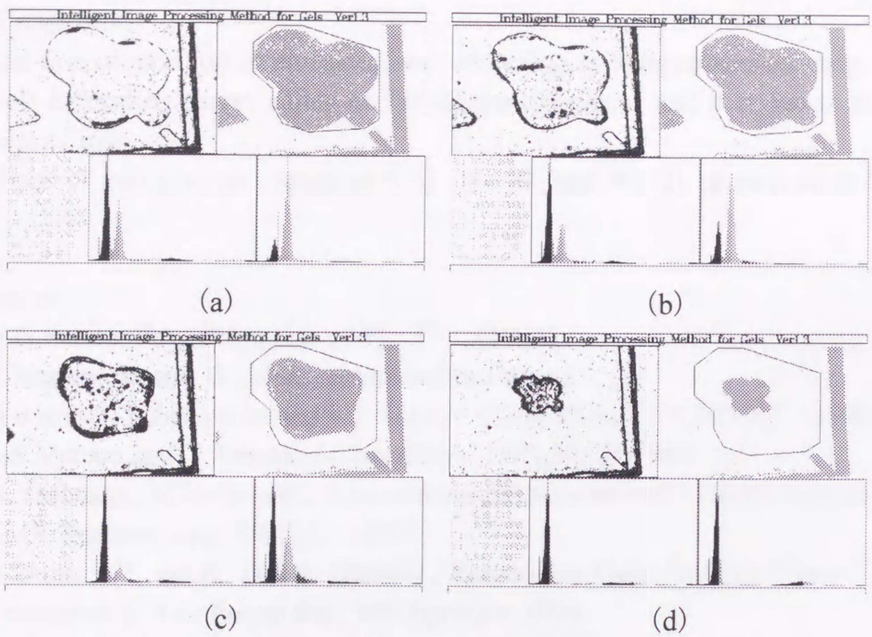

Figure 10. Shrinking process of clover type disk-like PNIPA gels using by graphical analysis. Time after jumping temperature at Tc+1.0℃ is (a) 7minutes (b) 19minutes (c) 30minutes (d) 42minutes.

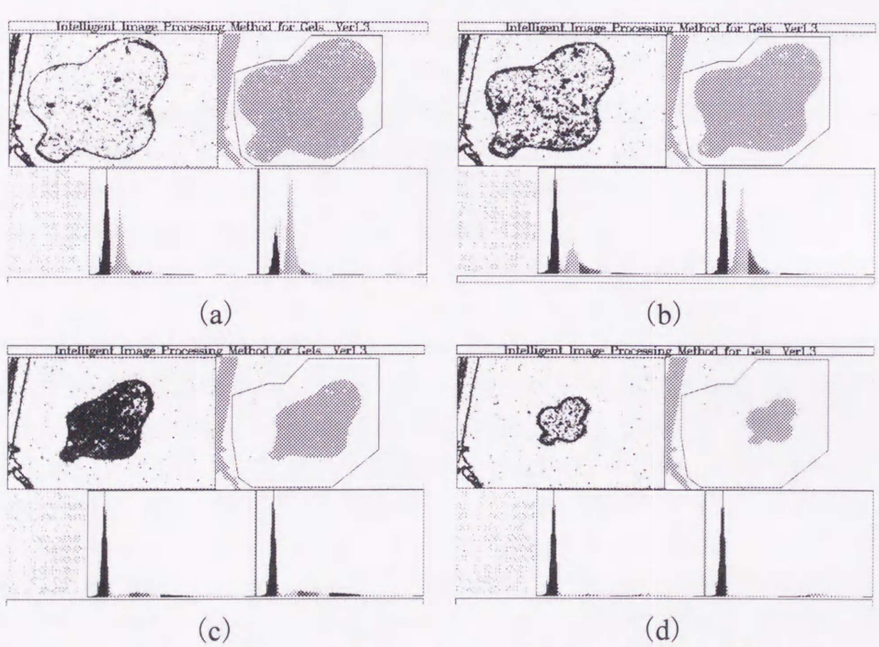

Figure 11. Shrinking process of clover type disk-like PNIPA gels using by graphical analysis. Time after jumping temperature at Tc+2.0℃ is (a) 5minutes (b) 6minutes (c) 8minutes (d) 10.5minutes.

4-4. Conclusion

(1) The synchronization of shrinking and whitening is independent on shape of gels.

(2) Gels deform its shape, called as "Kinchaku transition" and it is due to the elastic effect of gels.

(3) Shape of gels give no change of $S(t)$, $W_1(t)$ and $W_2(t)$ at various ΔT.

References

1. H.G.Schild, Prog.Polym.Sci., 163,(17) (1992)
2. C.Hashimoto and H.Ushiki, submitted to Poym.J.
3. B.Barriere, K.Sekimoto and L.Leibler, J.Chem.Phys.,1735,105(4) (1996)
4. E.S.Matsuo and T.Tanaka, J.Chem.Phys.,1695,89(3),1988
5. H.Yasunaga, M.Kobayashi, S.Matsukawa, H.Kurosu and I.Ando, Annual Rep. NMR Spectroscopy, 39,(34) (1997)
6. A.Onuki, 63, see K. Dusek (Editor), Responsive Gels: Volume Phase Transitions I, Adv.Polym.Sci., 109 Springer 1993
7. M.Shibayama, Macromol.Chem.Phys., 198 (1997)
8. H.Nakazawa and K.Sekimoto, J.Chem.Phys.,1675,104(4) (1996)
   K.Sekimoto, Phys.Rev.Lett.,4154,70(26) (1993)
   B.Barriere, K.Sekimoto and L.Leibler, J.Chem.Phys.,1735,105(4) (1996)
   K.Sekimoto,N,Suematsu and K.Kawasaki, Phys.Rev.A,39(9),4912 (1989)

Chapter 5. Bubbles Formation on Shrinking Process of PNIPA Gels

5-1. Abstract

Morphological patterns of shrinking Poly (N-isopropylacrylamide) (PNIPA) gels are observed using a single lens reflex camera and analyzed. PNIPA gels show two-step shrinking accompanied with turbidity after temperature jump above the critical temperature. In secondary shrinking, bubbles or interconnected network like neuron appear in gels with a strong multiple scattering. The power spectrum of 1-dimensional fast Fourier transformation (FFT) has 3 modes, that is, a sine, Markov noise and white noise. The temporal change of correlation strength of Markov noise is very similar to the temporal change of integral value of light intensities in gels. It indicates that the whitening amount of gels corresponds to Markov noise on the surface of gels. In addition, size of periodic structure due to the network is small at large ΔT and it is compatible with the tendency of phase separation.

5-2. Introduction

Volume change with remarkable pattern formations was observed on swelling and shrinking processes of gels[1-5]. T.Tanaka et. al. showed the morphological change of PNIPA gels in water[6]. Wrinkle patterns appear like surface of a brain when gels swell, while gels are covered with many bubbles when they shrink. They also showed that when acrylamide/sodium acrylate copolymer gels in acetone/water mixture shrink under a certain strain, gels behave various patterns, bubble, bamboo and so on[2]. These morphological patterns have been attracted many theorist. In case of swelling process, the morphological swelling process of spherical gels is described as an elastic body of which surface layer is swollen and attached to the shrunken inner part. However the shrinking mechanism is not so clear yet and skin layer has been structurally proposed by some researchers, which has so far been believed to be formed on the surface of gels and prevents solvents from permeating across the boundary when gels shrink. On the other hand, T.Tanaka et. al. proposed a single exponential function as a fitting function of volume change on swelling and shrinking processes, assuming the infinitesimal deformation of an elastic body[7,8]. Their theory has a good agreement with some swelling processes of gels, but does not explain shrinking processes of PNIPA gels shown in our experiments[6,9]. Elasticity due to crosslinking is also very important from a viewpoint of phase demixing between polymer network and solvents, that is, coupling between phase transition and elasticity is an essential concept for shrinking process of gels. Dynamics of gels are expected as combined effects of thermodynamic instability and nonlinear elasticity. H.Tanaka has studied asymmetric molecular dynamics and morphological pattern in phase separation process of polymer solution, considering volume phase transition phenomena of gels as an expanded problem[10].

Poly N-(isopropyleacrylamide) (PNIPA) gels are well known as nonionic polymer gels which show a large volume change by temperature. When PNIPA gels are put into hot water above the critical temperature, the transparent gels shrink and be opaque. They stop shrinking for a while and shrink again accompanied with some morphological change. T.Tanaka et al. showed that a sub-micron spherical gels consists of some bubbles on the second stage of shrinking[1]. Volume phase transition of gels has so far been discussed from the viewpoint of phase separation accompanied with strong elastic effect and the mechanism of such bubble formation will be due to elasticity of gels. H. Tanaka showed that some morpholoical pattern in phase separion of polymer solution. Morphological changes which appear while shrinking are very interesting and such dynamical phenomena of gels will be explained as combined effects of thermodynamic instability and nonlinear elasticity. There is no proper discrimination about the origin of such bubble formation. A lot of paper about phase diagram of gels involved the fluctuation of gels as an viscoelastic body and it is very important for the treatment of volume phase transition of gels as phase transition.

5-3. Experimental

1) Sample Preparation

Sample preparation was same as previous section (Chapter 1). Sheet-like PNIPA gels were synthesized between glass plates with a spacer of which thickness was about 0.4 mm. Disk-like gels were prepared by cutting the sheet-like gels with a cookie cutter of which diameter was 36mm. The sample was put into a 5.0mm thickness cell filled with distilled water and the cell was sealed with epoxy resin. The critical temperature (T_c) was close to 34.1℃ based on cloud point measurement.

2) Experimental Procedure

The sample cell was immersed in a thermostated water bath at ±0.02℃ as shown in Figure 1. The sample gels are lighted from above by a white light source. The whitening and shrinking of the gels were studied as a function of time at various destination temperatures $T_c + \Delta T$ with ΔT= 0.4℃ and 1.0℃. Images of the gels were intermittently recorded using a single lens reflex camera (Canon EOS). Photographs were converted into BMP form files throughout the scanner (Epson GT-5500 Wins) at a light intensity resolution of 256 and a spatial resolution of 320 ×200 dots.

Programs for graphical analysis and curve fitting were made by Delphi 5.0 (Borland). Various fitting functions can be always estimated for all data curves using nonlinear-least-squares method based on the quasi-Marquardt algorithm as a software part of PLASMA. Calculations were carried out on a personal computer (NEC:LM500J/3)

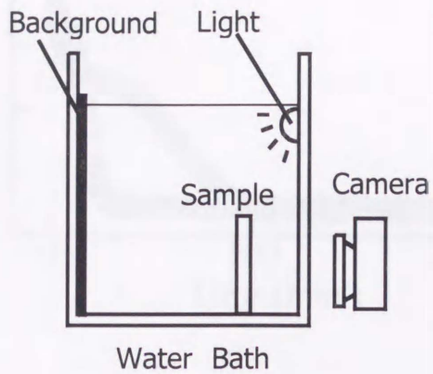

Figure 1. Apparatus for visual volume phase transition measurement

5-3. Results and Discussions

1) Shrinking and Whitening Processes of PNIPA Gels

Temporal change of size and whitening of PNIPA gels were evaluated from CCD video camera pictures as shown in previous section (Chapter 1). Since PNIPA gels are transparent at first, we cannot get images of disk-like gels clearly using a video camera. So a white plastic disk was used to estimate the initial gel size. On increasing scattered light on the gels, the disk-like gels become white and can be observed clearly against a black background. In our graphical analysis, the resolution of light was from 0 up to 255. Using a clipping procedure, we obtain black and white images of the disk-like gels. We introduced typical parameters $S(t)$, $W_1(t)$ and $W_2(t)$ transferred from these images. The area of a disk-like gels $S(t)$ was normalized to 1 at the initial value of area obtained using a white plastic disk of size the same as before shrinking. The integral value of light intensities in gels area is $W_1(t)$, normalized to 1 at maximum value. $W_2(t)$ is whitening per area of gel $W_1(t)/S(t)$, normalized to 1 at maximum value.

Plots of $S(t)$, $W_1(t)$ and $W_2(t)$ as a function of time at ΔT=0.4℃ and 1.0 ℃ are shown in Figure 2. $S(t)$ first decreases monotonically and remains constant for a while, then decreases and approaches a certain constant value. $W_1(t)$ and $W_2(t)$ first increase sharply and decrease gradually, reaching 0 at the final stage. The time at which $S(t)$ reaches a minimum corresponds to the time at which $W_2(t)$ is a maximum. The time of $W_2(t)$ is synchronized with that of $S(t)$ for each ΔT.

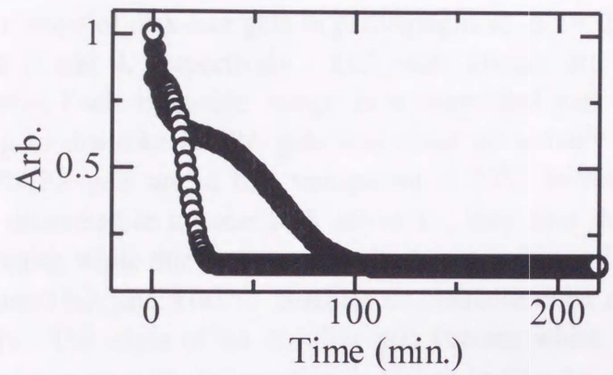

(a)

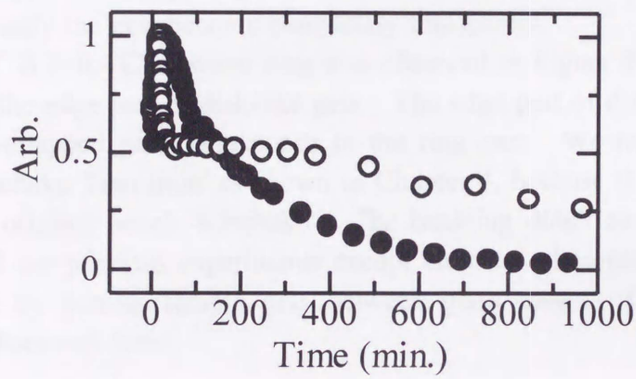

(b)

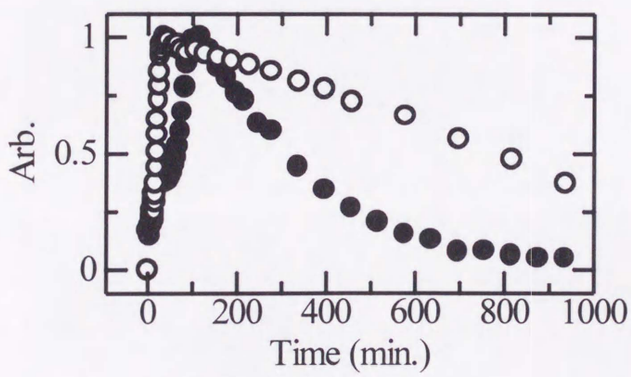

(c)

Figure 2. Plots of normalized area of gels S(t) (a), normalized whitening of gels $W_1(t)$ (b) and normalized whitening of gels per unit area $W_2(t)$ (c) as a function of time at ΔT=0.4℃ (●) and 1.0℃ (○).

2) Photographs of Disk-like PNIPA Gels

Temporal change of disk-like gels in photographs at $\Delta T = 0.4℃$ and $1.0℃$ are shown in Figure 3 and 4, respectively. Left -side images are whole gels against black background. Each right-side image is a magnified part of left-side image. Typical shrinking of disk-like PNIPA gels was observed visually in previous section (Chapter 1). PNIPA gels are at first transparent at 20℃ before shrinking. When PNIPA gels are immersed in a water bath above T_c, they first shrink monotonically. They become bluish white due to intense multiple scattering and gels stop shrinking for a while (Figure 3(a) and 4(a)). Bubbles or interconnected network like neuron appear in the gels. The edges of the disk-like gels become white. Then the disk-like gels shrink abruptly again with deformation as shown in Chapter 4. Shape of gels is restored after shrinking and whitening begins to disappear slowly. Gels show white and transparent spots randomly (Figure 4(e)). The white network-like spots slowly disappear and finally the gels become completely transparent.

In case of $\Delta T = 0.4℃$, a white ring was observed in Figure 4(c). It is due to the buckling of the edge part of disk-like gels. The edge part of disk-like gels turned over and the overlapped part corresponds to the ring part. We name this buckling phenomena 'Kinchaku Transition' as shown in Chapter 4, because the shape is similar to the japanese original pouch 'Kinchaku'. The buckling didn't clearly appear at $\Delta T = 1.0℃$. In all our previous experiments except for these photographs, the buckling was suppressed by putting sample gels between glass plates. Only the network pattern will be discussed here.

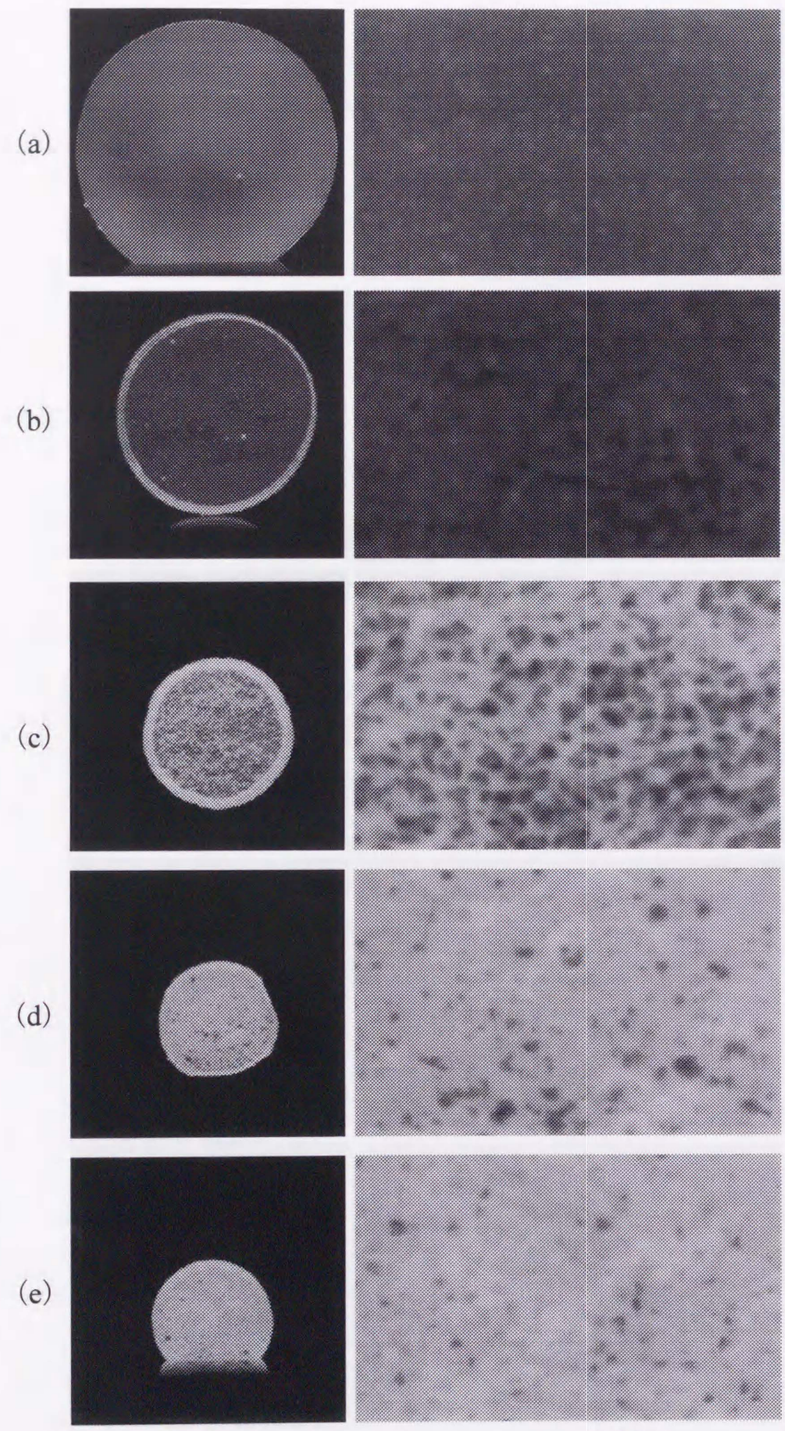

Figure 3. Temporal change of disk-like gels. Whole gels are shown at left-side and closed surface of gels are observed at right-side. Times after immersing sample into water at ΔT=0.4℃ are (a) 8min (b) 65min (c) 96min and (d) 136min (e) 150min.

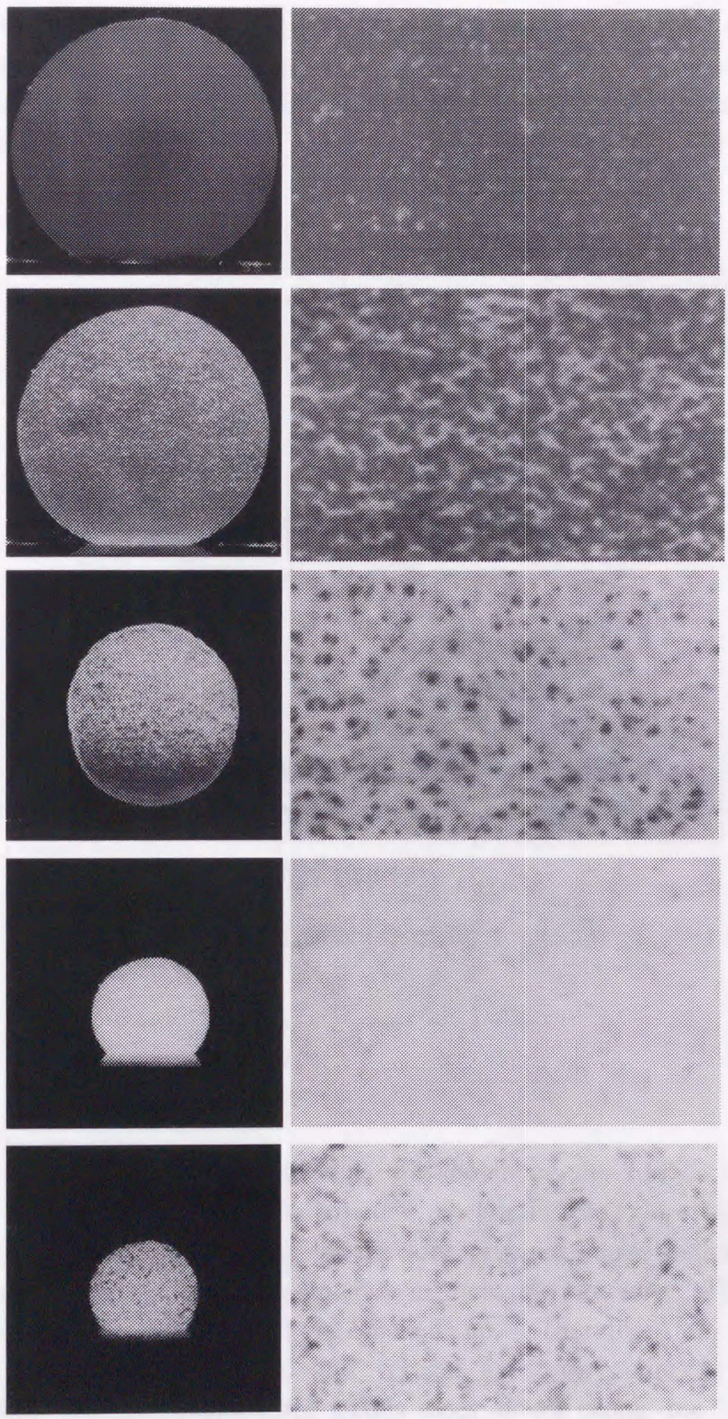

Figure 4. Temporal change of disk-like gels. Whole gels are shown at left-side and closed surface of gels are observed at right-side. Time after immersing sample into water at ΔT=1.0℃ are (a) 4min (b) 11min (c) 19.5min (d) 75min and (e) 150min.

3) Distribution of Light Intensity

Figure 5 shows distribution of light intensity in a unit area at $\Delta T=1.0℃$ using by magnified photographs shown in right-side images of Figure 4. The distribution shifts to higher intensity with time. Then it shifts back to lower intensity and finally disappears. This is same as previous reported one using by a CCD video camera (Chapter 1).

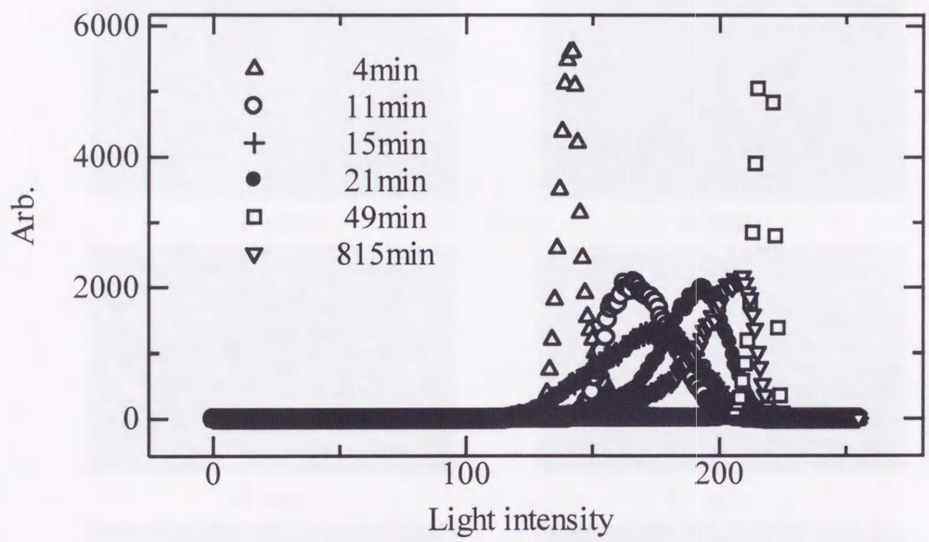

Figure 5. Temporal change of distribution of light intensity at $\Delta T=1.0℃$

4) Graphical Analysis of Photographs

White network and transparent domains are shown on the surface of gels in Figure 3 and 4. In order to obtain such structure, a clipping procedure was used in usual. However it was impossible to get the network structure image well using by a clipping procedure. It is due to the 3-dimensional network structure. That is, the network in back is dark and cannot be picked up. Therefore the following procedures were used along horizontal and vertical axes: we count 127 if light intensity difference between neighboring pixels goes down along the axis, then continue counting 127 along the axis till the light intensity difference is less than 0. When the difference is less than 0, we count 0 and continue counting 0 till the intensity goes up again along the axis. If the sum of both values along horizontal and vertical axes are 0, 127 or 255, put back black, gray and white dots, respectively. Using such a procedure, we obtain black, gray and white images of the disk-like gels

as shown in Figure 6. They clearly show the convexoconcave of light intensity on the surface of gels.

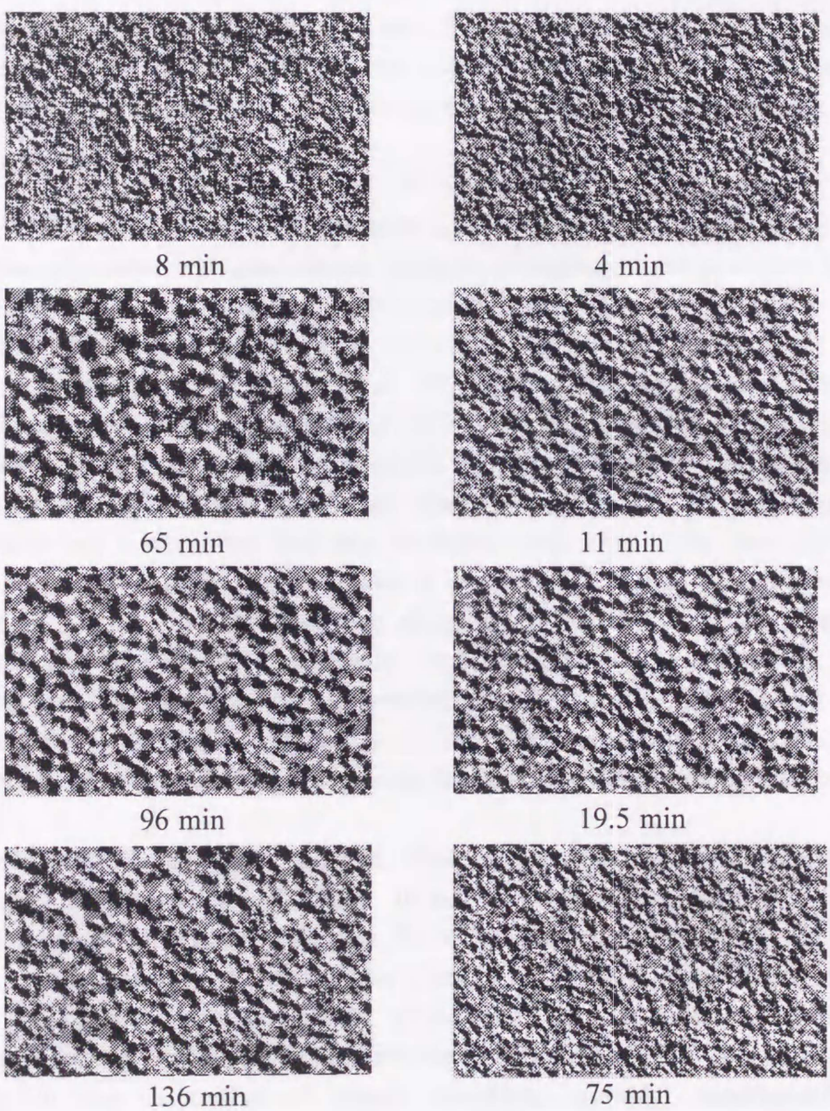

Figure 6. Temporal change of analytical images of PNIPA gels at ΔT=0.4℃ (left-side) and 1.0℃ (right-side)

5) 1D-FFT Analysis

Right-side images of Figure 6 were cut into 128x128 dots and 1-dimensional fast Fourier transformation (FFT) was carried on along vertical and horizontal axis of each image, respectively. Each power spectrum of horizontal and vertical axes is the average of 128 spectra. Temporal changes of power spectra are shown in Figure 7. X axis is wavenumber and we count 1 when a sine exists in 128 dots. Real measure is also shown. Y axis is fraction of the wave. At first there is no periodic structure on the surface of PNIPA gels. Then a sine appears at around 5 wevenumber and it corresponds to the size of characteristic network on the second stage of shrinking (about 0.86 mm). There is no difference between sizes of vertical and horizontal axes and it indicates that the network structure is isotropic. The following equation was proposed as a fitting function of these power spectra.

$$S(f) = A_3/2\left[\frac{1}{A_1^2 + 4\pi^2(f+f_0)^2} + \frac{1}{A_1^2 + 4\pi^2(f-f_0)^2}\right] + A_2 \qquad (1)$$

The first term represents a power spectrum of a sine and Markov noise, where f_0 is wavenumber of a sine. Autocorrelation function of Markov noise is written by $\exp(-A_1 t)$, where A_1^{-1} is strength of correlation of noise. The second term is a power spectra of white noise, where A_2 is the fraction of white noise. Data were fitted by equation (1) well as shown in Figure 8. It indicates that three modes exist on the surface of secondary shrinking disk-like PNIPA gels, that is, a sine, Markov noise and white noise. Fitting parameters of equation (1) are plotted as a function of time after putting the sample into thermostat water in Figure 9. The wavenumber of periodic structure f_0 decreases and then increases with time. The time at which f_0 reaches a minimum is larger than the time at which the gels size reach a minimum. As shown in Figure 2, needed times to shrink at ΔT= 0.4℃ and 1.0℃ are about 100 minutes and 25 minutes, respectively. It indicates that size of network becomes large when gels shrink, then size of network becomes small. The largest network size at ΔT=0.4℃ is larger than that at ΔT=1.0℃. It coinsides with the fact that small domains are formed when the quench depth is large in phase separation process in general.

White noise A_2 is almost constant, while correlation strength of Markov noise A_1^{-1} increases and decreases with time. In addition, temporal change of A_1^{-1} is very similar to normalized whitening of gels $W_1(t)$ as shown in Figure 10. It indicates that $W_1(t)$ corresponds to the correlation strength of Markov noise on the surface of gels and $W_1(t)$ is obtained without considering the network. In general the mechanism of phase transition phenomena has been discussed by phase diagram. According to the discussion of phase transition, spinodal decomposition and nucleation and nuclear formation progress at large and small ΔT, respectively. There has been discussed the possibility that such mechanism to volume phase transition. However there is turbidity like Markov noise appear and disappear while PNIPA gels shrink in spite of the formation of network. It can be considered that such Markov noise corresponds to the appearance of scattered light in spinodal

decomposition.

5-4. Conclusion

(1) New graphical analysis is proposed and network structure when gels shrink is evaluated.

(2) Power spectra on the surface of gels has three modes, a sine, Markov noise and white noise. Temporal change of correlation strength of Markov noise corresponds to normalized whitening amount of gels $W_1(t)$ as discussed in previous section.

References

1. E.S.Matsuo and T.Tanaka, J.Chem.Phys.,1695,89(3) (1988)
2. T.Tanaka,S.T.Sun,Y.Hirokawa,S.Katayama,J.Kucera,Y.Hirose and T.Amiya, Nature,,796,325(26) (1987)
3. S.Hirotsu, J.Chem.Phys.,88,1,427 (1988)
4. E.S.Matsuo and T.Tanaka, Nature,482,358(6) (1992)
5. M.Shibayama and M.Uesaka, J.Chem.Phys.,4350,105(10) (1996)
6. E.S.Matsuo and T.Tanaka, J.Chem.Phys.,1695,89(3),1988
7. T.Tanaka and D.J.Fillmore, J.Chem.Phys.,1214,70(3) (1979)
8. Y.Li and T.Tanaka, J.Chem.Phys.,1365,92(2) (1990)
9. C.Hashimoto and H.Ushiki, Polym.J.,32(10), 807 (2000)
10. H.Tanaka, Phys.Rev.Lett.,3158,71(19) (1993)

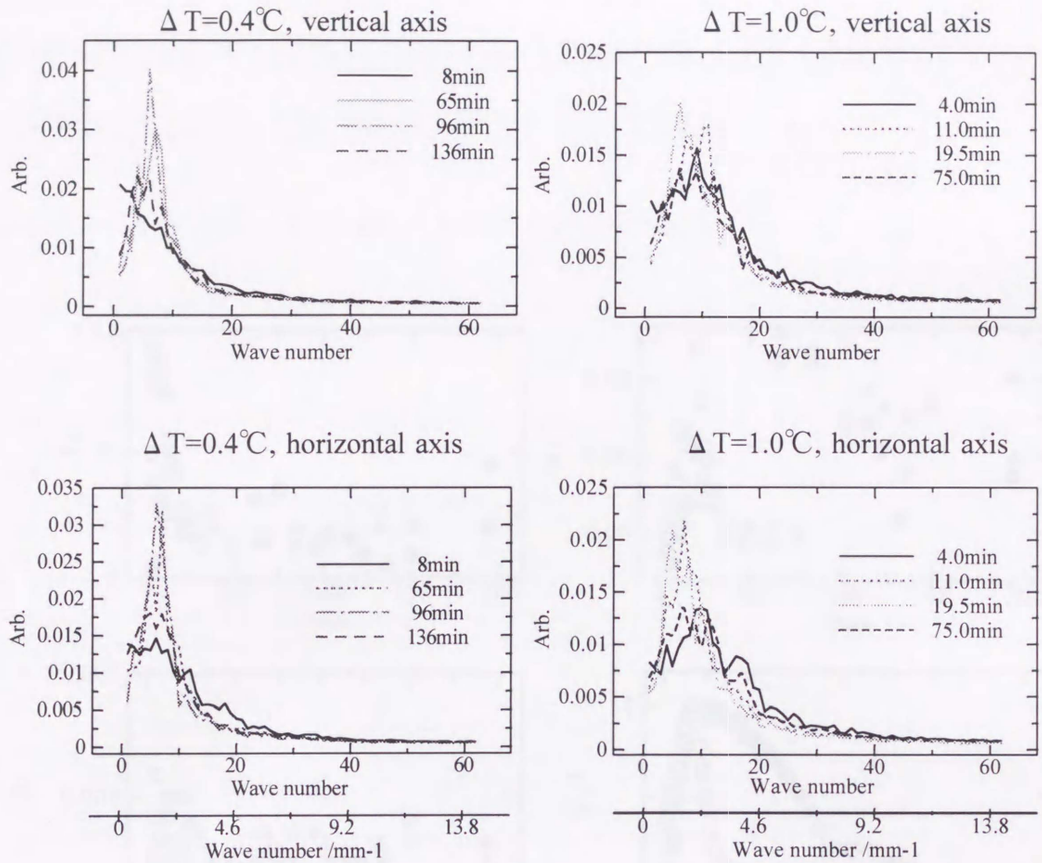

Figure 7. Temporal change of power spectra.

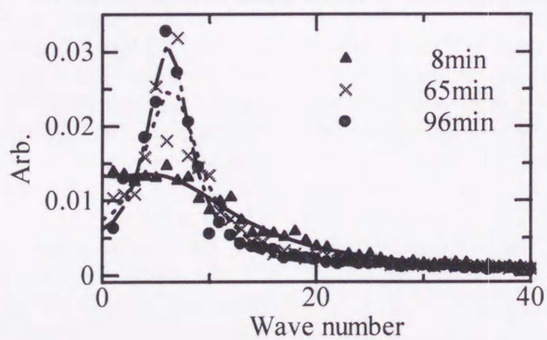

Figure 8. Temporal change of power spectra at Δ T=0.4℃ along horizontal axis. Lines trough the data are fits to equation (1).

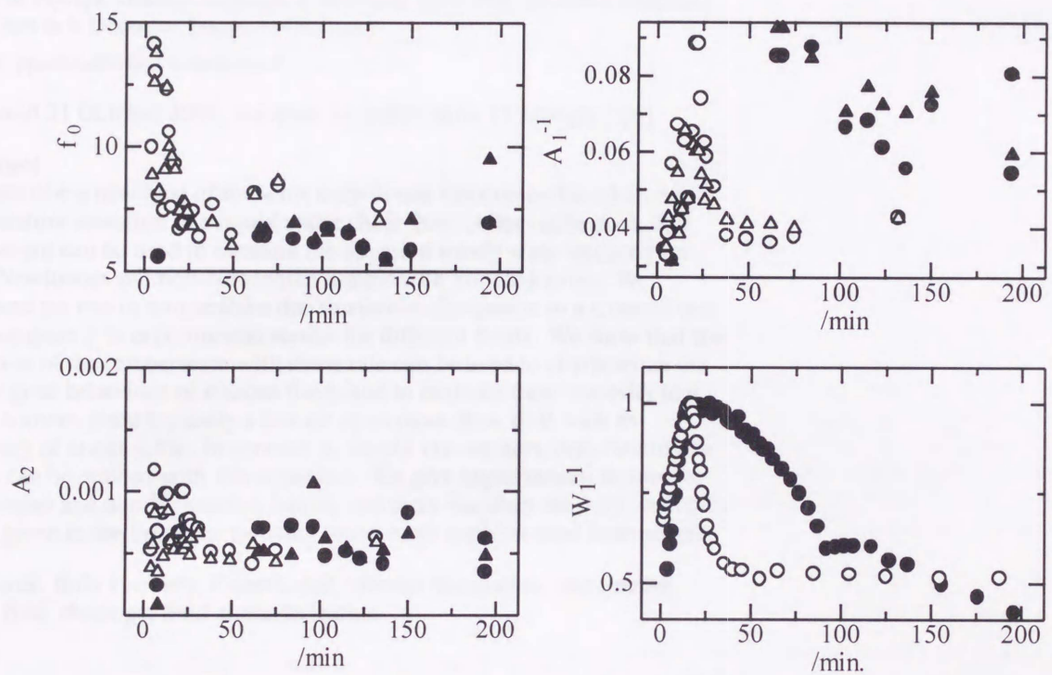

Figure 9. Fitting parameters of equation (1) against time after immersing sample into water. (○: Δ T=1.0℃, horizontal axis, △: Δ T=1.0℃, vertical axis, ●: Δ T=0.4℃, horizontal axis, ▲: Δ T=0.4℃,vertical axis)

INSTITUTE OF PHYSICS PUBLISHING MEASUREMENT SCIENCE AND TECHNOLOGY
Meas. Sci. Technol. **12** (2001) 1–5 www.iop.org/Journals/mt PII: S0957-0233(01)18472-9

Low-cost viscometer based on energy dissipation in viscous liquids

C Hashimoto[1], G Cristobal, A Nicolas, P Panizza[2], J Rouch and H Ushiki[1]

Centre de Physique Moléculaire Optique et Hertzienne, UMR 5798, Université Bordeaux I, 351, Cours de la Libération, Talence 33400, France

E-mail: ppanizza@cribx1.u-bordeaux.fr

Received 31 October 2000, accepted for publication 11 January 2001

Abstract

We describe a new type of low-cost easy-to-use viscometer based on the temperature elevation in a liquid under shear flow. After calibration, this instrument can be used to measure the apparent steady state viscosity for both Newtonian and non-Newtonian liquids with no yield stress. We compute the rise in temperature due to viscous dissipation in a Couette cell and compare it to experimental results for different fluids. We show that the variation of the temperature with shear rate can be used to characterize the rheological behaviour of viscous fluids and to evaluate their viscosity in a large domain, from typically a few cP up to more than 10 P, with an accuracy of about ±5%. In contrast to simple viscometers, non-Newtonian fluids can be studied with this apparatus. We give experimental results for Newtonian and non-Newtonian liquids and show that they are very similar to those given in the literature by using much more sophisticated instruments.

Keywords: fluid viscosity, Couette cell, viscous dissipation, viscometer, shear flow, rheology, fluid characterization

1. Introduction

It is well known that simple viscometers like capillary tubes or falling-ball instruments give precise values of the viscosity of liquids, but in a quite restricted range for a given instrument. Furthermore they are unable to give information on non-Newtonian fluids. Indeed non-Newtonian regimes are usually connected to structural changes of the fluid microstructure under flow. The transient time to reach steady state under stress can be long, from a few minutes up to hours. Therefore capillary or falling-ball viscometers are unsuitable to study non-Newtonian fluids since the steady state under stress can never be obtained with these types of instrument. To gain information on non-Newtonian fluids, expensive rotating rheometers have to be used. In this paper we first evaluate the thermal elevation (in a stationary state) due to viscous dissipation of a liquid in a Couette cell. Even at moderate shear rates, we show that this temperature elevation can be significant and therefore quite easy to measure with a standard laboratory instrument. On this basis, we describe an easy-to-use low-cost instrumental set-up (about 1/15 of the cost of a commercial rheometer) which allows us to characterize the rheological behaviour of Newtonian or non-Newtonian fluids. Using this set-up we give experimental results both for Newtonian (water–glycerol solutions, micro-emulsion systems) and for non-Newtonian liquids like quaternary solutions made of brine, surfactant, dodecane and pentanol. After calibration, the value of the temperature, shear and time-dependent viscosity can be measured with an accuracy of about ±5% in a large domain, from few cP up to more than 10 P, for shear rates varying continuously from 0 up to 1000 s^{-1}.

2. Experimental set-up

We used a home made set-up depicted in figure 1. It consists of a Couette cell made of two concentric cylinders of respective radii $R_0 = 25$ mm and $R_1 = 26$ mm, and of heights $H =$ 60 mm. The inner cylinder is fixed while the outer one rotates at a given angular velocity, ω, by using a variable rotating

[1] On leave from Tokyo University of Agriculture and Technology, 3-5-8, Saiwai-cho, Fuchu-shi, Tokyo 183-8509, Japan.
[2] To whom correspondence should be addressed.

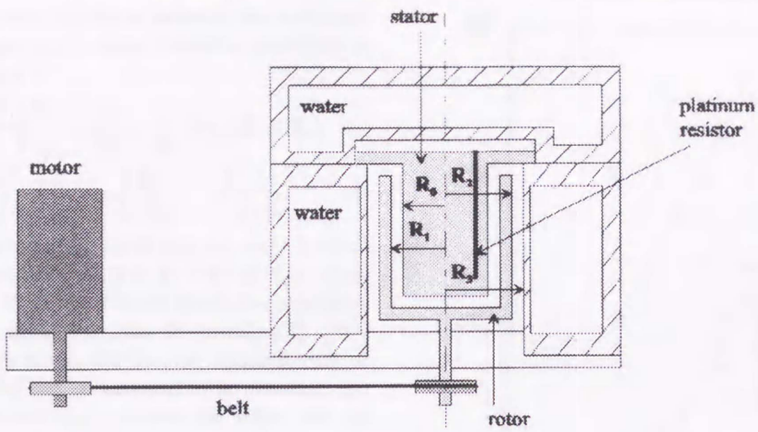

Figure 1. Schematic diagram of the set-up.

speed motor GR21M from MATTKE. The fluid filled the gap of width $e = R_1 - R_0 = 1$ mm between the two cylinders. For Newtonian fluids, at not too high angular velocities, and because the gap is narrow, the Couette geometry yields a simple laminar flow with a shear rate $\dot{\gamma}$ uniform across the gap and given by $\dot{\gamma} = R_1\omega/e$. The shear rate, which is imposed by the selected rotating speed of the motor, can be varied continuously from 0 up to 1000 s^{-1}. For non-Newtonian fluids the flow may be more complex; however we keep the same notation $\dot{\gamma}$ for $R_1\omega/e$, this quantity representing the mean shear rate within the cell. The rotor, which is made of ertacetal as the stator, is a cylindrical tube whose outer radius is $R_2 = 30$ mm. Note that ertacetal is both a good electrical insulator and has a low thermal conductivity. As we shall see below, its low value of the thermal conductivity enhances the temperature gradient inside of the cell and makes temperature measurements easier.

The Couette cell (stator + rotor) is placed inside a thermostatted housing consisting of two concentric cylindrical tubes of thickness $d = 20$ mm. The inner radius of the inner cylinder is $R_3 = 30$ mm and the gap between R_2 and R_3 is filled with air. The inner tube is made of brass to ensure a good conduction of heat with the Couette cell while the outer one is made of ertacetal. The gap between these two tubes is filled with circulating water from a water bath whose temperature is controlled within an accuracy of 0.01 °C. Another enclosure, connected to the same water bath, is placed on the top of the Couette cell to insulate it from outside. A platinum resistor (Pt 100), connected to a Wheatstone bridge, measures the temperature inside the stator with an accuracy of 0.02 °C. Its distance to the fluid is 1 mm. When the system is at rest, the temperatures of the stator and of the water bath are the same to within experimental errors. When the rotor is rotating, due to the energy dissipation inside of the viscous fluid, a temperature gradient is observed between the bath and the stator. This temperature gradient can be up to 10 °C for glycerol at a shear rate of 1000 s^{-1} and is therefore very easy to measure with standard equipment. As we shall see below, a simple model allows us to connect this temperature gradient to the viscous properties of the sample, both for Newtonian and non-Newtonian liquids.

3. Model

The temperature profile within the Couette cell is first calculated by solving Fourier's equations in cylindrical coordinates, when a stationary state is obtained ($\partial T/\partial t = 0$). We consider an elementary volume sandwiched between two concentric cylinders whose radii are respectively r and $r + dr$ and draw up the corresponding energetic balance accounting for the energy due to viscous height dissipation inside of the fluid. To simplify, we assume that the cylinders have an infinite height. By symmetry, the temperature profile $T(r)$ only depends on the radial distance r to the axis.

In the fluid ($R_0 \leqslant r \leqslant R_1$), $T(r)$ is given by the equation

$$-\lambda_f \left[\frac{1}{r}\frac{d}{dr}\left(r\frac{dT}{dr}\right)\right] = \eta\dot{\gamma}^2 \tag{1}$$

where λ_f and η are respectively the thermal conductivity and the viscosity of the fluid. The term on the right-hand side of (1) represents the creation of energy per unit volume due to viscous dissipation. The general solution of this differential equation is

$$T(r) = -\frac{r^2}{4}\frac{\eta\dot{\gamma}^2}{\lambda_f} + C_1 \ln(r) + C_2 \tag{2}$$

where C_1 and C_2 are constants.

Outside the fluid (i.e. for $r \leqslant R_0$, $R_1 \leqslant r \leqslant R_2$ and $R_2 \leqslant r \leqslant R_3$), the temperature is given by

$$-\lambda_i \left[\frac{1}{r}\frac{d}{dr}\left(r\frac{dT}{dr}\right)\right] = 0 \tag{3}$$

where λ_i represents the thermal conductivity of the materials air and ertacetal.

The general solution of equation (3) is

$$T(r) = C_3 \ln(r) + C_4 \tag{4}$$

where C_3 and C_4 are constants.

The temperature profile within the cell can then be fully determined by using the boundary condition $T(R_3) = T_{th}$, where T_{th} is the fixed temperature of the thermostat and the continuity of the temperature and heat flux across the different

regions. The temperature difference between the isothermal stator (C_3 has to be zero for the stator to avoid a singularity at $r = 0$) and thermostat is

$$T(\text{stator}) - T_{\text{th}} = \frac{\eta\dot{\gamma}^2}{2}\left\{\frac{R_0^2}{\lambda_f}\log\left(1+\frac{e}{R_0}\right) + e(R_1+R_0) \times\left[\frac{1}{\lambda_{\text{air}}}\log\left(\frac{R_2}{R_3}\right)+\frac{1}{\lambda_{\text{erta}}}\log\left(\frac{R_1}{R_2}\right)-\frac{1}{2\lambda_f}\right]\right\}. \quad (5)$$

Since the gap between the stator and the rotor is small compared to their respective radii ($e = R_1 - R_0 \ll R_0$), a first-order expansion in e/R_0 shows that the thermal conductivity of the fluid does not come into play in formula (5). In a reasonable temperature range, the thermal conductivities of the air and the ertacetal can be assumed to be constant. So the temperature difference ΔT between the stator and the thermostat—or between the rotating stator and the stator at rest—turns out to be the product of three terms: the viscosity η of the fluid, the square of the applied shear rate, $\dot{\gamma}^2$, and an instrumental constant, C, which can be deduced by calibration, using Newtonian fluids of known viscosity:

$$\Delta T = T_{\text{stator}}(\dot{\gamma}) - T_{\text{stator}}(0) \approx C\eta\dot{\gamma}^2 \quad (6)$$

where the instrument constant C is given by

$$C = \frac{1}{2}\left\{(R_1^2 - R_0^2)\left[\frac{1}{\lambda_{\text{air}}}\log\left(\frac{R_2}{R_3}\right)+\frac{1}{\lambda_{\text{erta}}}\log\left(\frac{R_1}{R_2}\right)\right]\right\}. \quad (7)$$

Note that the low thermal conductivity of ertacetal enhances the temperature gradient inside the cell by increasing the constant C and therefore makes temperature difference measurements easier. On the other hand, it takes a few tens of minutes to reach a stationary temperature of the stator. It has to be emphasized that formula (6) still holds even if the fluid is non-Newtonian i.e. if the apparent viscosity ($\eta = \sigma/\dot{\gamma}$) depends on the shear rate (σ is the stress) and provided the fluid does not possess a yield stress. For Newtonian liquids a plot of ΔT versus $\dot{\gamma}^2$ should be a straight line, whose slope gives the viscosity. On the other hand, deviations of ΔT from a linear dependence on $\dot{\gamma}^2$ should be observed for non-Newtonian liquids. In this case, at a given the shear rate, we can infer the value of the shear-dependent viscosity from the slope of ΔT versus $\dot{\gamma}^2$.

4. Experimental results

4.1. Newtonian liquids

As we said above, in the absence of shear flow, the temperature of the stator is equal to the temperature of the thermostat (the thermal conductivity of brass is so high that the temperature gradient within the brass tube is negligible). However, when the fluid is sheared, the temperature of the stator increases due to viscous dissipation and is modelled by equation (6). In order to compare the model with experimental results, we measure the temperature of the stator first at rest and then after setting the shear flow and reaching the steady state.

Figures 2 and 3 show the variation of the stationary increase of temperature ΔT as a function of shear rate observed with Newtonian liquids, namely binary mixtures of glycerol and water at different water content and micro-emulsion systems. The viscosities are quite low for micro-emulsion systems and for water–glycerol solutions at high water content. In this case, the temperature increase ΔT is not too high (at most a few K) and it increases linearly with the second power of the applied shear rate (straight lines of slope 2 in a log–log diagram) as expected from the simple theoretical model. Since the behaviour of the temperature increase with shear rate is in agreement with our simple model, we can easily deduce the shear viscosity of these liquids after calibration. In order to do so, we have first measured the temperature rise for liquids of known viscosity such as long chain alcohols and nitrobenzene and then fitted these data with equation (6).

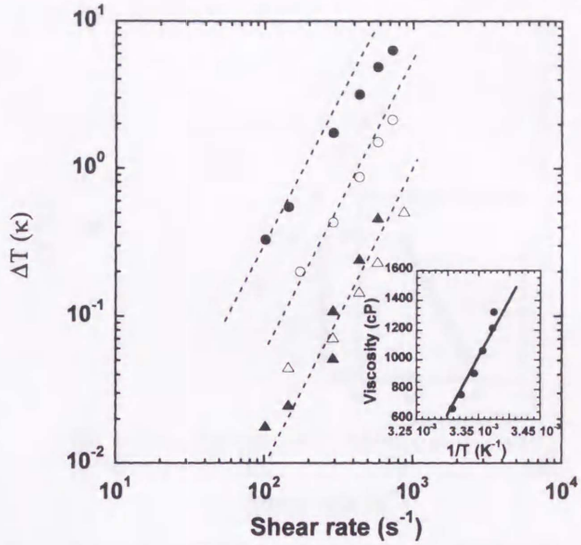

Figure 2. Log–log plot of the temperature increase versus the shear rate. Full circles: pure glycerol; empty circles: water–glycerol solution at 90% of glycerol; triangles: water–glycerol solution at 70% of glycerol. The dashed lines are power laws with a slope of 2. The inset shows the viscosity of pure glycerol as a function of temperature. Full circles: experimental results, solid line: data from literature.

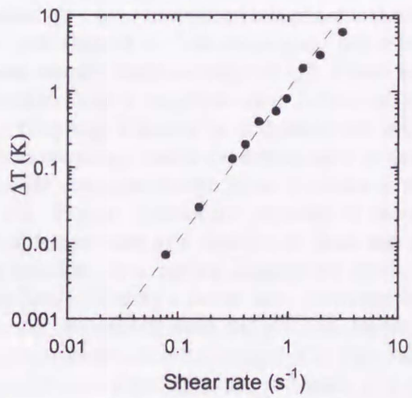

Figure 3. Log–log plot of the temperature increase as a function of the shear rate for a ternary micro-emulsion, water, AOT, decane at a molar ratio of 40.8 and a volume fraction 40%. The dashed line is a power law with a slope of 2.

For pure glycerol and low water content water–glycerol solutions, ΔT is large, up to 10 K at a shear rate of 1000 s^{-1}. For these solutions, two regimes are observed (see figure 2

for pure glycerol): the first one, observed at low shear rates, corresponds to a weak temperature increase and is characterized by a straight line of slope 2 in the log–log plot. For higher shear rates, when the temperature increase is high, a second regime takes place, leading to a curvature of the plot. A similar but less pronounced curvature of the plot can be observed for the micro-emulsion in the same domain of ΔT (figure 3). This last effect is due to the strong temperature variation of the viscosity with temperature even in a reduced temperature range (tables give a variation of a factor of two of the viscosity of glycerol in a range of temperature of 10 K around room temperature). To model this effect we assume that the viscosity follows an Arrhenius law, which is a typical variation for most liquids:

$$\eta = \eta_0 \exp \frac{U}{RT} \tag{8}$$

where η_0, U and R are respectively the infinite temperature viscosity, the activation energy/mol and the molar Boltzmann constant. To account for this effect, Fourier's equation has to be solved again. This cannot be achieved analytically and a numerical solution would be obtained. In our case, however, since the accuracy of our simple instrument is only a few per cent, a first approximation is to assume that the viscosity is temperature independent in Fourier's equation and to introduce the temperature-dependent viscosity in the final result. This approximation leads to

$$\Delta T = T_{\text{stator}}(\dot{\gamma}) - T_{\text{stator}}(0) \approx C\eta_0 \exp \frac{U}{RT_{\text{stator}}(\dot{\gamma})} \dot{\gamma}^2. \tag{9}$$

In the inset of figure 2, we have plotted the viscosity of glycerol as a function of the inverse of temperature. The dots are our experimental results obtained by fitting our data to equation (9) whereas the straight line corresponds to data obtained from the literature. A good agreement between these data is found.

From the plot of ΔT versus $\dot{\gamma}^2$ and after calibration, we can easily measure the viscosity of liquids in the range from a few cP up to more than 10 P, and its temperature dependence. The accuracy is of the order of $\pm 5\%$ for the viscosity of Newtonian fluids and of the order of $\pm 10\%$ for the activation energy for highly viscous liquids.

4.2. *Non-Newtonian liquids*

As we said above, simple viscometers (such as capillary tubes or as falling spheres) are not suitable to deduce the rheological properties of non-Newtonian liquids. In what follows we show that our instrument can provide also valuable information for this type of fluid when a stationary state of temperature is reached inside the cell ($\partial T/\partial t = 0$). We have performed the same type of experiment with a lyotropic lamellar phase exhibiting a non-Newtonian behaviour [3]. We have studied a lamellar phase made of sodium dodecyl sulphate (SDS), pentanol, dodecane and water with a SDS/water mass ratio of 1.55. The phase diagram of this system has been extensively studied by Roux and Bellocq [2]. We have prepared a solution composed in weight percentage of 15.1% SDS, 23.35% (water), 14.55% pentanol and 47% dodecane. This lamellar phase can be seen as constituted of water film surrounded by surfactant molecules and separated by a solvent

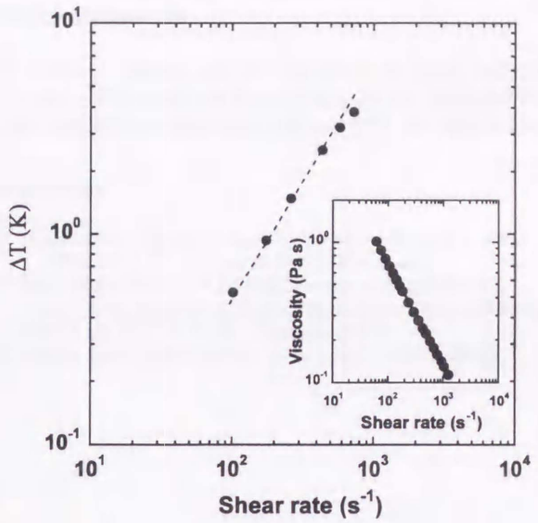

Figure 4. Log–log plot of the temperature increase versus the shear rate for a non-Newtonian fluid. The dots are experimental results whereas the dashed line is the best fit to a power law with slope 1.2. The inset shows experimental data obtained with a SR5 rheometer from Rheometrics for the same system. The full line is the best fit to the data with a power law of slope -0.75.

which is a mixture of 91% weight fraction of dodecane and 9% pentanol. We have introduced this phase into the Couette cell and have sheared it. The rheological behaviour of this system has already been investigated [3]. Under shear flow, this system exhibits a non-Newtonian behaviour as a result of strong couplings between its microstructure and the flow field. These couplings lead to the formation of an assembly of multilamellar vesicules, known in the literature as the 'onion texture' [4]. Figure 4 shows the variation of the stationary increase of temperature as a function of shear rate measured with this solution. In a log–log diagram we obtain here also a straight line, indicating a power law. However, in contrast to Newtonian mixtures of water and glycerol, for instance, the slope is lower, about 1.2 ± 0.1 instead of 2. This value shows that the solution is shear thinning, and leads to a scaling of the viscosity with shear rate as $\dot{\gamma}^{-0.8}$. To check this scaling, we have measured the rheological properties of the same sample with a sophisticated stress control rheometer, RS5, from Rheometrics. The scaling law we obtained is depicted in the inset of figure 4. The slope we infer from the double log plot is -0.7 ± 0.05, in agreement with literature data [4]. These data clearly show the consistency of the experiments made with our simple apparatus.

5. Conclusion

We have investigated the effect of thermal heating due to the viscous energy dissipation obtained when shearing fluids in a Couette cell. When the steady state is reached the increase of temperature is significant and its variation with shear rate can be used to gain valuable information about the rheological behaviour of the fluid. For Newtonian liquids, after calibration, this allows the determination of the viscosity in a large range, from few cP up to more than 10 P with a quite good accuracy,

typically ±5%, and the determination of the activation energy with an accuracy of the order of ±10%. This technique can also be used to study non-Newtonian fluids in the range 0–1000 s^{-1}. For the non-Newtonian quaternary mixture we have studied, it provides good scaling of the viscosity with the shear rate. The cost of this set-up is less than 10% of the cost of a more sophisticated commercial viscometer. Besides there is no need to proceed to the difficult measurement of a torque although it works at imposed shear rate. Therefore this device can be considered as an easy-to-use low-cost viscometer specially designed to study the rheological behaviour of viscous complex fluids.

Acknowledgments

We thank T Douar and M Winckert for their technical assistance. This work was supported by the PICS No 610 from CNRS and Région Aquitaine (contract CTP No 980209202).

References

[1] *Handbook of Chemistry and Physics* 46th edn, ed R C weast (Cleveland, OH: Chemical Rubber Company)
[2] Roux D and Bellocq A M 1985 *Physics of Amphiphiles* ed V Degiorgio and M Corti (Amsterdam: North-Holland)
[3] Diat O and Roux D 1993 *J. Physique* II **3** 9
[4] Diat O, Roux D and Nallet F 1993 *Europhys. Lett.* **24** 53

List of publications

1. C.HASHIMOTO, P.Panizza, J.Rouch and H.Ushiki,
   "Graphical Analysis in Gels Morphology I. General Method"
   Polymer Journal, (2000) Vol 32, No.10, 807-816
2. C.HASHIMOTO, G.Cristobal, P.Panizza, J.Rouch and H.Ushiki;
   "Law Cost Viscometer Based on Energy Dissipation in Viscouse Liquid"
   Meas. Sci. Technol., (2001) 12, 1-5
3. C.HASHIMOTO, P.Panizza, J.Rouch and H.Ushiki;
   "Graphical Analysis in Gels Morphology II. Physical Meaning of Stretched Exponential Function with $\beta > 1$"
   submitted to Journal of Physics Condensed Matter
4. C.HASHIMOTO, P.Panizza, J.Rouch and H.Ushiki;
   "Graphical Analysis in Gels Morphology III. Effect of Temperature-jumping for Volume Phase Transition of Poly(N-isopropylacrylamide) Gels"
   submitted to Polymer Journal
5. C.HASHIMOTO, P.Panizza, J.Rouch and H.Ushiki,
   "Graphical Analysis in Gels Morphology IV.
   Whitening Process in Volume Phase Transition of Poly(N-isopropylacrylamide) Gels"
   submitted to Polymer Journal
6. C.HASHIMOTO and H.Ushiki;
   "Graphical Analysis in Gels Morphology V. Relationship between Volume Change and Whitening in Volume Phase Transition of Poly(N-isopropylacrylamide) Gels"
   submitted to Polymer Journal
7. S.Kawahara, S.Bushimata, T.Sugiyama, C.Hashimoto, Y.Tanaka;
   "A Novel Method for ^{13}C-NMR spectroscopy of Polymer in Emulsion. I -Quantitative Analysis of Microstructure of Crosslinked Polybutadiene in Latex-"
   submit to Macromolecules

List of other publications I

1. H.Ushiki, C.Hashimoto, J.Rouch;
   "PLASMA XXV -Kinetic Study on Shrinking and Whitening Processes in Volume Phase Transition of Poly(N-isopropylacrylamide) Gels at Above Critical Temperatures-"
   Rep.Prog.Polym.Phys.Jpn., (1996) Vol.39, 179
2. H.Ushiki, C.Hashimoto, J.Rouch;
   "PLASMA XXVI -Volume Phase Transition Behaviours of Poly(N-isopropylacrylamide) Gels-"
   Rep.Prog.Polym.Phys.Jpn., (1997) Vol.40, 171
3. H.Ushiki, C.Hashimoto, J.Rouch;
   "PLASMA XXVII -Dependence of Temperature Quench Depth on Volume Phase Transition and Phase Separation Behaviour of Poly (N-isopropylacrylamide) Gels-"
   Rep.Prog.Polym.Phys.Jpn., (1997) Vol.40, 175
4. H.Ushiki, A.Ikehata, C.Hashimoto, J.Rouch;
   "PLASMA XXVIII -Additional Effects of Various Metal Ions to Volume Phase Transition Temperatures of Poly(N-isopropylacrylamide) Gels-"
   Rep.Prog.Polym.Phys.Jpn., (1997) Vol.40, 179
5. H.Ushiki, C.Hashimoto, J.Rouch;
   "PLASMA XXXII

-Kinetic Study on Volume Phase Transition Process of Poly(N-isopropylacrylamide) Gels-" Rep.Prog.Polym.Phys.Jpn., (1998) Vol.41, 165

6. H.Ushiki, T.Suzuki, A.Ikehata, C.Hashimoto, J.Rouch, K.Hamano; "PLASMA XXXVIII -Turbid Processes of Poly(N-isopropylacrylamide) Gels at near Critical Temperature Monitorede by Microscope Techniques-" Rep.Prog.Polym.Phys.Jpn., (1999) Vol.42, 67
7. H.Ushiki, C.Hashimoto, J.Rouch, K.Hamano; "PLASMA XXXIX -Phenomenological Analysis of Turbid Processes of Poly (N-isopropylacrylamide) Gels at near Critical Temperature-" Rep.Prog.Polym.Phys.Jpn., (1999) Vol.42, 71
8. H.Ushiki, A.Ishii, S.Irisawa, C.Hashimoto, J.Rouch, K.Hamano; "PLASMA XL -Algorithm Physics for Analysis of TitrationCurves in Yogurt Production Process-" Rep.Prog.Polym.Phys.Jpn., (1999) Vol.42, 539

＜紀要＞

1. 牛木秀治, 橋本千尋, 生駒丈善, J.Rouch; ”太陽と大地，そして人間－複雑系化学物理学への招待－ I. Cooking Chemical Physics”, 「人間と社会」東京農工大学一般教育部紀要，1998 年 3 月, Vol.9, 211-262
2. 牛木秀治, 橋本千尋, 勝本之晶, J.Rouch; ”太陽と大地，そして人間－複雑系化学物理学への招待－ II. 反要素還元と分布関数”, 「人間と社会」東京農工大学一般教育部紀要，1999 年 3 月, Vol.10, 133-197

＜総説＞

1. 牛木秀治，橋本千尋；”形態形成ダイナミックス－温度誘起型体積相転移ゲルのダイナミックス－” 高分子加工，1997 年 Vol.46, No.273, 33

List of other publications II

＜口頭発表＞　注）○は発表者を意味する。

1. 牛木秀治，山口睦穂，○橋本千尋; "PNIPA ゲルの体積相転移における機能水の役割について" 電気化学協会年次大会 東京 1996 年 4 月
2. ○橋本千尋, 牛木秀治; "高分子鎖ダイナミックスの階層構造[LXXI]－画像解析法による PNIPA ゲルの体積相転移近傍における白濁消失速度について－" 高分子年次大会 名古屋 1996 年 5 月
3. ○橋本千尋, 牛木秀治; "高分子鎖ダイナミックスの階層構造[LXXVI]－温度ジャンプによる PNIPA ゲルの体積相転移過程のビデオ画像解析－" 高分子討論会 広島 1996 年 10 月
4. ○橋本千尋, 牛木秀治; "高分子鎖ダイナミックスの階層構造[LXXX]－画像解析法による PNIPA ゲルの体積相転移におけるスキン層効果について－" 溶液化学シンポジウム 佐賀 1996 年 11 月
5. ○牛木秀治, 橋本千尋; "高分子鎖ダイナミックスの階層構造 － PNIPA ゲルの体積相転移現象の画像解析－" 科研費総合研究A「ソフトマテリアルの構造とダイナミックス」箱根 1997 年 1 月
6. ○牛木秀治, 池羽田晶文，橋本千尋; "PNIPA ゲルの体積相転移温度の金属イオン添加依存性について" 電気化学協会年次大会 横浜 1997 年 3 月　依頼講演
7. ○橋本千尋, 牛木秀治，Jaques Rouch; "形態形成ダイナミックス III － PNIPA ゲルの体積相転移現象の画像解析－" 高分子年次大会 東京 1997 年 5 月
8. ○牛木秀治，池羽田晶文，橋本千尋; "形態形成ダイナミックス IV － PNIPA ゲルの体

積相転移温度への金属イオン効果－" 高分子年次大会 東京 1997年5月
9. ○池羽田晶文, 橋本千尋, 牛木秀治; "形態形成ダイナミックスVII － PNIPAゲルの体積相転移における水の役割について－" 高分子討論会 名古屋 1997年10月
10. ○橋本千尋, 牛木秀治, Jaques Rouch; "形態形成ダイナミックスVIII －画像解析によるPNIPAゲル体積相転移過程のダイナミックス－" 高分子討論会 名古屋 1997年10月
11. ○橋本千尋, 牛木秀治; "画像解析法によるPNIPAゲル体積相転移過程の解析" 旧科研費総合A研究会 京都 1998年1月
12. ○橋本千尋, 牛木秀治, Jaques Rouch; "形態形成ダイナミックスXI －画像解析によるNIPAゲルのキネティックス－" 高分子年次大会 京都 1998年5月
13. ○角森史昭, 橋本千尋, 牛木秀治; "形態形成ダイナミックスXII － NIPAゲルの中の低分子の拡散について－" 高分子年次大会 京都 1998年5月
14. ○ H.Ushiki, C.Hashimoto and J.Rouch; "Phenomelogical Analysis for Volume Phase Transition Behaviours of Poly(N-isopropylacrylamide) Gels" II Workshop on Non Equilibrium Phenomena in Supercooled Fluids, Glasses and Amorphous Materials, Pisa (Italy) 1998年9月
15. ○橋本千尋, 牛木秀治, Jacques Rouch; "形態形成ダイナミックスXV －画像解析によるPNIPAゲルの形態変化－" 高分子討論会 名古屋 1998年9月
16. ○橋本千尋, 牛木秀治; "PNIPAゲルの体積相転移の画像解析" 科研費基盤研究C 1 「インテリジェント高分子の機能と構造・ダイナミックス：乱れと秩序の解析と組織化」 犬山 1999年1月
17. ○橋本千尋, 角森史昭, 牛木秀治; "形態形成ダイナミックスXX － PNIPAゲルの体積相転移と相分離の現象論的解析－" 高分子年次大会 京都 1999年5月
18. 牛木秀治, ○橋本千尋, 角森史昭; "形態形成ダイナミックスXXI －高分子鎖に導入されたプローブ色素の発光寿命分布関数の添加高分子依存性－" 高分子討論会 新潟 1999年10月
19. ○石井暁子, 橋本千尋, 牛木秀治; "形態形成ダイナミックスXXIII －カゼイン／オレイン酸／水系の新たなｐH曲線解析法について－" 高分子討論会 新潟 1999年10月
20. ○橋本千尋, 牛木秀治; "形態形成ダイナミックスXXV －画像解析によるPNIPAゲルの収縮及び白濁生成・消失過程－" 高分子討論会 新潟 1999年10月
21. ○遠藤淳, 橋本千尋, 牛木秀治; "形態形成ダイナミックスXXVI － PNIPAゲルの体積相転移における「巾着転移」の画像解析－" 高分子討論会 新潟 1999年10月
22. ○ H.Ushiki, C.Hashimoto and J.Rouch; "Dynamics of Morphological Formation -Power Law Analysis on Temperature-Induced Vlume Phase Transition Process of PNIPA Gels-", International Symposium on Electrokinetic Phenomena, Dresden (Germany) 2000年10月

THE PUBLIC LIBRARY OF THE CITY OF BOSTON